NORTHWESTERN UNIVERSITY

MicroRNA *MiR-7* Regulation of Insulin-like Peptides in *Drosophila*

A DISSERTATION

SUBMITTED TO THE GRADUATE SCHOOL IN PARTIAL FULFILLMENT OF REQUIREMENTS

for the degree

DOCTOR OF PHILOSOPHY

Field of Interdisciplinary Biological Sciences Program

By

Pamela Agbu

EVANSTON, ILLINOIS

September 2020

Abstract

The insulin/Insulin-Like Growth Factor (IGF) pathway is essential for linking nutritional status to growth and metabolism. MicroRNAs (miRNAs) are short RNAs that are players in the regulation of this process. The miRNA *miR-7* shows highly conserved expression in insulin-producing cells across the animal kingdom. However, its conserved functions in regulation of insulin-like peptides (ILPs) remain unknown. Using *Drosophila* as a model, I demonstrate that *miR-7* limits ILP availability by inhibiting its production and secretion. Increasing *miR-7* alters body growth and metabolism in an ILP-dependent manner, elevating circulating sugars and total body triglycerides, while decreasing animal growth. These effects are not due to direct targeting of ILP mRNA, but instead arise through alternate targets that affect the function of ILP-producing cells. The Drosophila F-actin capping protein alpha, CPA, is a direct target of *miR-7*, and knockdown of CPA in IPCs phenocopies the effects of *miR-7* on ILP secretion. This regulation of CPA is conserved in mammals, with the mouse ortholog Capza1 also targeted by *miR-7* in β-islet cells. This result supports a conserved role for *miR-7* regulation of an actin capping protein in insulin regulation, and highlights a conserved mechanism of action for an evolutionarily ancient microRNA.

Acknowledgements

First and foremost, I would like to thank my advisor Rich – without his knowledge, guidance, and generosity, none of this work would have been possible. I am thankful for his support, his willingness to give advice, and for his patience with me during all these years. I have learned many lessons from him throughout my years in his lab and I am grateful to have had the experience.

I would also like to thank my thesis committee. Greg, Sadie, and Chris. They have been very supportive through the years and their guidance and suggestions helped get my project to where it is today.

Next, I would like to thank Justin, who I worked very closely with to make my paper and this thesis possible. Justin took me under his wing when I first joined the lab, and although he left a few years into my time in the lab, he taught me a lot about fruit flies, research in general, and about *miR-7*. He was always happy to give his time to help me and anyone else in the lab, whether it was coming up with new ideas to test or troubleshooting failed experiments. This project would not have been possible without him and I am grateful that my time in the lab overlapped with his.

To my Carthew Lab mates - research is hard, but one of the things that made it easier is the people that I worked with every day. Thank you for all the tea trips and vending machine trips, but also for listening to me and giving me advice whenever I needed it. I am lucky to have found such a great people to spend the past few years with.

Lastly, I would like to thank my friends and family for their support and encouragement.

Table of contents

List of Figures

CHAPTER 1: A PRIMER ON PANCREATIC β-CELLS AND DROSOPHILA IPCS

DEVELOPMENT OF THE VERTEBRATE ENDOCRINE SYSTEM

The vertebrate neuroendocrine system consists of neurons, glands, and non-endocrine tissue that produce hormones, and the organs that their axons target. Components of this system include the hypothalamus and the pituitary, peripheral neurons of the autonomic nervous system, and notably, the pancreas. In this system, cells secrete long range signals, known as hormones, into the circulatory system to target cells, which contain receptors for those hormones. The downstream actions mediated through hormone receptors regulate many aspects of animal physiology and behavioral state, including food intake, growth, water balance, lifespan, and reproduction.

One of the roles of the endocrine system is to couple the nutrient status of an organism to downstream functions of growth and maintenance of metabolic functions. At the core of this system in vertebrates is the pancreas, which has two main functions: The first is an endocrine function, consisting of islet cells that secrete hormones in response to nutrient cues to maintain blood glucose levels[1]. The second is an exocrine function, made up of acinar cells that secrete digestive enzymes through the pancreatic duct into the small intestine[1]. The pancreatic islets are composed of several different cell types, with insulin-secreting β-cells making up the bulk of the endocrine cells at 50-75 percent of the population, while α, δ, pp, and Ɛ cells, comprise much smaller percentages of the endocrine cell population(Figure 1) [2].

Figure 1 - The vertebrate pancreas

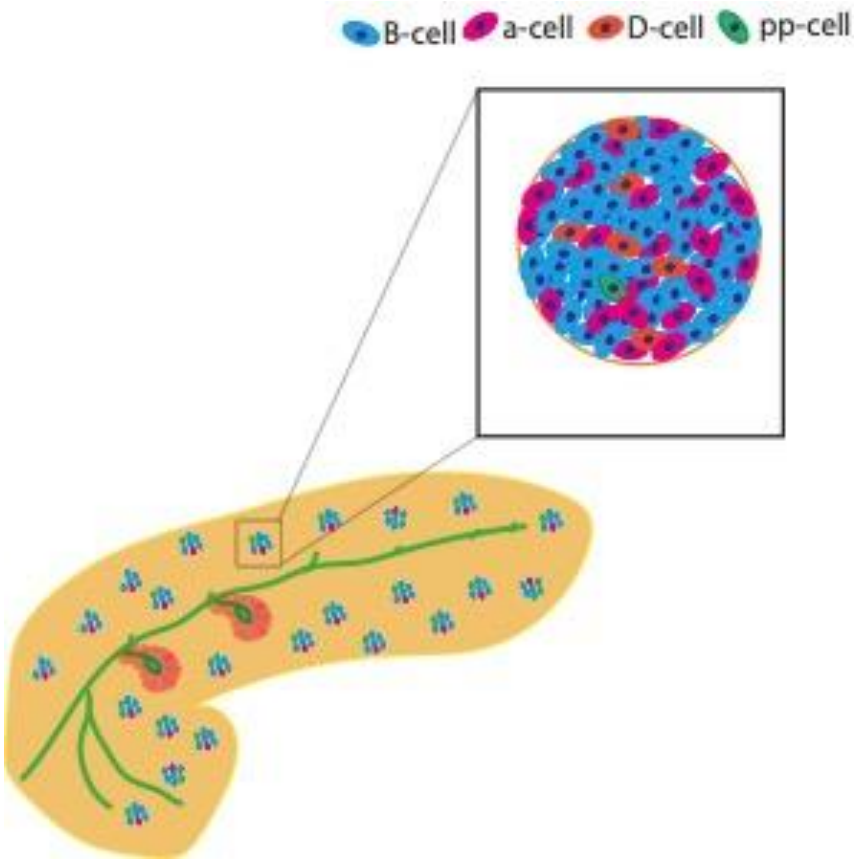

Figure 1: The vertebrate pancreas - The pancreas has an endocrine component, which consists of islet cells that release hormones into the circulatory system, and an exocrine component, which consists of acinar cells that release digestive enzymes into the intestine through the pancreatic duct. The islet cells of the endocrine pancreas include insulin-secreting β-cells (50-75%), glucagon-secreting α-cells (25-35%), somatostatin-secreting δ-cells (10%), with ε-cells and pp-cells making up much smaller percentages of the islet(~1%). Figure modified from Noguchi et al 2019 [2].

Pancreatic specification begins with the primary transition, which is characterized by the activation of TGFB proteins of the activin and nodal families, retinoic acid signaling, and FGF signaling (Figure 2) [3]. The combined action of these signals at the pre-pancreatic endoderm inhibit the expression of Sonic Hedgehog (Shh), whose expression would normally prevent the acquisition of pancreatic fates[4, 5]. Pdx1 is expressed in this Shh-excluded zone, with its expression coinciding with the outgrowth of dorsal and ventral pancreatic buds. Ptf1a and Pdx1, together with Sox17 and Hb9 are necessary to specify pancreatic fates[6-8]. However, the expression of Pdx1 and Ptf1a demarcate the pre pancreatic endoderm, and with the exclusion of a few glucagon-expressing cells that differentiate during early pancreatic bud formation, Pdx-1 and Ptf1a expressing cells will give rise to all cell types of the mature pancreas (Figure 2). Notch signaling is necessary to enforce pancreatic endodermal fate specification, with the expression of Hairy and enhancer of split (Hes1) restricting the expression domain of Ptf1a to the pre-pancreatic endoderm.

Intrinsic and extrinsic signals are necessary to maintain a sufficient pool of multipotent progenitor cells that will differentiate into the various pancreatic cell types. Extrinsic signals include Isl1, Wnt, BMP, and FGF signals, which originate from the nearby mesenchyme to promote growth and proliferation of the multipotent progenitor cell population[9-14]. Additionally, intrinsic cues from Notch signaling are also essential for progenitor pool maintenance, with the absence of Notch signaling resulting in pancreatic hypoplasia due to premature cell cycle arrest[15-17].

As development progresses, pancreatic progenitor cells acquire distinct cells fates, including islet and acinar fates. This fate specification is dependent on Nkx6 and Ptf1a, with Ptf1a expression marking acinar cells, while Nkx6 expression marks the endocrine and ductal cell populations[18].

Endocrine cell fates are assigned during a process known as the secondary transition. Initiating this process is the transcription factor Neurogenin3 (Ngn3), which is expressed in a short pulse, followed by its subsequent downregulation. The pulsatile expression of Ngn3 is regulated by Hes1, with high levels of Hes1 inhibiting Ngn3 expression(Figure 2). The timing of this Ngn3 pulse is important, with earlier pulses specifying α cell fate, and progressively later pulses specifying β and δ cell fates [19].

Despite being short-lived, this pulse in Ngn3 expression results in the activation of endocrine cell type specific downstream transcriptional activators, including Isl1, Ia1, and Neurod1, that enable terminal differentiation of the different endocrine cell types(α, β, δ, pp, Ɛ) (Figure 2). Neurod1 and Ia1 are co-expressed in the differentiating pancreatic islet, with mutations in Ia1 expression leading to decreased α-cell and β-cell populations, while Neurod1 mutations lead to disorganization in islet structure due to endocrine cell apoptosis, particularly in β-cell populations [20, 21].

Specification of one pancreatic cell type often occurs at the expense of another pancreatic cell population. For instance, the transcription factors Arx and Pax4 function antagonistically to specify different fates in the endocrine cell lineage, with Arx expression restricting cells to α-cell and pp- cell fates, while Pax4 restricts cells to β-cell and δ cell fates

(Figure 2). Mutations in Arx results in a decrease in α-cells while causing a concomitant increase in β-cells and δ cells, while mutating Pax4 increases β-cells while causing an increase in the ghrelin expressing Ɛ cell populations[22, 23].

Following another downregulation of Ngn3 expression, the tertiary transition occurs. During this stage, the different endocrine cell types undergo additional rounds of proliferation and organize into islet structures[24].

Figure 2- Development of the vertebrate endocrine system

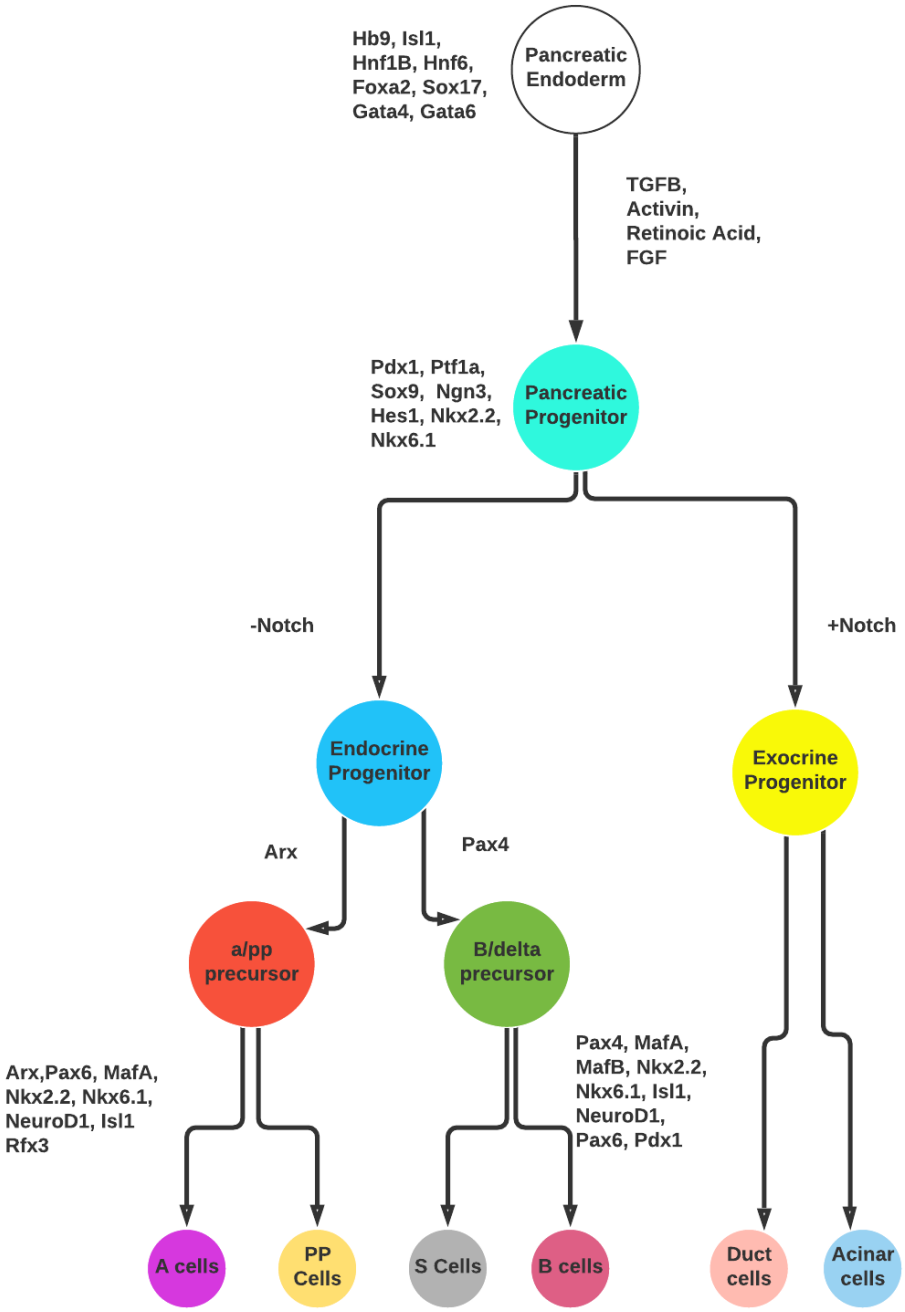

Figure 2: Development of the vertebrate endocrine system - The pancreatic cell lineage from the foregut of the endoderm to various differentiated cell types in the mature pancreas.

REGULATION OF INSULIN PRODUCTION AND SECRETION IN PANCREATIC B-CELLS

Insulin transcript production is primarily dependent on the presence of glucose, with upstream signals from glucose leading to the activation of MAPK pathway component ERK1/2, which activate downstream factors important for insulin gene activation. Glucose action leads to the binding of key transcription factors to the insulin promoter, with many of the identified transcription factors having played earlier roles in β-cell development and differentiation. Characterization of the structure of the insulin promoter in humans has identified elements that regulate insulin mRNA expression and the transcription factors to which they bind (Table 1).

Table 1 - Regulation of insulin transcription in vertebrates

Binding Site	Function
A	Contains binding site for Pdx1 and Isl1
C1	Inhibits insulin expression in response to prolonged exposure of fatty acids by inhibiting MAFA binding
C2	Contains binding site for Pax6
E	Contains binding site for BHLH family of transcription factor NeuroD1/Beta12, which forms a heterodimer with E47 to bind the promoter. Mutations in this site results in massive β-cell apoptosis
Z	Binds Pdx1 and MAFA. Is necessary to activate the A element
CRE	Contains binding sites for members of the CREB/ATF family

Table 1 – Regulation of insulin transcription in vertebrates - Gene expression is regulated by binding of transcriptional activators and repressors to different elements of insulin gene promoter.

In addition to increasing insulin transcription, glucose also increases the stability of insulin mRNA, with stabilization dependent on binding of polypyrimidine tract binding protein and other stabilizing elements to the mRNA 3'UTR. Although changes in insulin gene expression are regulated by nutrient cues, the amount of insulin in circulation is primary regulated at the level of secretion [25]. Glucose is the primary nutrient activating insulin release from pancreatic β-cells. Fatty acids and amino acids can also elicit insulin release, however the amount of insulin released is at much lower levels.

The insulin secretory pathway begins with glucose entering the cell through a Glut-2 transporter. Glucose then undergoes metabolism in the mitochondria to generate increases in β-cell ATP:ADP ratio, with the increase triggering closure of ATP-sensitive potassium channels, plasma membrane depolarization and calcium influx[26-29]. This leads to a number of downstream events that culminate in the SNARE-dependent fusion of insulin-containing secretory granules with the membrane, and subsequent release of insulin into circulation[26].

Insulin secretion occurs in two phases[30, 31]. The first phase consists of the secretion of the readily-releasable pool, which makes up only about 1% of the β-cell's insulin stores, and occurs soon after nutrient sensing. In this phase, insulin vesicles pre-docked at the cell membrane rapidly fuse and release their contents. This first phase can be elicited by nutrient and non-nutrient secretagogues, and occurs about five to ten minutes after glucose sensing[32]. The second phase of insulin secretion however is more sustained, occurs only in response to nutrient secretagogues, and involves substantial cytoskeletal rearrangements to transport of insulin vesicles from intracellular stores to the plasma membrane[33, 34].

REGULATION OF INSULIN-LIKE GROWTH FACTORS

Insulin and Insulin-like growth factors (IGFs) diverged at the base of the vertebrate lineage with vertebrate insulins primarily regulating metabolism, while IGFs primarily regulate growth[35, 36]. There are two IGF genes in vertebrates, IGF I and IGF II, and both signal through an IGF I receptor to mediate their effect on growth[37-39]. Binding of IGF to its receptor triggers the activation of the AKT signaling pathway which feeds into the mTOR, MAPK, and FoxO pathways to promote growth, proliferation, and cell survival[39].

Despite their divergence in vertebrates, limited crosstalk exists between insulin and IGF signaling. Each peptide shows some ability to bind the others receptor, although this binding occurs with lower affinity with their cognate receptors[40]. IGF receptor and insulin receptor can also dimerize to form hybrid receptors that are able to bind either IGF or insulin[41]. Downstream signaling of insulin and IGF are orchestrated primarily through the same pathway; however differences in tissue specificity of receptor expression and time of expression during development govern their distinct functions. For instance, IGF receptors predominate in adipocytes prior to differentiation, and upon differentiation these IGF receptors become downregulated and replaced by insulin receptors[42, 43]. In contrast, differentiated muscle tissue show high enrichment for IGF expression, but very little expression of insulin receptor[43].

IGFs function through both endocrine and autocrine/paracrine mechanisms[39]. The majority of endocrine IGFs in vertebrates are produced in the liver and then secreted into the circulatory system to regulate growth. In addition to their endocrine functions, IGFs are also produced at low levels by almost all cell types. Unlike liver-produced IGFs, these cell-specific IGFs primarily function in an autocrine and paracrine manner to promote growth[42].

Production of IGF primarily occurs in response to Growth Hormone[39]. Growth Hormone is produced in the pituitary, and its synthesis and secretion is induced by a hypothalamus-derived signal mediated by Growth Hormone Releasing Hormone[44, 45]. The levels of IGFs in circulation are stabilized through a feedback mechanism, with elevated circulating IGFs feeding back to the pituitary to inhibit Growth hormone release[44, 45]. Nutritional inputs also play a role in increasing serum IGFs, with IGF secretion being especially sensitive to overall protein levels[46]. IGF secretion can also occur in a nutrient independent manner. Nutrients also indirectly regulate IGF levels through regulation of the insulin pathway, and diseases that decrease insulin, such as Type I diabetes, also result in decreased IGF production[47, 48].

THE DROSOPHILA NEUROENDOCRINE SYSTEM

The *Drosophila* neuroendocrine axis consists of neurons located in the pars intercerebralis, pars lateralis, and the dorsal medial protocerebrum in the brain. Neuropeptides are produced in these neurons and travel up axons to the neurohemal release sites in the ring gland, where they are released into the circulatory system (Figure 3). The *Drosophila* ring gland consists of three different components: the corpora cardiaca neurons, which secrete the hormone glucagon and also serve as the primary neurohemal release site, the corpora allata, which is important for the secretion of juvenile hormone, and the prothoracic gland, which secretes hormone ecdysone during larval molting.

Similar to vertebrates, *Drosophila* possess insulin producing cells (IPCs) that produce and secrete insulin-like peptides in response to nutrient cues[49]. Unlike pancreatic β-cells which have endodermal origins, however, the *Drosophila* IPCs originate from ectoderm[50]. The IPC neuroblasts originate from pars intercerebralis primordium in a region known as the procephalic neuroepithelium (Pdm)[50]. The development of the *Drosophila* neuroendocrine center begins in the head midline dorsomedial procephalic neuroepithelium (Pdm), where prior to neurogenesis, the neuroepithelium loses its sheet-like morphology and starts expressing proneural factors (Figure 4). The neuroepithelium consists of three distinct regions, each demarcated by the expression of a unique transcription factor[50]. The region that will give rise to the IPCs, the pars intercerebralis primordium, is marked by the expression of Chx.

Neighboring regions are the pars lateralis and pars medialis, each marked by the expression of Fas2 and the transcription factor Rx respectively[50].

Within the Pdm neuroepithelium, all cells in the invaginated placode are fated to assume neuroblast identity, with the pars intercerebralis and pars lateralis giving rise to neural stems cells comprising the brain-ring gland complex [50]. The firstborn neuroblast to be specified within the IPC primordium is the IPC neuroblast, uniquely marked by its expression of the transcription factor Dachshund. Neuroblast formation begins with the expression of lethal of scute, a pro-neural factor that is essential for neurogenesis. Asymmetric division of the neuroblast leads to the generation of ganglion mother cells (GMC), with each GMC undergoing additional rounds of cell division to generate the IPC neurons[51]. IPC fate acquisition also coincides with the activation of Notch signaling pathway, with successive delamination of neuroblasts from the epithelial placode coinciding with the activation of the enhancer of split genes, e(spl)m5 and e(spl)m8[51]. The birth of the IPC neuroblast is followed by the delamination of multiple non-IPC neuroblasts. The inhibition of Notch signaling is necessary to ensure that the correct number of IPC neuroblasts are specified, with Notch signaling inhibition causing later born neuroblasts in the placode to assume IPC neuroblast fate[51].

In addition to sharing homologous insulin secretory cell types, Drosophila and vertebrates also share homologies in the expression of glucagon-secreting cell types, with flies possessing corpora cardiaca cells that secrete the hormone AKH[52]. Unlike what is observed in pancreatic β-cells and α-cells however, IPCs and CC cells originate from different germ layers in *Drosophila,* with IPCs originating from the giant expressing head ectoderm, while CC cells originate from Glass-expressing precursors in the head mesoderm[50, 53]. Notch signaling also

plays essential roles in CC cell development, with Notch and downstream factor Tinman acting in concert with transcription factor Daughterless to specify CC precursors from head mesoderm[53]. Similar to its role in maintaining proper numbers of IPC neuroblasts, Notch signaling also regulates CC cell precursor formation. In contrast to the IPC hypoplasia seen in some Notch mutants however, loss of Notch signaling resulted in increased CC cell specification, with Notch mutants showing almost a ten-fold increase in the number of cells assuming CC fate[51, 53].

Figure 3- The Drosophila neuroendocrine system

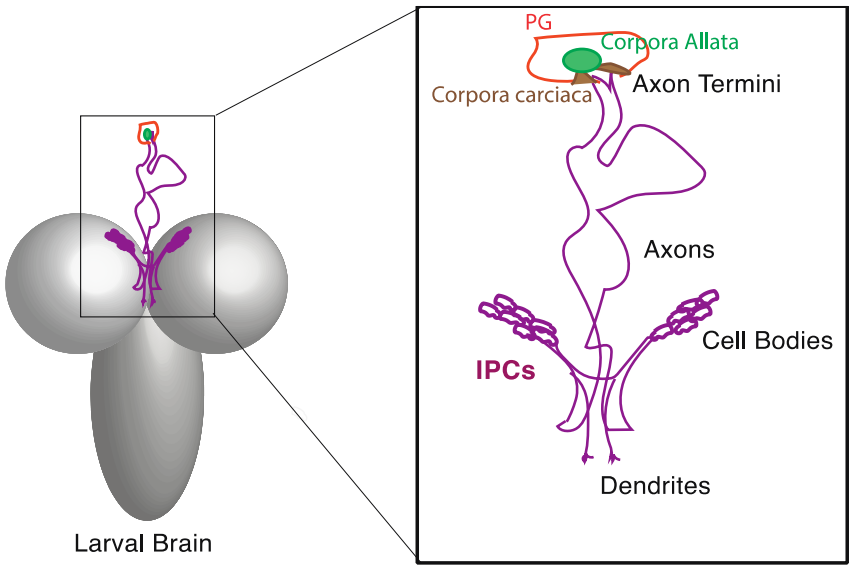

Figure 3: The Drosophila neuroendocrine system – the neuroendocrine control center is located in the pars intercerebralis region of the drosophila brain, and it includes the insulin producing cells (IPCs), and corpora cardiaca cells (CC), which secrete the Drosophila glucagon analog, AKH. The IPC axons project to the corpora cardiaca and the corpora allata in the ring gland, where the hormones are released into the circulatory system[54].

Figure 4- Insulin Producing Cell Development in Drosophila

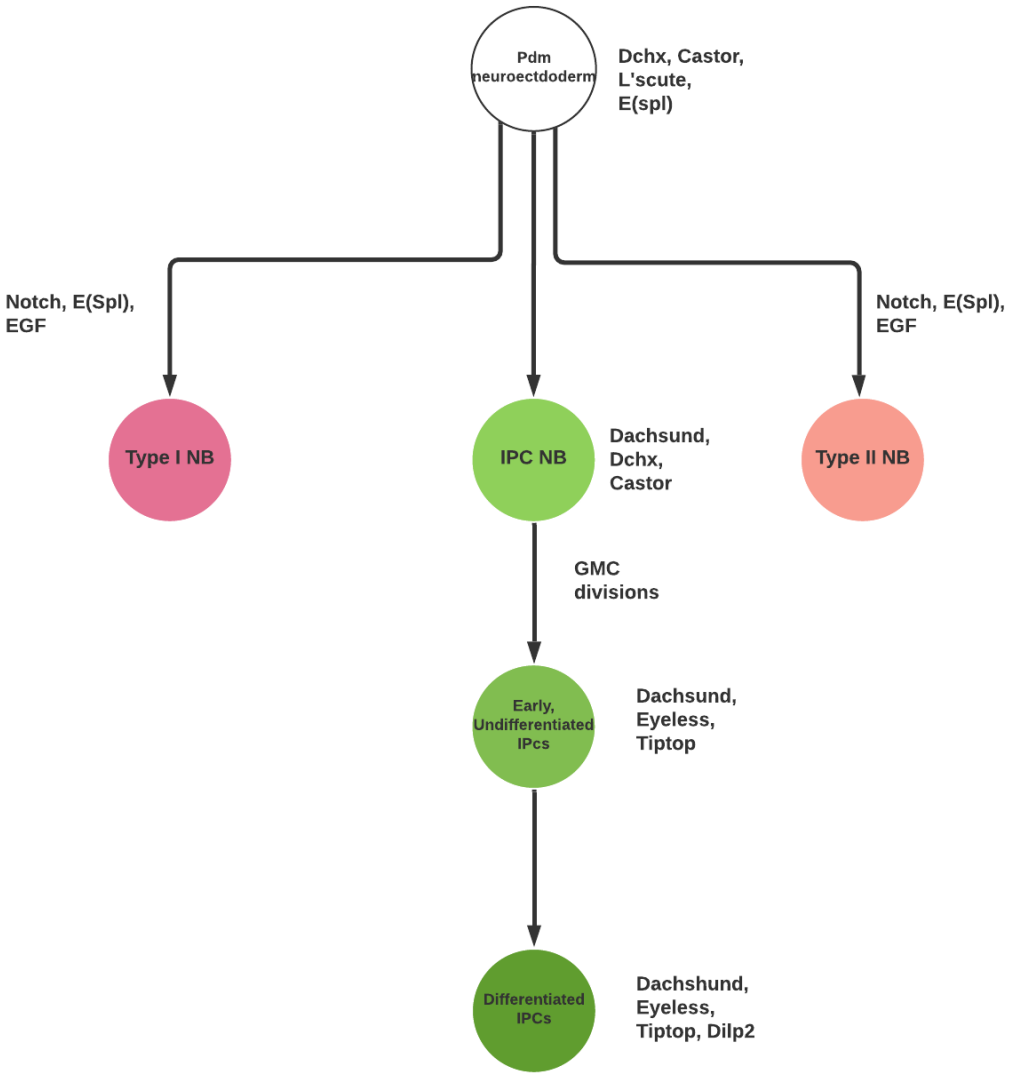

Figure 4: Insulin producing cell development in Drosophila - The development of the Drosophila IPCs from the neuroectoderm of the dorsal medial brain region of the early blastoderm

REGULATION OF DROSOPHILA INSULIN-LIKE PEPTIDE PRODUCTION AND SECRETION

In contrast to the expression of a single insulin gene in humans, *Drosophila* express 8 different Drosophila insulin-like peptpides (Dilp) genes, with the expression of each Dilp regulated independently [55-58]. These Dilps are thought to have partially overlapping downstream functions, with the loss of a certain Dilp often resulting in compensation by another[59]. The primary Dilp expressed in IPCs are Dilp 2,3, and 5, with the expression of Dilp 3 and 5 increasing in response to dietary sugar, while Dilp2 transcription is able to proceed independently of nutrients. Dilp secretion has also been shown to be somewhat independently regulated. For instance, Dilp2 is released in response to amino acids in larval stages, and Dilp 3 can be selectively co-released with AKH in the presence of glucose[60, 61].

A number of studies performed to identify the specific factors binding to Dilp promoters, have identified parallels between pancreatic β-cell insulin regulation and Dilp regulation in IPCs. The Dilp5 promoter regulation has been extensively characterized, and the results show that the transcription factors Dachshund and Eyeless, *Drosophila* homologs of vertebrate Dachs1/2 and Pax6, bind to the Dilp5 promoter and activate its transcription[62, 63]. This result is of note because Pax6 is a known regulator of insulin in vertebrates, with vertebrate Pax6 binding to the C2 element of the insulin gene to promote its transcription (Table 1). Vertebrate Dachs1/2 has not been shown to directly regulate insulin gene expression, however it does play roles in regulating pancreatic β-cell development[64]. Other transcription

factors identified in vertebrates have been shown to regulate Dilp expression. The protein ChREBP in mammals is essential for coordinating carbohydrate status with insulin expression. The *Drosophila* ChREBP ortholog, *Mlx interactor* (Mio), activates the expression of Dilp3 transcripts in IPCs in response to glucose[57]. Additionally, the *Drosophila* ortholog of mammalian *Glis3, Lameduck* (Lmd) have also been shown to activate Dilp2 production[65]. It remains to be determined however, whether this regulation occurs through direct binding of the Dilp promoter or indirectly, and future studies focusing on characterizing the different Dilp promoters and the factors which they bind could result in the identification of additional shared mechanisms of regulation.

The physiology of IPCs differs slightly between adults and larvae. While adult IPCs are nutrient responsive, larval IPCs do not sense nutrients directly. Rather, nutrient sensing occurs through external sources which indirectly regulate IPC responses[60, 66]. The fat body contains a nutrient sensor, *Slimfast*, that senses amino acids and signals to IPCs in a TOR-dependent manner to promote the release of Dilp2[67]. Corpora cardiaca cells nearby IPCs also possess glucose sensing abilities in the larval stages and express the *Drosophila* ortholog of the ATP sensing subunit of the mammalian pancreatic β-cell ATP potassium channel[52]. Adult IPCs however, respond to glucose by expressing a Glut1 protein, possess potassium channels that sense ATP, and express voltage-sensitive calcium channels[66, 68].

Comparing pancreatic β-cells to neurons identifies many similarities[69]. Pancreatic cells demonstrate a similar gene expression profile to neurons during their development[70-73]. In pancreatic β-cell development and in neuronal development, Ngn3 functions downstream of Notch signaling to regulate neuronal fate specification [74, 75]. NeuroD1/Beta2 which is

downstream of Ngn3 in the pancreas, is also necessary for proper expression of the insulin gene and is important for neuronal development [74, 75]. In addition to the expression of a common set of genes, β-cells and neurons also demonstrate shared absence in expression of a gene that inhibits cells from assuming neuronal fate. The NRSF/REST complex is a transcriptional repressor that is only expressed in non-neuronal tissue, and its expression is also absent in pancreatic β-cells[76].

When comparing pancreatic β-cells and IPCs specifically, gene expression profiling of *Drosophila* IPCs identified many similarly expressed genes. Transcription factor FoxO which regulates β-cell proliferation is also enriched in IPCs and has been shown to regulate ILP transcription[77]. Amon, a *Drosophila* homolog of Proconvertase 2, is essential for the processing of proinsulin to insulin[77, 78]. Additionally, many genes regulating dense core vesicle formation and insulin secretion signal transduction are co-expressed between the two insulin secretory systems[77].

INSULIN IN OTHER ORGANISMS

Jellyfish, which arose earlier in the evolutionary tree, have extensive neuronal networks through which they secrete insulin[79]. Gut-based cells that secrete insulin however, are not seen in evolutionary history until *C.elegans*, which contain both gut and brain neurons that secrete insulin in response to dietary changes[80]. In addition to their standard expression domain, almost all *Drosophila* Dilps show expression in the gut. Perhaps these gut insulin-secreting neurons paved the way for the appearance of islet-like structures later in evolution.

At the base of the vertebrate tree, jawless fish show islet-like structures that secrete insulin along with other hormones[81]. A proposed explanation for these similarities is a shared evolutionary origin for β-cells and neurons, with speculation that perhaps the regulatory programs for neuronal development and physiology were co-opted by cells in the gut during the course of evolution[69].

MICRORNAS IN PANCREATIC B-CELLS

In addition to the well-characterized roles of transcription factors in regulating development and function of pancreatic β-cells, evidence has accumulated that microRNAs are embedded in the regulatory networks at various stages of pancreatic development and function (Figure 5). MicroRNAs are a class of short RNA transcripts that regulate gene expression by binding the 3'UTR of target genes, leading to transcript degradation or translational inhibition. Mutating Dicer, an enzyme necessary for generation of all mature microRNAs results in defects in all pancreatic lineages, with the most severe phenotypes seen in the pancreatic β-cell lineage[82]. A potential cause of this defect was proposed to be an increase in the expression of Notch target gene Hes1, along with a downregulation of the Hes1 target gene Ngn3[82].

There are hundreds of distinct microRNA genes expressed in human pancreatic β-cells, and mutations in individual microRNAs impacts processes ranging from β-cell development, differentiation, and maintenance of mature β-cell function (Figure 5). For instance, microRNAs miR-26, miR124a and miR-375, are important for regulating proper islet development[83-85]. MiR-375 is a major player in all stages of pancreatic function. In early pancreatic development,

miR-375 shows highly enriched expression in endodermal pancreatic progenitor cells, and activation of its expression is dependent on key pancreatic differentiation genes, including Pdx1, Ngn3, and NeuroD1[85, 86]. Additionally, both upstream activators and downstream targets are known to play roles in pancreatic progenitor specification and in endocrine cell maturation[85, 86]. Downstream targets of miR-375 include key players in pancreatic development and differentiation, including Gata6, Hnf1B, and Pax6[85]. Increasing the levels of miR-26 in the developing pancreas was shown to increase the number of Ngn3-expressing progenitor cells and to increase the numbers of cells differentiating into β-cells. MiR-124a inhibits islet developmental transcription factors including Foxa2 and Neurod1[87]. In addition to the genes described above, other microRNAs, including *miR-7*, miR-9, miR-15a/b, miR-124a, miR-195 (Figure 5) have been shown to play roles in early pancreatic development.

Like many pancreatic transcription factors that play roles in pancreatic β-cell development, many miRNA genes from pancreatic development are later recycled to regulate the functions of mature pancreatic β-cells (Figure 5). In addition to its role in pancreatic β-cell development, miR-375 inhibits glucose stimulated insulin secretion by targeting a gene necessary for insulin vesicle transport in mature β-cells, thereby decreasing insulin exocytosis[88]. miR-124 regulates secreted insulin by inhibiting ATP-sensitive potassium channels, which are essential for plasma membrane depolarization, and by targeting SNARE proteins and Rab GTPases, which are involved in fusing insulin-containing vesicles to the plasma membrane[89, 90]. MiR-124 also regulates insulin gene production in mature β-cells by targeting the transcription factor Neurod1[87].

Figure 5 - MicroRNAs in pancreatic β-cells

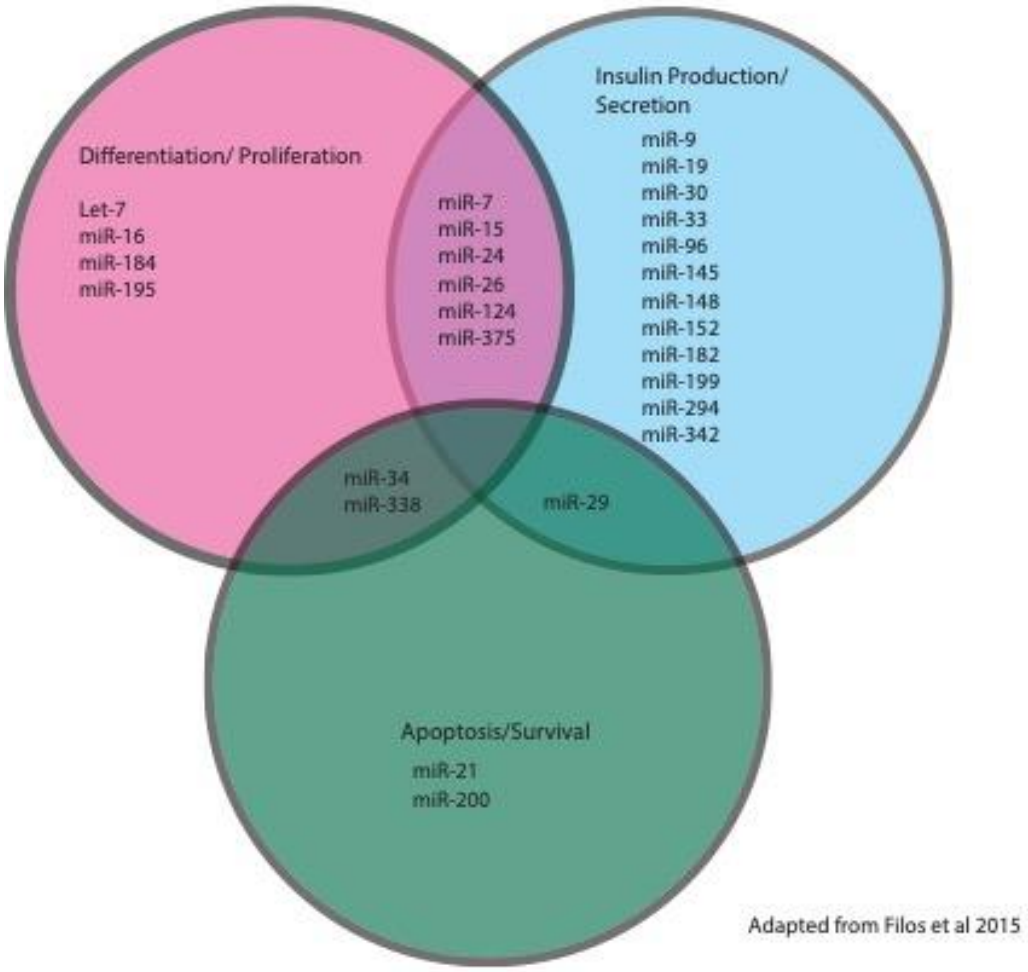

Figure 5: MicroRNAs in pancreatic β-cells – MicroRNAS play diverse roles in pancreatic β-cells including regulating differentiation and proliferation, insulin production and secretion, and β-cell apoptosis and survival. A subset of these microRNAs also play roles in overlapping processes.

MICRORNAS IN DROSOPHILA ENDOCRINOLOGY

Adapted from review article "MicroRNAS in Drosophila melanogaster" published in Seminars in Cell and Developmental Biology 2017.

The neuroendocrine control center of *Drosophila* is located in the brain, in a region known as the pars intercerebralis. Here, Dilps that regulate body growth and metabolism are produced [91]. Dilps are produced and secreted from a cluster of fourteen IPCs which are regulated by various inputs such as nutrient availability and certain neuropeptides. One such neuropeptide, short Neuropeptide F (sNPF) modulates IPC function by binding its receptor, sNPFR on the IPC cell surface. This results in activation of ERK-mediated signaling and stimulation of Dilp production to promote body growth.

Regulation of Dilp production by sNPF is mediated by the miRNA miR-9a [92]. miR-9a modulates body size through its repression of sNPFR1 levels in IPCs. miR-9a mediated sNPFR1 repression results in a decrease in Dilp production and a concomitant decrease in body size (Fig. 6). Interestingly, this interaction is conserved in mammalian insulin endocrinology. The sNPF ortholog NPY modulates insulin production in the β-islet cells of mammals. The miR-9 ortholog represses NPY receptor NPY2R expression in a rat insulinoma cell line [92].

Dilp production is also under the control of miR-14 [93]. miR-14 mutants have decreased levels of Dilps, and mutants show elevated triglyceride stores as a consequence. Additionally, miR-14 mutants have increased sensitivity to starvation as a result of defective mobilization of

energy stores, since a certain level of Dilp production may be necessary for fat mobilization. The transcription factor Sugarbabe is directly targeted by miR-14, and Sugarbabe otherwise inhibits Dilp transcription in IPCs (Figure 6).

Another important hormone in *Drosophila* is the molting hormone ecdysone, which negatively regulates body growth. Dilps stimulate production of ecdysone in the prothoracic gland (PG) of the brain. They do so by inhibiting a miRNA in the PG (Figure 6). The bantam miRNA promotes systemic growth through its inhibition of ecdysone production [94]. However, Dilp inhibit bantam expression in the PG, thus bantam mediates Dilp-dependent expression of ecdysone.

Ecdysone not only triggers molting, but it also inhibits body growth. It does so by its action on the fat body [95]. The fat body is the insect liver, and in addition to metabolism, the fat body also regulates body growth. Fat body miR-8 has been shown to serve as a key link between ecdysone and body growth [96]. Without miR-8 expression in the fat body, ecdysone is unable to repress body growth. miR-8 directly represses expression of U-shaped, which is an inhibitor of PI3K [97]. Since PI3K is a key transducer of Dilp signals in fat body cells, indirect upregulation of PI3K by miR-8 potentiates the response of the fat body to Dilp (Figure 6). However, ecdysone represses the expression of miR-8 in the fat body, thereby antagonizing Dilp-induced signal transduction [96].

The fat body is itself a site of hormone production. Production of several of these factors is down-regulated by miR-8 [98]. Imp-L2 is one of these factors, and it is indirectly down-regulated by miR-8 through miR-8's action on U-shaped (Figure 6). Imp-L2 protein is

secreted by the fat body under starvation conditions, and it binds to and inhibits humoral Dilp [99]. Since Imp-L2 expression is induced by ecdysone [100], it is likely that ecdysone regulation of miR-8 in the fat body is one means by which ecdysone stimulates Imp-L2. In turn, this would antagonize Dilp-induced body growth. However, this mechanism is not sufficient to account for the effect of miR-8 and ecdysone on body growth [98].

Ecdysone also antagonizes juvenile hormone (JH). Pulses of ecdysone trigger metamorphosis, whereas JH acts in the opposing direction to repress metamorphosis. The miR-2 family of miRNAs are involved in this process, with loss of miR-2 resulting in impaired induction of metamorphosis [101]. miR-2 acts by repressing the transcription factor Kruppel homolog-1, which functions downstream of JH. By rapidly clearing Kruppel homolog-1 mRNA in the last larval instar, miR-2 miRNAs ensure that the transition to metamorphosis is able to progress.

Figure 6- MicroRNAs in Drosophila endocrinology

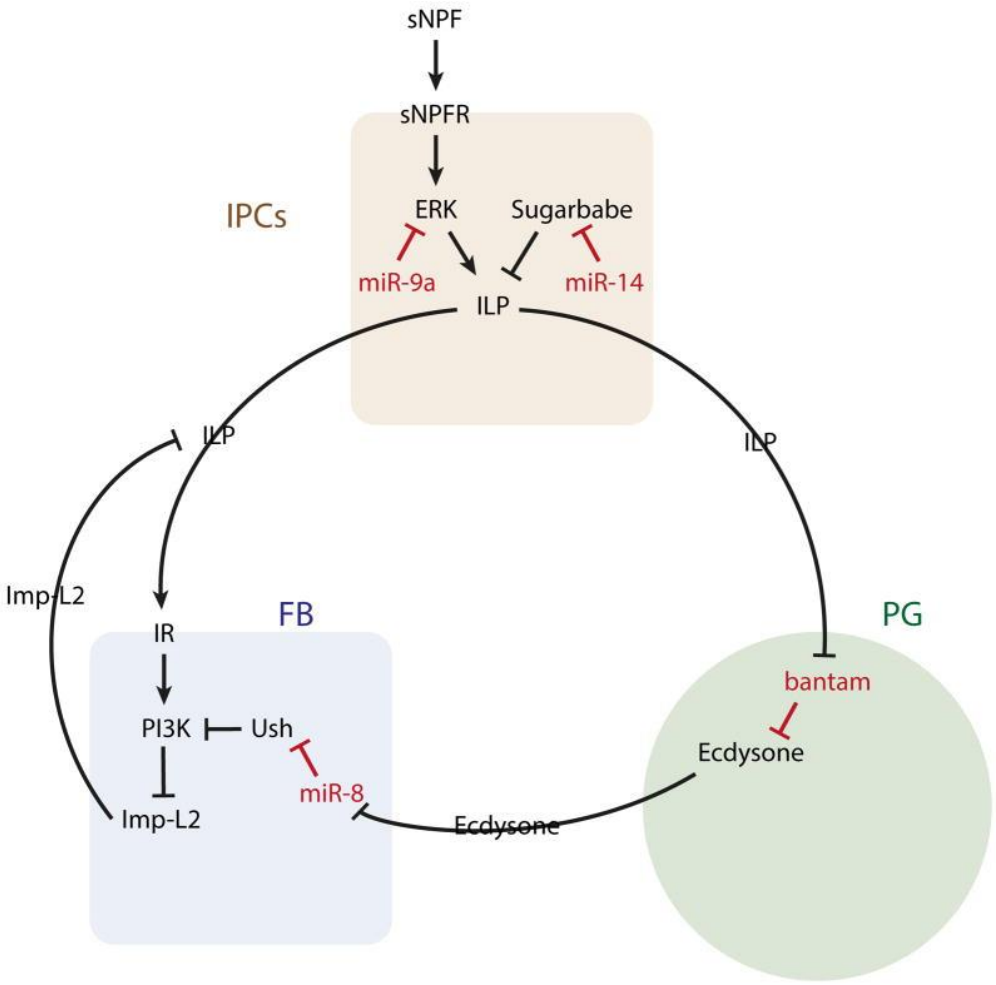

Figure 6: MicroRNAs in Drosophila endocrinology – miR-14 and miR-9 play roles in regulating IPC ILP levels. No other microRNAa have been demonstrated to play roles in regulating drosophila IPC functions, however, the microRNA miR-8 regulates insulin signaling reception, while bantam also play roles in regulates ecdysone levels in the prothoracic gland.

DIABETES, FLYABETES, AND DROSOPHILA AS A MODEL ORGANISM

Adult diabetes is a metabolic disease characterized by defects in insulin production and utilization. Millions of people are diagnosed with this disease worldwide, and the numbers of those afflicted are predicted to steadily increase[102]. Progression of Type II Diabetes involves the interplay between insulin and blood glucose levels, with initial disease stages characterized by insulin resistance and hyperinsulinemia[103]. In more advanced stages of Type II Diabetes, insulin secretory ability becomes further compromised and results in hyperglycemia[104]. The net result is a dysfunction in carbohydrate homeostasis, which if left untreated leads to additional health complications.

Obesity is thought to be the main driving factor for the insulin resistance and the hyperinsulinemia that precedes Type II Diabetes. The widespread availability of high calorie foods coupled with sedentary lifestyles assumed by much of the world fuels much of the current obesity epidemic, and as a result the rates of Type II Diabetes have also increased[105, 106]. Despite the general acceptance of obesity as the main determining factor, however, it is also clear that there are genetic components contributing to disease acquisition and progression. For instance in certain cases, obesity never progresses to full blown Type II Diabetes, while in others, disease onset occurs at a weight that is much lower than would be expected[106]. This suggests genetic components, independent of obesity, that govern disease susceptibility.

Efforts to identify markers governing disease predisposition have led to the insight that a large number of the mutations impact pancreatic β-cell function, with very few of the

identified mutations governing insulin sensitivity[107]. The most consistently identified mutation in Type II Diabetes patients is a mutation in the gene TCF7L2, which encodes a Wnt pathway transcription factor[108-110]. These patients have elevated levels of this protein variant, with elevation leading to impairment in β-cell performance by inhibiting the processing of proinsulin to insulin[111]. These findings suggest that focusing efforts on better understanding of β-cell function could yield notable gains in understanding of how diabetes progression occurs.

Scientists have made use of animal models in order to gain insights on how organism development and metabolism occur. One of the most useful animal models for answering questions in biology is the fruit fly *Drosophila melanogaster*. *Drosophila* possesses many useful traits including small size, fast reproduction time, and a large toolkit for genetic manipulation that have made them a model organism highly favored by scientists[112]. The *Drosophila* genome is comparatively smaller than the vertebrate genome, thereby increasing the likelihood of observing mutant phenotypes due to decreased likelihood of compensation by functionally redundant genes.

Drosophila make excellent model organisms for answering questions pertaining to metabolism. As detailed above and in the coming chapters, the systems governing circulating sugar regulation have been largely conserved in flies, with flies possessing insulin secretory neurons that secrete insulin-like peptides in response to dietary cues[49, 60]. Specific ablation of these neurons results in a significant decrease in the levels of circulating insulin, leading to growth defects and phenotypes seen in humans with diabetes, including elevated circulating carbohydrates and triglycerides[49]. It has also been shown that feeding *Drosophila* a high

sugar diet leads to increased adiposity, insulin resistance and hyperglycemia, with the mechanism of disease acquisition showing similarities to mechanisms leading to Type II Diabetes in humans[113]. These commonalities show that better understanding of insulin regulatory functions in *Drosophila* could lead to better understanding of how this process can become defective in humans, and yield insight on ways to better prevent or treat Type II Diabetes.

UNCOVERING A CONSERVED ROLE FOR *MIR-7* IN INSULIN REGULATION

Although there are thousands of microRNA genes in the human genome, very few show as high a level of conservation as *miR-7*[114]. The mature *miR-7* RNA sequence is identical between humans and *Drosophila*, suggesting very strong selective pressure to maintain gene identity over 600 million years of earth history (Figure 7). *miR-7* is also the most abundantly expressed of all microRNAs in the human pancreas, and shows specific conserved expression in insulin secretory cells across species[115-117] (Figure 7). These observations suggest that *miR-7* may play a conserved role in maintaining the function of insulin secretory cells.

Characterization of *miR-7*'s role in the vertebrate pancreas shows that *miR-7* regulates multiple aspects of β-cell function, including differentiation, proliferation, and secretion[118-120]. In developing β-cells, *miR-7* is activated downstream of Ngn3 and NeuroD1/Beta2, with its expression levels increasing during the course of differentiation[118]. Additionally, specific overexpression of *miR-7* in β-cell and α-cell precursors inhibited differentiation, with *miR-7* overexpression in β-cells and α-cells causing a decrease in the levels of essential endocrine genes including Arx, Pax4, and Pax6 [118]. These cells additionally showed decreased levels of insulin and glucagon.

miR-7 also affects the function of mature pancreatic β-cells. Mice that are mutant for *miR-7* showed increased circulating insulin levels, and mutant animals also had lower circulating glucose levels than wildtype[120]. The converse situation was also shown to hold true, with *miR-7* overexpression decreasing circulating insulin levels and thereby raising blood glucose levels[120]. These animals also had changes in insulin mRNA expression, demonstrating that in

addition to inhibiting insulin secretion, *miR-7* also inhibits insulin at the mRNA level. The effect of *miR-7* on insulin secretory levels mainly occurred through its regulation of the exocytic protein, alpha synuclein (SNCA). Other targets were additionally identified, including cytoskeletal regulators Pfn2, Wipf2, Basp1, and Phactr1. Additionally, *miR-7* insulin gene repression was found to occur through its regulation of β-cell transcription factors Pdx1, Nkx6.1, MafA, Neurod1, and Pax6[120].

Despite *miR-7*'s well-characterized role in mammals, there are still outstanding questions regarding *miR-7*'s conserved functions. While it is known that *miR-7* is expressed in vertebrate insulin secretory cells, it remained to be determined whether it is also expressed in invertebrate insulin secretory cells, and if so, what roles it plays in invertebrate insulin regulatory functions. Given the similarities between vertebrate and invertebrate insulin regulation, and *miR-7*'s high level of sequence conservation across the animal kingdom, I was additionally curious to determine whether *miR-7* functioned through a conserved mechanism to regulate insulin-like peptides. Despite the wealth of information known about microRNAs and vertebrate β-cells, the function of very few microRNAs have been characterized in *Drosophila* IPCs. In my thesis, I have used *Drosophila* to study *miR-7*'s role in insulin regulation, and I have identified a novel, evolutionarily conserved mechanism through which *miR-7* regulates circulating insulin.

Figure 7 -miR-7 expression in vertebrate insulin secretory cells

A

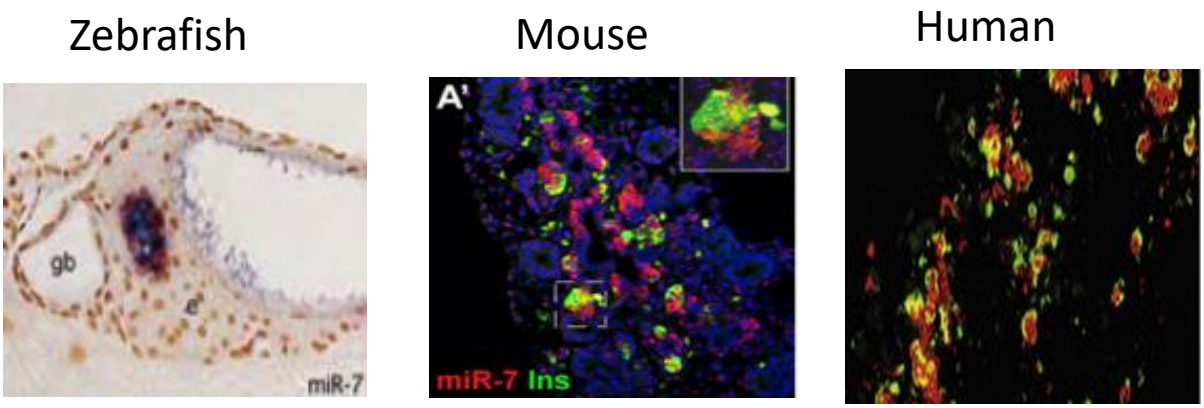

B

D. melanogaster	UGGAAGACUAGUGAUUUUGUUGUU
D. rerio	UGGAAGACUAGUGAUUUUGUUGUU
M. musculus	UGGAAGACUAGUGAUUUUGUUGUU
H. sapiens	UGGAAGACUAGUGAUUUUGUUGUU

Figure 7: *miR-7* expression in vertebrate insulin secretory cells - (A) Left shows 5 day old zebrafish pancreas. e is exocrine pancreas, while i is pancreatic islet, gb gallbladder. *miR-7* expression, purple, is enriched in the zebrafish pancreatic islet. Middle - *miR-7* expression in mouse pancreatic islets. *miR-7* fluorescent in situ hybridization is combined with protein immunofluorescence analysis. *miR-7* expression, red, colocalizes with insulin, green. Right - *miR-7* expression in human pancreatic islets – In situ hybridization of fetal human pancreas. Green shows insulin, glucagon, and somatostatin. Red pseudocoloring is *miR-7* expression. Images from Wienholds et al 2005, Kredo-Russo et al 2012, and Correa-Medina et al 2009. **(B)** Alignment of the mature *miR-7*-5p sequence (5' - 3') from different animal species. Highlighted

in green is the seed sequence. Shown are the *miR-7*a-1 (zebrafish and mouse) and *miR-7*-1 (human) paralogs.

CHAPTER 2: METABOLIC PHENOTYPING OF *MIR-7* MUTANTS

Introduction

The fruit fly *Drosophila melanogaster* has proven to be a useful model to study questions related to insulin/IGF effects on growth and metabolism[49, 121]. In vertebrates, insulins and Insulin-like Growth Factors (IGFs) mediate separate functions. Human insulin is encoded by a single gene, expressed in the pancreatic β-cells, that regulates metabolism in classic insulin-responsive tissue including the adipose, muscle, and the liver [122]. IGFs however are primarily produced in the vertebrate liver with their main roles focused on regulating organismal growth. Humans express two IGF genes, with IGF-1 regulating both pre and postnatal growth, while IGF-2 is primarily active during gestation[123-125].

Insulin is regulated at multiple levels, with the bulk of regulation occurring at the level of its secretion[25]. At this level, the presence of glucose leads to downstream changes that promote the fusion and release of insulin vesicles from the cell membrane [26]. Glucose metabolism also leads to the activation of MAPK pathway components ERK1/2, which activate downstream factors, like PDX-1 and Beta2/NeuroD,1 that play roles in insulin gene transcription[126]. In addition to its role in transcription and secretion, glucose activity in pancreatic β-cells also increases insulin levels by promoting insulin mRNA stability and increasing its translation [127].

Drosophila encode 8 different insulin like peptides, with each of these Dilps performing distinct though somewhat overlapping functions[54]. Unlike vertebrate insulin and IGFs, all Dilps, with the exception of Dilp8, bind to and signal through a single Drosophila Insulin-like receptor[54]. Each Dilp is independently regulated, showing activation by distinct transcription

factors[60, 65, 128]. They additionally demonstrate distinct responses to nutrients, express at different times during development, and demonstrate unique patterns of secretion [49, 58, 129]. Evidence however, also demonstrates some redundancy in their function. For instance, deletion of a Dilp gene often results in a compensatory increase in the expression of other Dilps[59]. Genetic ablation of the IPCs, which removes all Dilps expressed in these neurons (Dilp 2,3,5), results in elevated circulating sugar levels. Overexpression of a single Dilp, Dilp2, is sufficient to rescue this phenotype [49, 129].

Dilp2 is the first of the three core IPC Dilp to be expressed in embryogenesis, with expression starting in early embryos and persisting through adulthood [50, 129]. Of the three IPC Dilps, Dilp2 is the most highly expressed, the most potent regulator of growth, and the most highly related to insulin, with 35% sequence identity[49, 129]. Dilp2 is secreted from larvae from a TOR-dependent fat body-derived signal triggered by amino acid availability[60]. Although Dilp2 expression can increase in response to nutrients, its expression is also nutrient independent in that transcripts in larvae can be continuously produced during times of starvation [130].

Characterization of other Dilps has also yielded insight into their regulation. Dilp1 is expressed in the IPCs in a transient period from early pupal stages to the first few days of adult life[131]. Expression is extended under conditions of reproductive diapause, suggesting a role in regulating growth during conditions of low nutrient intake. Dilp 3 and 5 make up the other Dilps expressed in IPCs, and their expression is dependent on sensing of nutrients[58]. Interestingly, Dilp5 expression is activated by Dachshund and Eyeless, *Drosophila* orthologs of key pancreatic β-cell transcription factors Dachs1/2 and Pax6[63]. Other notable Dilps include Dilp6, which

displays high similarity to IGFs in vertebrates, and is expressed in the fat body, similar to IGF expression in the liver [132]. Dilp8, is thought to be function more similarly to Relaxins in vertebrates, and is the only Dilp that does not signal through the insulin-like receptor (INR)[133].

Insulin's main role is as a regulator of whole body growth and metabolism (Figure 8). Downstream mechanisms of Dilps on growth and metabolism have been largely conserved between *Drosophila* and vertebrates (Figure 9). These signals are initiated by binding to the insulin-like receptor[134]. Signaling occurs through the PI3K signaling cascade, and results in the activation of GSK3, Forkhead protein, and TOR signaling components[134]. Dilp binding to the INR results in receptor autophosphorylation and the phosphorylation of the insulin receptor substrate, Chico, which goes on to activate downstream kinase AKT through PI3K[134, 135]. Mutations in the catalytic subunit of PI3K, DP110 or in the adaptor subunit P60 result in small larvae that are unable to grow past the early third instar larval stage due to an inability of cells to properly proliferate or increase in size[134, 136]. AKT, however, is required in *Drosophila* for cell growth, with loss of function mutants showing smaller cell size relative to wildtype counterparts[137, 138]. Cell number however, is not affected[134, 137, 138].

Downstream of AKT, the insulin pathway feeds in to the conserved TOR signaling pathway through its activation of dS6K[134]. TOR regulates cell growth and proliferation in response to nutrients. Signaling through the INR also inhibits the Forkhead-type transcription factor FoxO and the glycogen synthase kinase GSK3. AKT phosphorylation of FoxO sequesters it in the cytoplasm, thereby inhibiting its downstream functions of adipolysis, gluconeogenesis, and the inhibition of cell growth and survival[139]. GSK3 plays regulatory roles in

glycogenolysis and triglyceride synthesis from fatty acids. In the absence of insulin, GSK3 normally promotes glycogenolysis by phosphorylating glycogen synthase and inhibiting its activity[140]. Inhibition of GSK3 by insulin prevents its kinase activity while simultaneously activating a glycogen synthase dephosphorylase[140]. This permits the buildup of circulating sugars into glycogen, which can be utilized as a fuel source during low nutrient conditions.

The mature *miR-7* sequence is perfectly conserved between *Drosophila* and humans, suggesting strong functional conservation (Fig 5). Moreover, *miR-7* shows conserved expression in neurosecretory cells of invertebrates and vertebrates[141]. While a conserved *miR-7* sequence is present in the *Drosophila* genome, it remains unknown whether *miR-7* is expressed in the fly insulin secretory cells, and whether its insulin secretory function, characterized in mice, is broadly conserved. The following experiments aim to answer these questions and determine whether in addition to regulating vertebrate insulin biology, *miR-7* could also be a regulator of invertebrate insulin-like peptides.

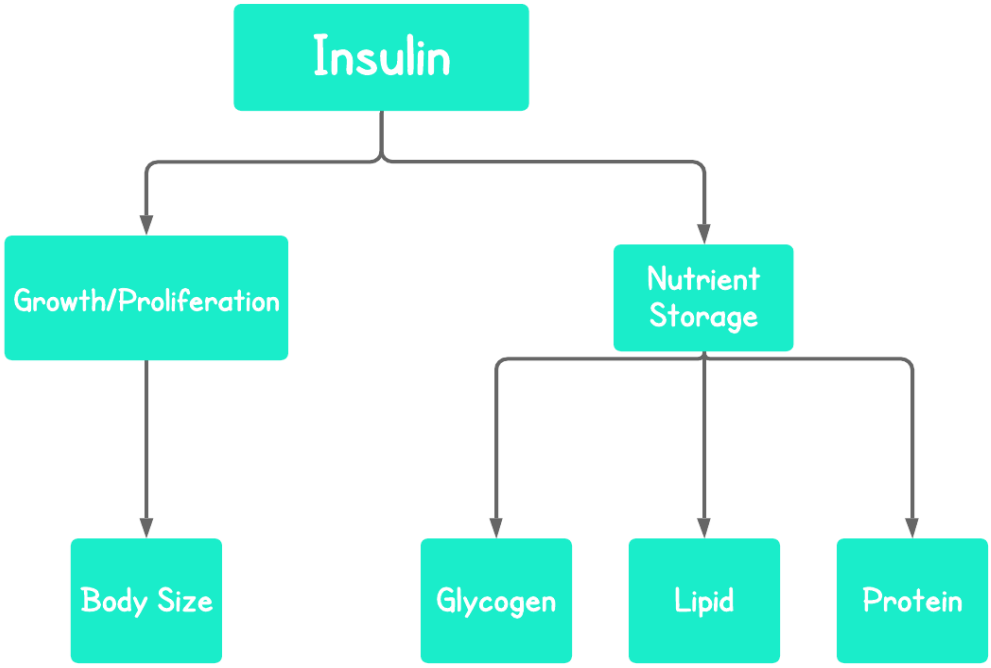

Figure 8: Insulin signaling in growth and metabolism - Insulin action on target tissue results in initiation of nutrient storage through the increased storage of glycogen, lipids, and protein, and in growth and proliferation by increasing body size.

Figure 9 – Conservation of insulin receptor signaling between Drosophila and mammals

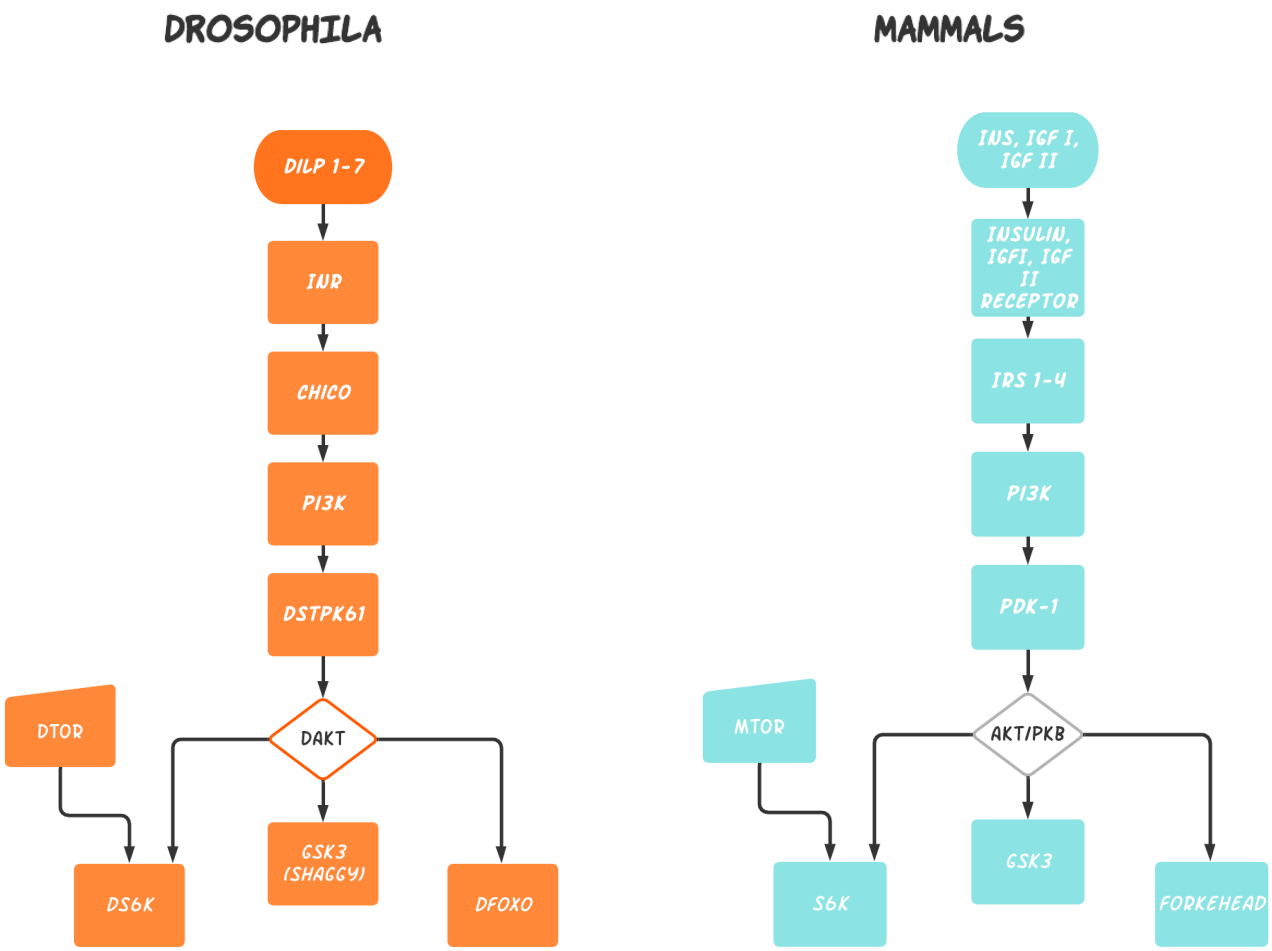

Figure 9 – Conservation of insulin receptor signaling between Drosophila and mammals – Left, insulin receptor signaling pathway in Drosophila. Right, insulin receptor signaling in mammals. Dilps bind insulin-like receptor to initiate downstream signaling cascade through AKT to activate TOR, GSK3 and FoxO. In mammals, insulin, insulin-like peptides, or IGFs bind cognate receptors to initiate a downstream signaling cascade through PI3K/AKT that activates mTOR, GSK3, and Forkhead proteins.

Results

MIR-7 IS EXPRESSED AND ACTIVE IN DROSOPHILA IPCS

Results are published in "MicroRNA *miR-7* Regulates Secretion of Insulin-Like Peptides" in Endocrinology, Feb. 2020.

miR-7 is expressed in insulin-producing cells of vertebrate species[115, 116, 120]. However, it is unclear whether *miR-7* is expressed in the IPCs of *Drosophila*. In order to answer this question, I examined a transgenic reporter gene for *miR-7* expression. This transgene has the transcriptional enhancer of the *miR-7* gene fused to a minimal promoter driving transcription of GFP. The reporter faithfully reproduces the expression pattern of *miR-7* in various tissues of the fly [142]. The transgene showed clear expression in the larval brain, as evident by nuclear-localized GFP fluorescence. To mark the location of the IPCs, I co-expressed membrane-bound RFP specifically in IPCs using the *Dilp2* gene promoter to drive expression. The IPCs occupy a stereotyped position in the larval brain with seven cells residing on either the left or right hemisphere of the brain (Figure 3). Moreover, IPC structure is highly organized and coordinated. This organization could be visualized with the membrane RFP marker (Figure 10). Clearly, the IPCs were labeled with nuclear GFP, suggesting that the *miR-7* enhancer is active in IPCs. To further validate our conclusion, I examined GFP expression from a reporter gene in which two binding sites for bHLH transcription factors were mutated in the enhancer. These binding sites are essential for *miR-7* expression in other tissues of *Drosophila* [142]. The mutant

enhancer was completely inactive in the larval IPCs (Figure 11). Thus, the *Drosophila miR-7* gene requires bHLH factors to augment *miR-7* expression in IPCs. This is comparable to the requirement of the bHLH factor *NeuroD/Beta2* for *miR-7* transcription in mouse β-cells [143].

Figure 10 - miR-7 is expressed in Drosophila IPCs

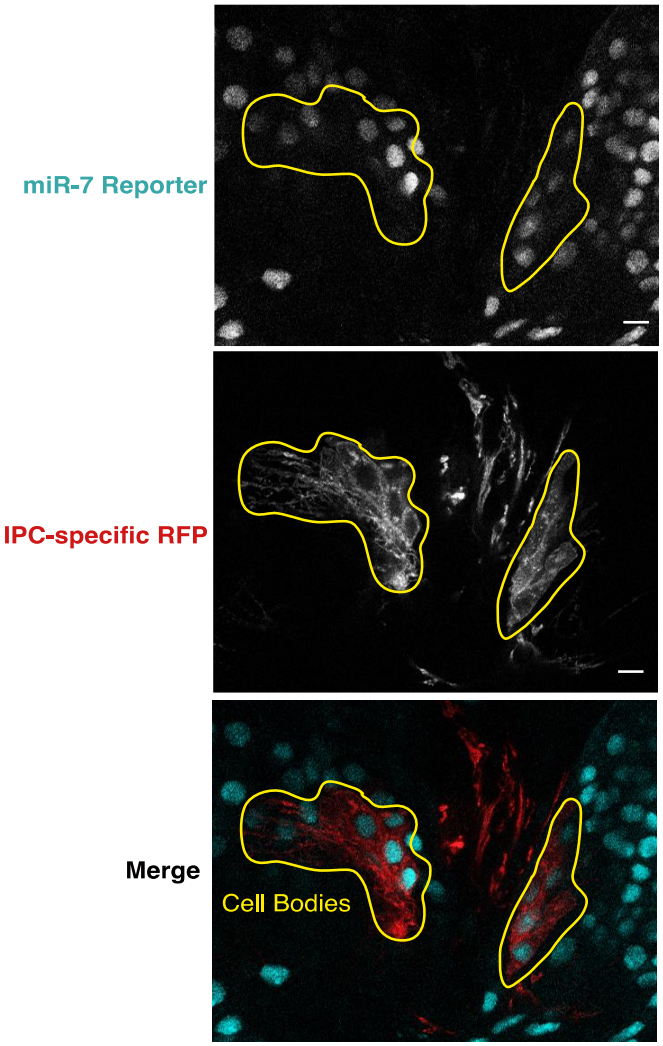

Figure 10: *miR-7* is expressed in *Drosophila* IPCs - Transgene reporter of *miR-7* enhancer activity as reported by nuclear GFP. Two clusters of IPC cell bodies are specifically highlighted by RFP fluorescence in the larval brain.

To demonstrate that *miR-7* RNA is functionally active in IPCs, I used a transgenic sensor for *miR-7* silencing activity [144]. Transgenic mRNA is transcribed ubiquitously in all cells, and it contains two perfect binding sites for *miR-7*. If *miR-7* is loaded into the miRNA Induced Silencing Complex (miRISC), it inhibits the synthesis of the GFP protein product of the transgene in that cell. Thus, reduction of GFP fluorescence is an indicator of *miR-7* silencing activity. The *miR-7* sensor showed weak GFP expression in larval IPCs (Figure 11). As a control, a transgene sensor lacking *miR-7* binding sites was also examined for GFP expression in IPCs. As expected, the control sensor gave strong ubiquitous GFP expression in larval IPCs (Figure 11). Thus, *miR-7* is not only expressed but is functionally active in the IPCs of growing *Drosophila*.

To further validate our conclusion, we examined GFP expression from a reporter gene in which two binding sites for bHLH transcription factors were mutated in the enhancer. These binding sites are essential for *miR-7* expression in other tissues of *Drosophila*40. The mutant enhancer was completely inactive in the larval IPCs (Figure 12). Thus, the *Drosophila miR-7* gene requires bHLH factors to augment *miR-7* expression in IPCs. This is comparable to the requirement of the bHLH factor NeuroD/Beta2 for *miR-7* transcription in mouse β-cells [143].

Given the IPCs role in responding to nutrients, I wondered whether the *miR-7* transcriptional enhancer activation would be nutrient-dependent. Feeding or 24 hour starved early wandering third instar larval brains were imaged to determine how nutrients affected enhancer expression (Figure 13). No difference was observed between the two groups, suggesting that enhancer activation is not dependent on nutrients.

Figure 11 - miR-7 is active in Drosophila IPCs

Figure 11: *miR-7* is active in Drosophila IPCs - Transgenic sensors expressing GFP under constitutive promoter control. Right, a sensor containing two perfect binding sites for *miR-7* in its 3'UTR. Left, a sensor lacking such binding sites. Each image shows two IPC clusters from a larval brain, marked by RFP fluorescence. For panels C - E, anterior is top.

Figure 12: Atonal activates the miR-7 enhancer

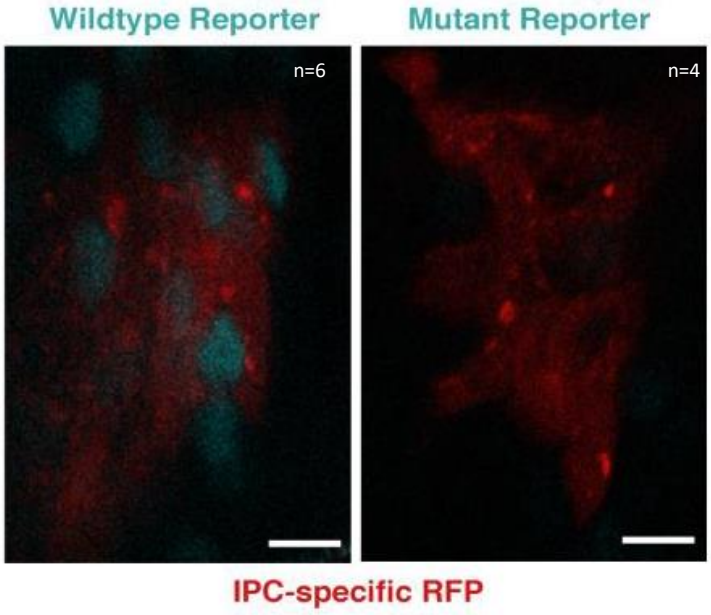

Figure 12: Atonal activates the *miR-7* enhancer- An IPC cluster expressing the GFP reporter that either contains a wildtype *miR-7* enhancer or a mutant enhancer in which two bHLH binding sites are altered. Scale bar = 7.6 µm.

Figure 13 - miR-7 enhancer is not glucose responsive

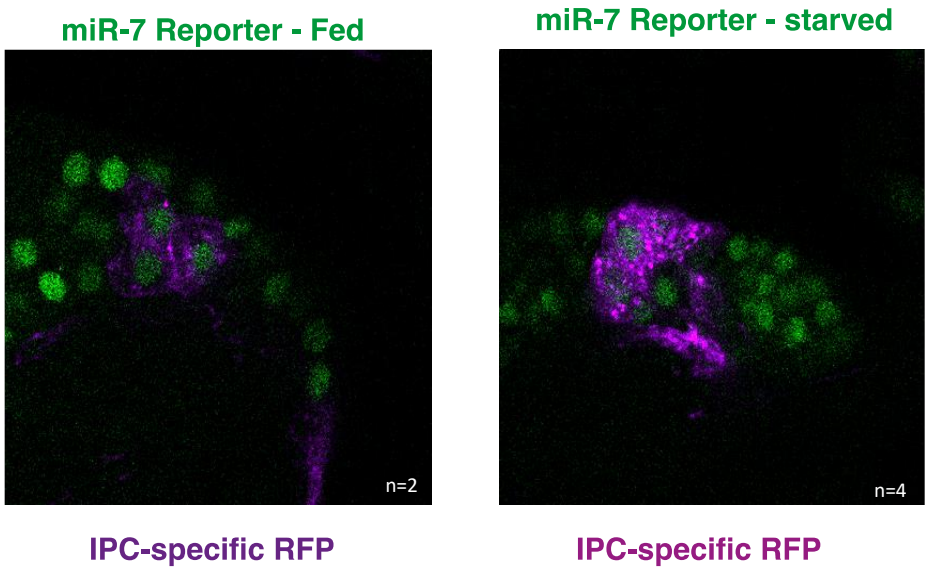

Figure 13: *miR-7* enhancer is not glucose responsive - *miR-7* enhancer expression in Drosophila IPCs. Fed and starved wandering 3rd instar larvae IPCs were imaged to determine nutrient dependency of enhancer expression. Green indicates GFP expression under the control of the *miR-7* enhancer. Purple indicates Drosophila IPCs.

IPC-SPECIFIC *MIR-7* REGULATES BODY WEIGHT AND METABOLITE LEVELS

Growth in *Drosophila* is facilitated by the IPCs in the larval brain. I wondered if *miR-7* plays a role in IPC regulation of growth. Therefore, I made gain-of-function and loss-of-function perturbations of *miR-7* specific to IPCs and not to other cells of the body. I reasoned that since *miR-7* is expressed in many tissues [142], classical *miR-7* mutations might produce confounding effects not directly related to IPC function. I overexpressed *miR-7* specifically in IPCs by combining *Dilp2-Gal4* and *UAS-miR-7* transgenes in animals. Since Gal4 is only present in IPCs due to the *Dilp2* gene promoter, *miR-7* is only overexpressed in these cells. I weighed such animals when they reached adulthood, and observed a decrease in mean body weight compared to wildtype siblings (Figure 14). Ablation of all larval IPCs also results in smaller adults [49]. Ablation is made possible by expressing the pro-apoptotic gene *Reaper* in IPCs using *Dilp2-Gal4*, causing the death of all IPCs. I compared the effects of *miR-7* overexpression with IPC ablation by *Reaper*. The effect of *miR-7* overexpression on adult body weight was less potent than the effect of IPC ablation on body weight (Figure 14).

IPCs primarily regulate adult body size by affecting the growth rate during the juvenile phase of the life cycle [49]. To determine whether *miR-7* regulates larval growth, I weighed animals at the larval-to-pupal molt. As observed in adults, *miR-7* overexpression caused a decrease in body size at this stage (Figure 15).

Figure 14 - miR-7 regulates adult body weight

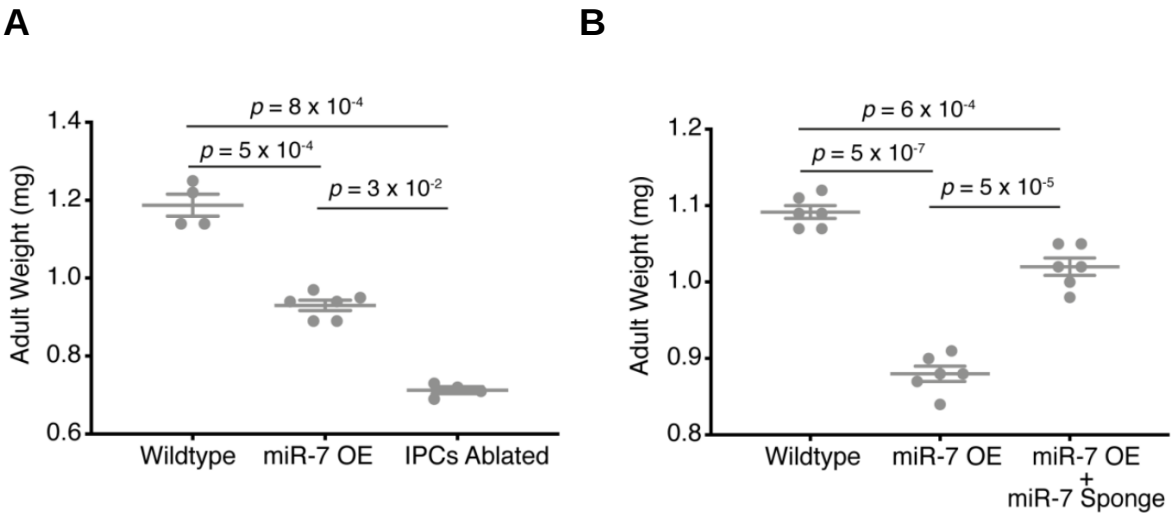

Figure 14 - *miR-7* regulates adult body weight- (A) Mean adult weight of females that have *miR-7* overexpression (OE) in IPCs or have had their IPCs ablated. Each condition is paired with a wildtype control line that contains the *Dilp2-Gal4* driver used in each experiment. **(B)** Mean adult weight of females that have *miR-7* overexpression (OE) compared to wildtype. One set of *miR-7* OE animals also had the *miR-7* Sponge co-expressed in their IPCs.

To generate a loss-of-function perturbation, I inhibited *miR-7* by overexpressing a *miR-7* sponge RNA specifically in IPCs. Sponge RNAs contain partially complementary binding sites to a miRNA of interest, and are produced from transgenes within cells [145]. When overexpressed, sponge RNAs sequester the miRNA of interest and titrate it away from its natural targets. The *UAS-miR-7 sponge* transgene expresses mRNA with ten tandem copies of a sequence complementary to *miR-7* inserted in the 3' UTR [145]. To confirm the potency of the *miR-7* sponge, I co-expressed the sponge along with *UAS-miR-7* in IPCs using *Dilp2-Gal4*. This largely neutralized the effect of *miR-7* overexpression on body weight (Figure 14). When I expressed just the *miR-7* sponge alone in IPCs, there was a small but significant increase in body weight of animals at the larval-to-pupal molt (Figure 15). Thus, both loss-of-function and gain-of-function experiments indicate that IPC-specific *miR-7* inhibits growth of *Drosophila*.

One possible role for *miR-7* in IPCs might be for their development and survival. If so, I predicted that *miR-7* mutants would display an abnormal number or morphology of IPCs. However, null *miR-7* mutants and *miR-7* overexpression mutants had the normal number and arrangement of IPCs (Figure 15).

Figure 15 - miR-7 regulates larval body weight

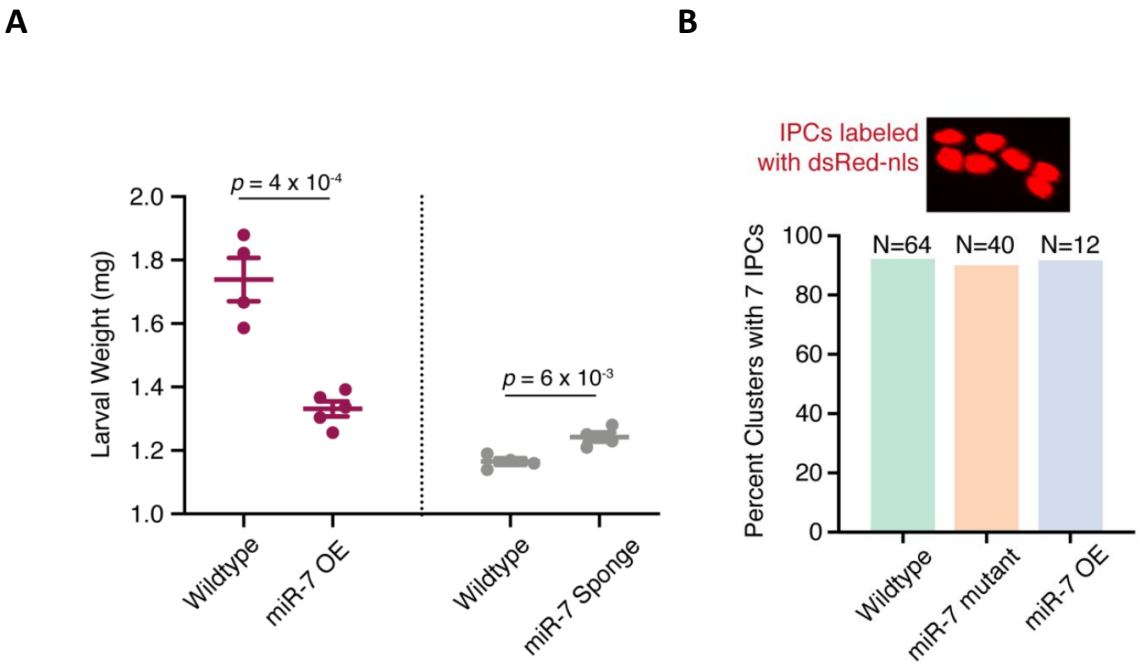

Figure 15 - *miR-7* regulates larval body weight- (**A**) Mean weight of female larvae at the pupal molt that have *miR-7* overexpression (OE) or the *miR-7* Sponge expressed in IPCs. Each condition is paired with a wildtype control line that contains the *Dilp2-Gal4* driver used in each experiment. Different *Dilp2-Gal4* drivers affect body weight on their own, which requires rigorous pairing for controls. (**B**) Shown on top is nuclear dsRed fluorescence in IPCs within one larval brain cluster. Note there are seven nuclei. At bottom is the percent of larval brain clusters having seven IPCs from animals with different genotypes. Number of scored clusters range from 12 to 64. A Chi-Square test on the data showed that none of the treatments had significantly different percentages (p = 0.93). For panels A - C, error bars represent the standard error of the mean. *P* values are derived from unpaired two-tailed student T-tests.

Growth is controlled by the balanced utilization and storage of carbohydrates and lipids. Impaired insulin signaling in diabetic patients is characterized by fasting hyperglycemia. Late third instar *Drosophila* larvae undergo cycles of feeding and fasting as they prepare for the pupal molt. Fasting animals can be easily identified by their clear digestive systems when given colored food. I extracted hemolymph from fasting late third instar larvae and measured their circulating sugar levels. Insects have two types of carbohydrates in circulation: glucose and trehalose. Glucose is obtained from food sources, while trehalose (the disaccharide of glucose) originates from the fat body, and is the primary sugar consumed by cells. Although knockdown of *miR-7* in IPCs did not have a significant effect on circulating sugar levels, overexpression of *miR-7* in IPCs caused an increase in circulating sugars (Figure 16). Inhibition of Dilp expression or ablation of IPCs generate similar effects on circulating sugars, however overexpression of *miR-7* results in an effect that is half as severe as genetically ablating the IPCs [49, 59].

The storage of fat in insects is primarily in the form of triglycerides. The ratio of body triglyceride to protein is a measure of relative fat storage in *Drosophila*. I compared this ratio between *miR-7* overexpressing and wildtype larvae. There was a significant increase in normalized triglycerides when *miR-7* was overexpressed in IPCs (Figure 17). This phenotype is also observed when adults lack any IPCs [121]. Conversely, expression of *miR-7* sponge RNA in IPCs caused a decrease in total triglycerides (Figure 17). These effects were exerted on non-circulating triglycerides since there was little or no difference in circulating triglyceride levels in the different genotypes (Figure 17). Thus, both loss-of-function and gain-of-function experiments indicate that *miR-7* stimulates the storage of fats in growing larvae.

Figure 16 - miR-7 regulates circulating sugars

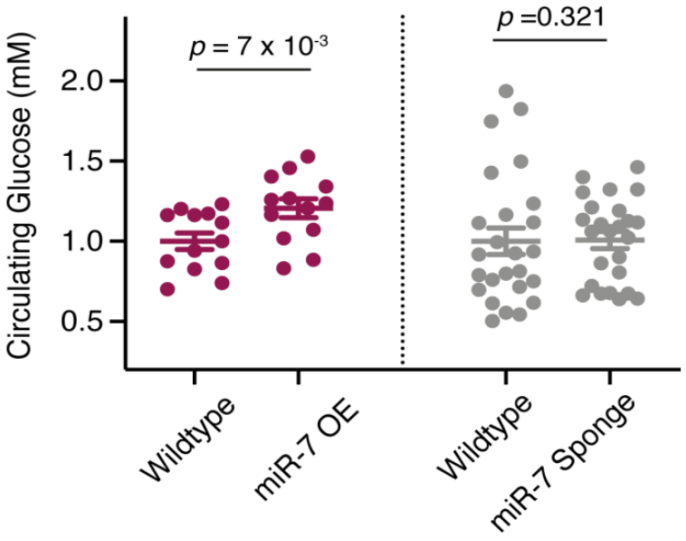

Figure 16 - *miR-7* regulates circulating sugars- Mean concentration of glucose (monosaccharide plus trehalose disaccharide) in larval hemolymph from animals that have *miR-7* overexpression (OE) or the *miR-7* Sponge expressed in IPCs. Each condition is paired with a wildtype control line that contains the *Dilp2-Gal4* driver used in each experiment.

Figure 17 - miR-7 regulates total body triglycerides

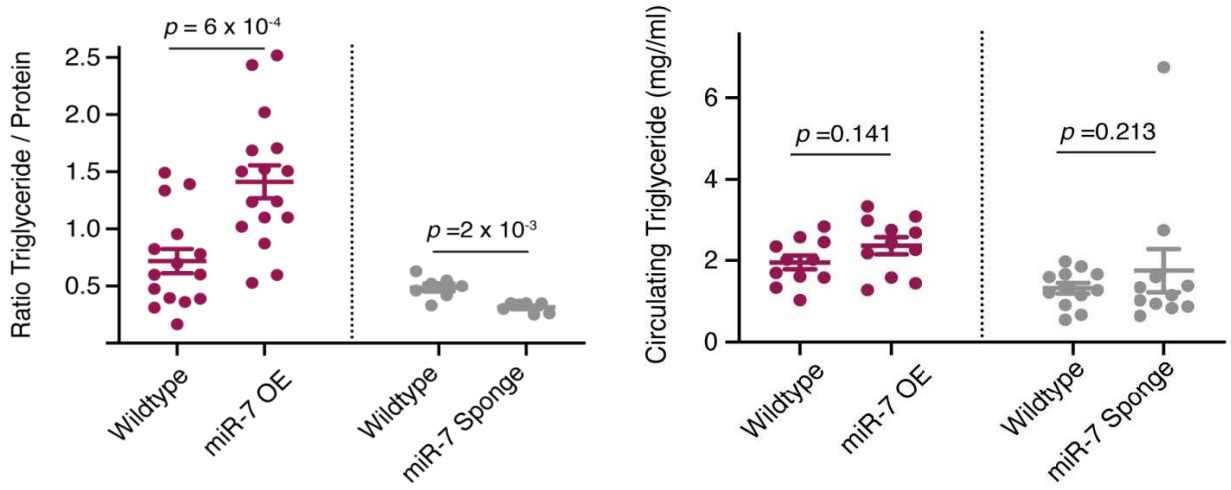

Figure 17 - *miR-7* regulates total body triglycerides- Average ratio of total body triglyceride to protein (w/w) in larvae that have *miR-7* overexpression (OE) or the *miR-7* Sponge expressed in IPCs. Each condition is paired with a wildtype control line that contains the *Dilp2-Gal4* driver used in each experiment. (**C**) Mean concentration of triglyceride in larval hemolymph from animals that have *miR-7* overexpression (OE) or the *miR-7* Sponge expressed in IPCs. Each condition is paired with a wildtype control line that contains the *Dilp2-Gal4* driver used in each experiment. Error bars represent the standard error of the mean. *P* values are derived from unpaired two-tailed student T-tests.

MIR-7 INHIBITS DILP SYNTHESIS AND RELEASE

miR-7's effects on fat stores, circulating sugars, and growth suggest that it might negatively regulate Dilps within IPCs. A genomic transgene containing the *Dilp2* transcription unit and regulatory sequences is sufficient to functionally replace the loss of the endogenous *Dilp2* gene[65]. Moreover, this transgene has been modified to place epitope tags fused to the Dilp2 product. Like insulin, Dilp2 is composed of A-chain and B-chain peptides linked via disulfide bonds. With a FLAG tag fused to the amino-terminus of the A chain and an HA epitope fused to the carboxy-terminus of the B chain, the resulting product is normally processed, secreted, and fully functional[65]. This *Dilp2HF* transgene enabled me to monitor both mRNA and peptide expressed from the IPCs. First, I asked whether *Dilp2HF* mRNA expression changed as a result of *miR-7* perturbation. *Dilp2HF* mRNA abundance was measured in whole brains of late third instar larvae by RT-qPCR. Sponge-mediated knockdown of *miR-7* resulted in an increase in *Dilp2HF* mRNA levels (Figure 18). Conversely, overexpression of *miR-7* decreased *Dilp2HF* mRNA abundance by three-fold (Figure 18). Thus, *miR-7* represses *Dilp2* mRNA levels.

Figure 18 - miR-7 inhibits Dilp2 synthesis

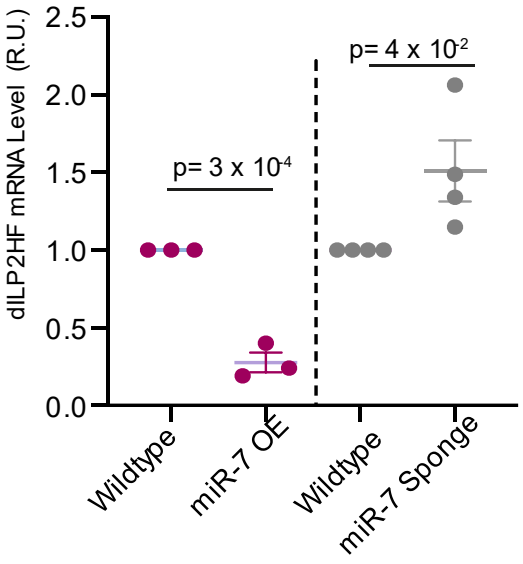

Figure 18 - *miR-7* inhibits Dilp2 synthesis- Normalized levels of *Dilp2HF* mRNA in larval brains from animals that have *miR-7* overexpression (OE) or the *miR-7* Sponge expressed in IPCs. Each condition is paired with a wildtype control line that contains the *Dilp2-Gal4* driver used in each experiment. Measurements made by RT-qPCR are presented in relative units.

To determine if these effects were also exerted at the peptide level, I performed an ELISA assay, which can accurately measure Dilp2HF peptide ranging from 40 attomoles to 4 femtomoles. I observed a two-fold increase in Dilp2HF peptide in larval brains when *miR-7* was knocked down by the sponge (Figure 19). Surprisingly, I saw that Dilp2HF peptide levels also increased when *miR-7* was overexpressed in IPCs, even though mRNA levels decreased (Figure 19).

Therefore, I measured the levels of Dilp2HF peptide in circulation. Knocking down *miR-7* in IPCs elevated circulating Dilp2HF levels consistent with its effects on brain Dilp2HF (Figure 19). Strikingly, *miR-7* overexpression decreased the levels of circulating Dilp2HF (Figure 19). Thus, when *miR-7* was overexpressed in IPCs, stored brain Dilp2HF rose but circulating levels dropped. This suggested that *miR-7* might inhibit the release of Dilp2HF from IPCs, thereby accounting for a buildup of stored Dilp2HF and a drop of Dilp2HF in circulation.

Another method to assess IPC Dilp2 is through visualization with antibodies. I hypothesized that the secretory defect for Dilp2 visualization in IPCs might correspond to changes in its localization in IPCs. Dilp2HF was expressed in animals coexpressing a membrane-localized mCD8-RFP in the IPC cell membranes. No clear difference in Dilp localization could be visualized by IPC *miR-7* knockdown (Figure 20). *miR-7* overexpression however resulted in ILP accumulation in IPCs. This accumulation seemed to be particularly prominent at the ILP release sites (Figure 20). Taken together, these results suggest that *miR-7* is inhibiting secreted ILPs from IPCs.

Figure 19 - miR-7 inhibits circulating Dilp2HF

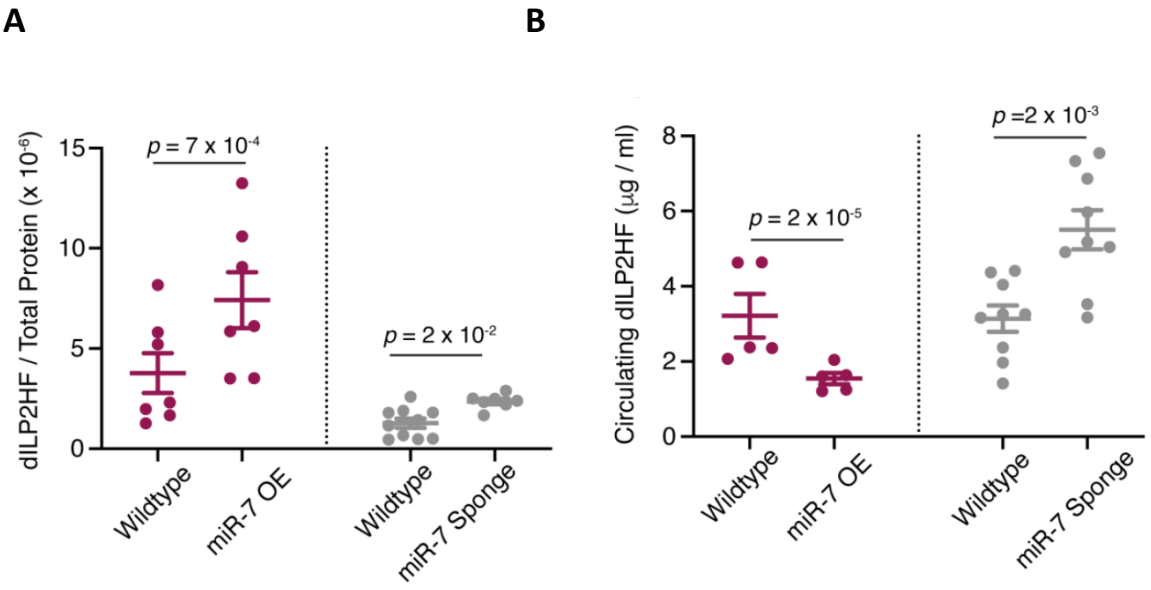

Fig 19: *miR-7* inhibits circulating Dilp2HF - (**A**) Fraction of total brain protein that is Dilp2HF peptide (w/w) in larvae that have *miR-7* overexpression (OE) or the *miR-7* Sponge expressed in IPCs. Each condition is paired with a wildtype control line that contains the *Dilp2-Gal4* driver used in each experiment. Different *Dilp2-Gal4* drivers affect Dilp2HF levels on their own, which requires rigorous pairing for control. (**B**) Concentration of Dilp2HF peptide in larval hemolymph from animals that have *miR-7* overexpression (OE) or the *miR-7* Sponge expressed in IPCs. Each condition is paired with a wildtype control line that contains the *Dilp2-Gal4* driver used in each experiment. Error bars represent the standard error of the mean, and *p* values are derived from unpaired two-tailed student T-tests.

Figure 20 – Visualization of Dilp2HF in IPCs

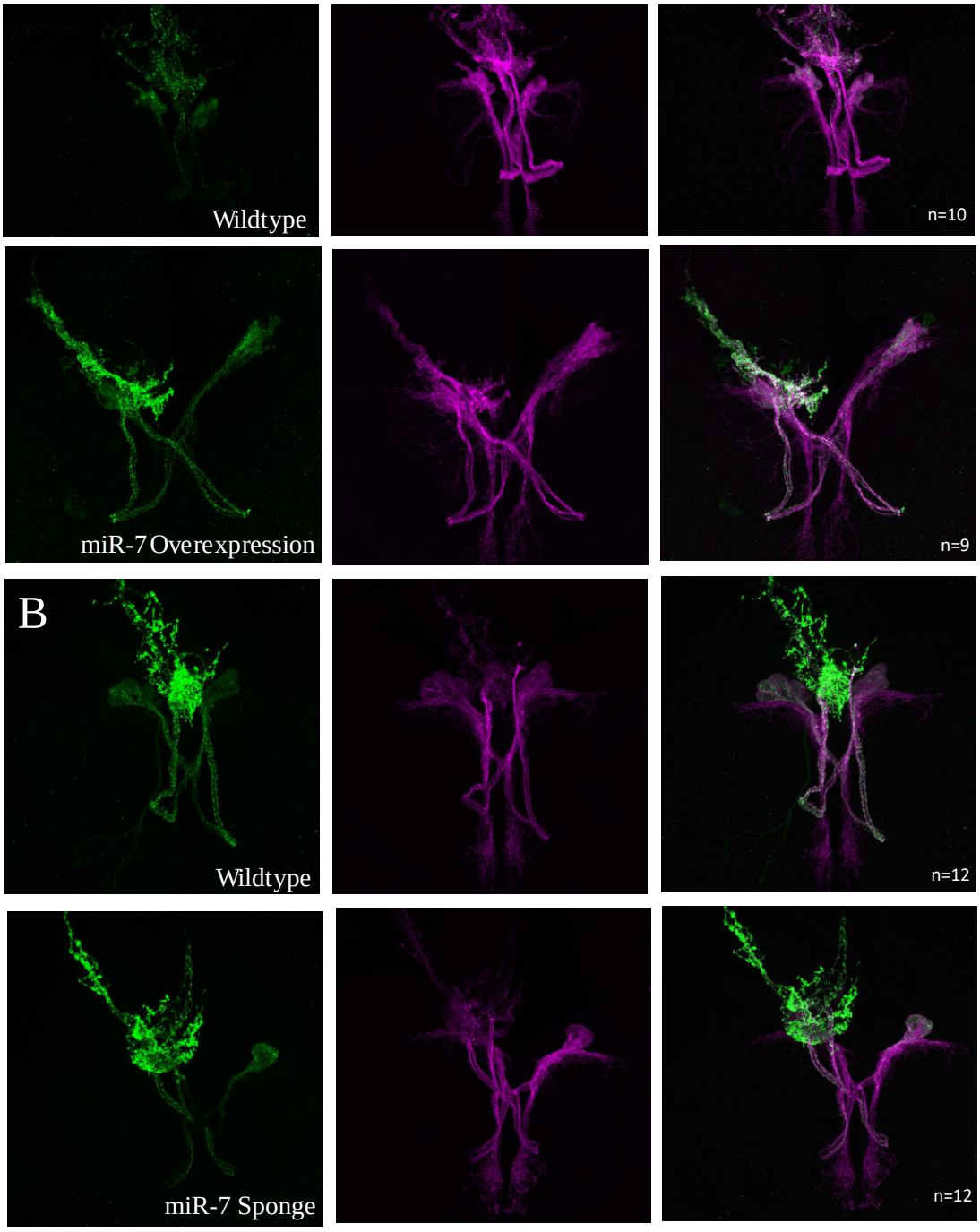

Figure 20 – Visualization of Dilp2HF in IPCs- Image is of Dilp2HF localization in IPCs of *miR-7* overexpression or *miR-7* knockdown wandering third instar larvae. Each condition is paired with a wildtype control line that contains the *Dilp2-Gal4* driver used in each experiment. Left - Green stain marks IPC Dilp2HF localization. Dilp2HF animals express a form of Dilp2 that has been

tagged with FLAG and HA. Antibody staining against HA is used to visualize tagged Dilp2HF. Middle - purple stain is a membrane localized CD8 RFP expressed under the control of a Dilp2gal4 driver. This marks the IPC cell membrane. Right – merge of Dilp2HF and IPC membrane. Each condition is paired with a wildtype control line that contains the *Dilp2-Gal4* driver used in each experiment. **(A)** Wildtype (top) and *miR-7* overexpression **(B)** Wildtype and *miR-7* sponge.

My results suggest that *miR-7* inhibits body growth, and *miR-7* also inhibits Dilp2 synthesis and release from IPCs. I wondered if the effect of *miR-7* on Dilp2 was responsible for its effect on growth. To test this idea, I overexpressed Dilp2 in IPCs that also overexpressed *miR-7* (Figure 21). The body weight of such individuals was partially rescued from the *miR-7* effect. Thus, Dilp2 at least partly mediates the effect of *miR-7* on growth. One possible explanation for the partial rescue is that Dilp2 overexpression does not necessarily alleviate the impact *miR-7* has on Dilp2 release from the IPCs.

Figure 21 - Partial rescue miR-7 OE adult weight by Dilp2 overexpression

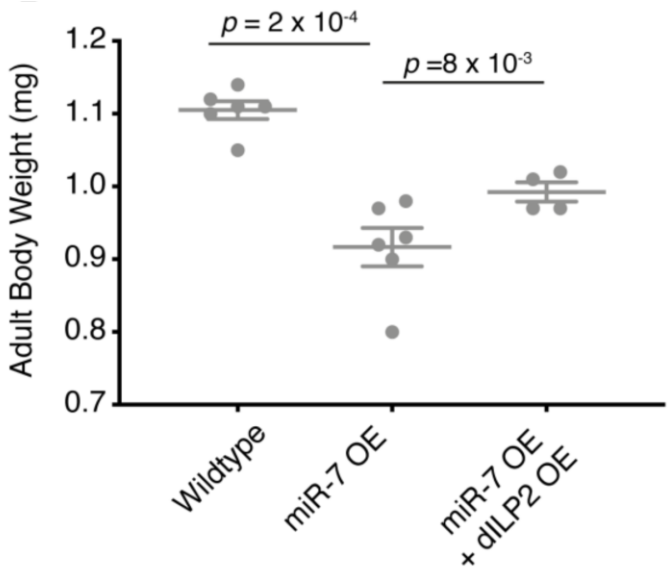

Figure 21 - Partial rescue *miR-7* OE adult weight by Dilp2 overexpression- Mean adult weight of females that have *miR-7* overexpression (OE) compared to wildtype. Each condition is paired with a wildtype control line that contains the *Dilp2-Gal4* driver used in the experiment. One set of *miR-7* OE animals also had Dilp2 overexpressed in their IPCs. Error bars represent the standard error of the mean, and *p* values are derived from unpaired two-tailed student T-tests.

Discussion

The microRNA *miR-7* shows highly conserved expression in vertebrate insulin secretory cells, however, it remained unclear what role it played in invertebrate insulin secretory cells. Here, I demonstrate that *miR-7* perturbation affects production and secretion from IPCs, and regulates processes downstream of insulin. *miR-7* inhibits overall animal growth, increases circulating sugars, and promotes total body triglyceride storage. These are suggestive of *miR-7* inhibition of insulin function. Consistent with this hypothesis, measurements of circulating Dilp2 were decreased with *miR-7* overexpression, and increased with *miR-7* knockdown. Mechanistic details of how *miR-7* exerts these functions will be further explored in the next chapter. However, I demonstrated that this effect is not due to *miR-7* affecting IPC survival, as IPC cell number remained the same in wildtype and in *miR-7* perturbed animals.

Assaying the regulation of *miR-7* expression shows that there are some parallels between the vertebrate and invertebrate systems. In vertebrates, the bHLH transcription factor NeuroD1 is essential for pancreatic development and for activation of insulin gene expression[146, 147]. Vertebrate NeuroD1 is thought to function downstream of Ngn3 to activate *miR-7* expression in pancreatic β-cells [143]. The *Drosophila* NeuroD1 ortholog is the transcription factor Atonal [148]. Atonal has previously been demonstrated to activate *miR-7* expression in the *Drosophila* eye[142]. Assaying activity of the *miR-7* enhancer in IPCs demonstrated that Atonal-mediated control of *miR-7* activation also extends to IPCs, as mutation of the Atonal binding sites in the *miR-7* enhancer prevented the enhancer from being

activated (Figure 12). Given NeuroD1/Atonal's roles in regulating *miR-7* in vertebrates and in *Drosophila*, a future question to answer is whether *Drosophila* Atonal could also be playing roles in regulating IPC development and Dilp transcription.

Since *miR-7* is embedded in the network that integrates responsiveness to upstream nutritional cues, I hypothesized that *miR-7* expression itself might be nutrient responsive. However, assaying *miR-7* enhancer activation during fed and starved conditions provided no indication that this was the case. Gene expression is regulated in a myriad number of ways. Perhaps regulation occurs through changes in miRNA localization or degradation. Circular RNAs have recently been demonstrated to regulate microRNA activity. One of the most well-characterized of these circular RNAs is CDR1as/Cirs-7. CDR1as contains 74 binding sites for *miR-7* and is highly enriched in sites of high *miR-7* expression, including in the brain, in the pituitary and in pancreatic β-cells[149]. It was recently demonstrated to regulate insulin secretion in pancreatic β-cells by decreasing the amounts of *miR-7* available to regulate its targets[149]. A *Drosophila* ortholog of CDR1as has yet to be discovered, however it is possible that *Drosophila* might utilize a similar mechanism to regulate *miR-7* expression.

The results from my experiments establish *miR-7* as a conserved regulator of invertebrate insulin-like peptides, with consequences of *miR-7* perturbation ranging from perturbed animal growth to disrupted metabolic homeostasis. Future experiments are aimed at clarifying the mechanisms through which *miR-7* regulates the function of *Drosophila* IPCs.

CHAPTER 3: IDENTIFICATION OF *MIR-7* TARGETS IN IPCS

Introduction

MicroRNAs are small non-coding RNAs that are transcribed from genes and processed from long precursor RNAs into 22-nucleotide single strands. They form a complex with Argonaute proteins and guide the miRISC complex to basepair with target mRNAs[150]. miRISC complexes seek out complementary sequences in the 3'UTRs of target mRNAs, and upon binding, destabilize mRNA transcripts and inhibit their translation capacity[150].

Since miRNAs mediate target recognition by basepairing complementary mRNA 3'UTRs, strong conservation of a miRNA at the sequence level might suggest strongly conserved regulatory targets. Indeed, studies of other strongly conserved miRNAs have demonstrated that this can be the case. Let-7, one of the first discovered miRNAs, shows conservation of not only its function in developmental timing, but also retention of key downstream targets. Let-7 regulates TRIM71 in humans, and in *C. elegans* it regulates the TRIM71 ortholog, Lin-41[151]. The miRNA miR-9a, also broadly conserved, shows similarly conserved downstream targets, with miR-9a regulating SNPFR1 in *Drosophila*, and its ortholog, NPY2R, in mammals[92].

Target prediction algorithms can predict the likelihood of interaction between a miRNA and its mRNA target. Each algorithm uses different sets of criteria to predict this interaction, which can result in a high rate of false positive predictions[152]. A common principle underlying the predictions made by many of these algorithms is the importance of the seed sequence, a 6-8 nucleotide string localized to a miRNA's 5' end[152]. This seed is accepted to be the most important predictor for productive miRNA-mRNA interactions, with each algorithm emphasizing

Watson-Crick base pairing between the miRNA seed and its mRNA target, with higher complementarity in this region indicating greater ability to silence expression of mRNA targets[152].

Emerging evidence has shed additional insight on the complexities of miRNA-target recognition, and could significantly improve efficacy of predictions. While standard prediction algorithms place heavy emphasis on the miRNA seed region, a recent study has shown that dinucleotide regions flanking the seed region can also have a large influence on the ability of mRNA target to repressed[153]. Additionally, while mRNAs with canonical target sites often show the highest affinity for miRNAs, target recognition patterns show unexpected miRNA-specific characteristics, with some miRNAs showing higher abilities to bind mRNA targets with non-canonical seed sequences than they do canonical seeds sequences[153].

In the previous chapter, *miR-7* was identified as an inhibitor of *Drosophila* IPC Dilp2 synthesis and secretion. However, it remains unclear how *miR-7* mediates its effects on IPC Dilp2. In this chapter, I utilize a combination of bioinformatics and experimental approaches to identify targets through which *miR-7* regulates IPC Dilp2.

Results

IDENTIFICATION OF *MIR-7* TARGETS IN IPCS

MicroRNAs repress their target genes by imperfect base-pairing to the 3'UTR of mRNAs. The primary recognition sequence is a 6 - 8 nucleotide seed that is located at the 5' end of a miRNA[154]. To identify mRNAs that are directly regulated by *miR-7*, computational algorithms that predict mRNA targets based on the presence of putative complementary sequences in annotated mRNA 3'UTRs were used (Analysis by Justin Cassidy). Different algorithms use different criteria when predicting the interaction between a miRNA and an mRNA. To reduce the risk of identifying false positives, five different target prediction algorithms were used in parallel. I initially asked whether any algorithm predicted a *miR-7* interaction with Dilp2 mRNA. My rationale was that since *miR-7* inhibits Dilp2 mRNA expression, it might do so directly. However, none of the algorithms predicted *miR-7* binding sites in the 3'UTRs of the *Dilp2, 3* and *5* genes (data not shown).

The 5 algorithms were independently run on the *Drosophila* transcriptome. Predicted targets were prioritized by only considering those genes identified by three or more different algorithms. A total of 97 genes were identified that fulfilled this criterion (Table 2). I next performed an experimental screen of these genes to determine if any of them might regulate IPC function. If a target gene directly mediates the effect of *miR-7* on growth control by IPCs, I reasoned that RNAi knockdown of the gene specifically in IPCs would resemble *miR-7* overexpression. The simplest phenotypic readout of growth control is adult body size, and *miR-*

7 overexpression causes adults to weigh less than normal (Figure 14). Adult body size scales proportionally with wing blade length: the distance between points where the third longitudinal vein intersects the wing margin and anterior crossvein (Figure 22) [92]. *miR-7* overexpression in IPCs reduced wing blade length as expected (Figure 22). I crossed *Dilp2-Gal4* to *UAS-RNAi* lines that knocked down individual candidate *miR-7* target genes, and measured blade length of affected animals. The screen identified *capping protein α* (*cpa*), two *Enhancer of split (E(spl)* genes - *E(spl)mγ* and *E(spl)m3*, and *dachshund* (*dachs*) as showing a statistically significant decrease in wing blade size as a consequence of RNAi knockdown in IPCs (Figure 21).

Table 2 - List of miR-7 predicted targets Drosophila

Drosophila *miR-7* predicted targets					
#	Gene	#	Gene	#	Gene
6	**Hairy**	4	Daughterless	3	SRPK
6	**E(spl)m3**	4	G-protein y	3	Abd-A
6	**E(spl)my**	4	MED19	3	Ptp10D
6	**Tom**	4	Olf186-F	3	Tweety
6	Capping protein a	4	Furin	3	CG2129
6	Myoblast City	4	DCX-Erv1AP	3	Tribbles
6	CG10444	4	Espinas	3	Mhc
6	CG4685	4	Cnk	3	RhoGAP100F
6	Lama	4	Costa	3	Heix
5	**Yan**	4	CG4898	3	CG32380
5	**E(spl)m5**	4	CG10338	3	TBP-AF13
5	**Bearded**	4	Fritz	3	Brinker
5	Rasputin	4	Gap1	3	Brown
5	CG6700	4	CG13213	3	CG11665
5	CG11319	4	CG5044	3	CG14989
5	iHog	4	Act88F	3	CG15727
5	CG18549	4	CG3967	3	Cpr64Aa
5	CG31472	4	CG8861	3	Cpr49Ae
5	Sticks and stones	4	DopR2	3	Him
5	CG10622	4	Egalitarian	3	Nomp-C
5	CG15113	4	Jim	3	Scabrous
5	Bowl	4	Legless	3	Tramtrackp69
5	Cad87A	4	Lame		
5	CG12488	4	Pdm2		
5	CG13908	4	Repo		
5	CG7272	4	CG12806		
5	CG9368	3	**Fringe**		
5	Dachs	3	**E(spl)mS**		
5	Jitterbug	3	CG5670		
4	**BobA**	3	Falafel		
4	p130CAS	3	CG10373		
4	Mito	3	eRF1		
4	Su(fu)	3	p16-ARC		
4	Ric8a	3	TRAM		
4	Pgant5	3	A3-3		
4	Ghost	3	Fax		
4	Spineless	3	Peanut		
4	DopR2	3	Deltex		

Identified target

Analysis by Justin Cassidy

Table 2: List of *Drosophila miR-7* predicted targets – Targets were predicted using Targetscan, PicTar, PITA, MiRanda, MiRTE, Sloan-Kettering target prediction algorithms. Red indicates a verified *miR-7* target in *Drosophila* and # indicates number of target prediction algorithms that predict the gene to be regulated by *miR-7*.

Figure 22 - RNAi screen to identify miR-7 IPC targets in Drosophila

A

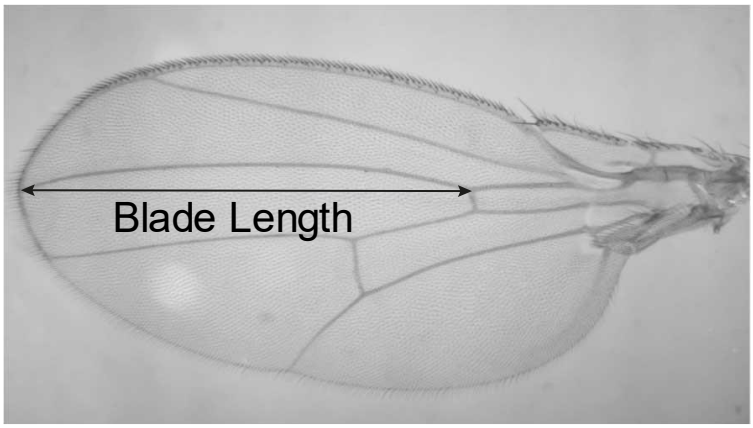

B

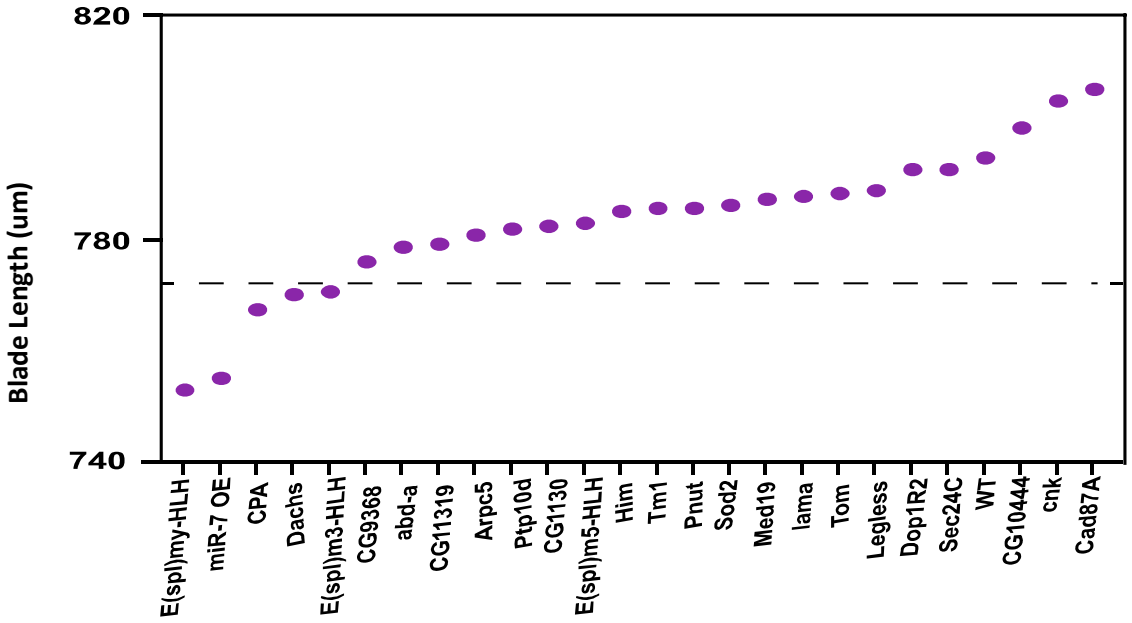

Figure 22 - RNAi screen to identify *miR-7* IPC targets in Drosophila - (A) An adult wing showing the measurement of blade length, from the margin to the anterior crossvein where both intersect the L3 vein. Scale bar = 100 µm. **(B)** A set of *miR-7* predicted targets in *Drosophila* were screened for wing size defects upon RNAi knockdown in IPCs. Dashed line indicates Bonferroni cutoff for statistical significance p=0.00192

Table 3 - List of miR-7 predicted targets in humans

Human *miR-7* predicted targets															
#	Gene	#	Gene	#	Gene	#	Gene	#	Gene	#	Gene	#	Gene	#	Gene
3	FBXL11	3	ARF4	3	ERLIN1	3	MED13L	3	SKP1A	2	ATP6V1A	2	VAMP2	2	BRWD1
3	G3BP2	3	ARF5	3	ESRRG	3	MKNK1	3	SLC38A2	2	DNAJB12	2	DLG3	2	C11ORF56
3	HERPUD2	3	ARID4A	3	FAM126B	3	MUSTN1	3	SLC38A4	2	DYRK1A	2	FRY	2	C18ORF23
3	OSBPL5	3	ARL4C	3	FAM19A1	3	NAB1	3	SLC4A4	2	GALNT7	2	IKZF2	2	C1ORF119
3	PGM2L1	3	ARL8B	3	FAM53C	3	NLGN2	3	SLC4A7	2	HDLBP	2	SRPK2	2	C20ORF112
3	SEC24C	3	ASXL1	3	FAM54B	3	NMT1	3	SMARCD1	2	NLK	2	TNKS	2	C20ORF23
3	CAPZA1	3	ATP2B2	3	FLJ20294	3	NR4A3	3	SMG6	2	NUDT4	2	CNTNAP1	2	C20ORF77
3	A2BP1	3	ATRX	3	FLJ36874	3	OGT	3	SMYD5	2	PPP2R2B	2	ENAH	2	C3ORF58
3	EIF4EBP2	3	BACE1	3	FLJ37078	3	OSBPL11	3	SNCA	2	SMEK1	2	FAM13A1	2	C5ORF13
3	ORAI1	3	C13ORF8	3	FLRT2	3	PAPPA	3	SOCS2	2	VANGL2	2	LPHN2	2	C6ORF107
3	PLCB1	3	C16ORF70	3	GAL3ST3	3	PCDHGA3	3	SP1	2	YPEL2	2	LPHN3	2	CAMSAP1L1
3	PPP1R2	3	C20ORF24	3	GATAD2B	3	PCSK7	3	SP3	2	C19ORF7	2	MPP5	2	CAPN2
3	RNF144A	3	C2ORF24	3	GATS	3	PDE4D	3	SRF	2	CACNA1C	2	RAB11FIP4	2	CAPN3
3	RYBP	3	CA10	3	GKAP1	3	PFN2	3	SUDS3	2	CUGBP2	2	SORBS1	2	CBX4
3	SEMA6A	3	CA7	3	GLTSCR1	3	PHF21A	3	TBC1D10B	2	DENND1A	2	TGFBR1	2	CCND2
3	SEMA6D	3	CALU	3	GPR88	3	PHOX2B	3	TCERG1	2	EPC2	2	ZFHX3	2	CCNY
3	SFRS1	3	CAND1	3	HELLS	3	PITPNA	3	TFRC	2	FXC1	2	HNRPA3	2	CCNYL1
3	TCF12	3	CCDC43	3	HMGA2	3	PLEC1	3	TNK2	2	HRNBP3	2	ABCD3	2	CD24
3	CNN3	3	CCDC76	3	HOXB5	3	PLP2	3	TNRC6A	2	KCNA1	2	ACVR2A	2	CD244
3	GATA6	3	CCNT2	3	HPCAL4	3	PLXNA1	3	TP53INP2	2	KIAA0460	2	ADAM10	2	CDC73
3	SEMMC	3	CEP350	3	IRS2	3	POGK	3	TTC26	2	LIN9	2	AEBP2	2	CFL2
3	SMG7	3	CGGBP1	3	ITCH	3	POLE4	3	TUSC2	2	MBNL2	2	ANKRD12	2	CHD9
3	SPATA2	3	CHKB	3	KCNH5	3	PPFIA3	3	UBE2D2	2	MITF	2	APL5	2	CHMP?
3	CHD3	3	CKAP4	3	KIAA0430	3	PSCD3	3	UBE2G1	2	NRF1	2	ARHGEF3	2	CLASP2
3	BMPR2	3	CLIP3	3	KIAA1128	3	PSME3	3	UBE2Z	2	PDPK1	2	ARID2	2	CLEC16A
3	BOC	3	CNOT6	3	KLF12	3	PTK2	3	ULK2	2	OKI	2	ASB6	2	CNNM4
3	GLI3	3	CNOT8	3	KLF4	3	PURB	3	USP52	2	RBM9	2	ASCL1	2	CNOT6L
3	MAP3K9	3	COL1A2	3	KLF9	3	RAF1	3	VDAC1	2	RPS6KB1	2	ATP2B3	2	CNP
3	REM1	3	COL2A1	3	KPNA1	3	RB1	3	VDAC3	2	SH3BGRL2	2	ATRN	2	CNTN2
3	KCNJ2	3	CPEB2	3	LEMD3	3	RNF141	3	VPS26A	2	SIN3A	2	ATXN1	2	COL12A1
3	AADACL1	3	CRY2	3	LINGO1	3	RSBN1	3	WAPAL	2	ZNF609	2	BMT	2	CORO2B
3	ABCG4	3	CXXC6	3	LOC339745	3	SATB1	3	WDR47	2	SEMA3C	2	BASP1	2	CPEB4
3	ABHD8	3	DACH1	3	LRRC59	3	SCAMPS	3	WIPF2	2	YWHAG	2	BCL9	2	CPT1B
3	ACSL4	3	DDIT4	3	LSM12	3	SERAC1	3	ZBTB4	2	PIK3AP1	2	BCLAF1	2	CRKL
3	ADAM11	3	EGR3	3	MAPK4	3	SERP1	3	ZNF294	2	SEMMG	2	BIRC4	2	CSMD1
3	ADCY9	3	EIF2C1	3	MBD2	3	SETD8	3	ZNF313	2	SLC25A23	2	BLR1	2	CSNK1E
3	AMD1	3	EPHA3	3	MDGA2	3	SGK	3	ZNF395	2	TLK1	2	BNC1	2	CTF8
3	ANKFY1	3	ERBB4	3	MECP2	3	SHANK2	2	ARL5B	2	TRIM2	2	BRD3	2	CUL3

Pancreatic β-cell Pituitary Both Hypothalamus

Analysis by Justin Cassidy

Human *miR-7* predicted targets															
#	Gene	#	Gene	#	Gene	#	Gene	#	Gene	#	Gene	#	Gene	#	Gene
2	CUL4B	2	GPR126	2	LHX6	2	NFIB	2	PPAP2B	2	RNF20	2	SPTBN4	2	WDR44
2	CYFIP2	2	GRIN2A	2	LOC130074	2	NHLH2	2	PPARGC1A	2	RNF38	2	SR140	2	WHSC1
2	DCUN1D1	2	GRIN3A	2	LOC203547	2	NKRF	2	PPFIA1	2	ROBO2	2	SRGAP2	2	WNK3
2	DIRAS1	2	HBP1	2	LOC400451	2	NR2C2	2	PPM1E	2	ROD1	2	SSH3	2	WWP1
2	DNAJB2	2	HDAC?A	2	LPGAT1	2	NR3C2	2	PPAP2B	2	SCN2B	2	STC1	2	XRN1
2	DOCK9	2	HIC2	2	LRCH2	2	NR5A2	2	PPARGC1A	2	scoc	2	STRN3	2	YOD1
2	DPF2	2	HLF	2	LRRC62	2	NRCAM	2	PPFIA1	2	SCRT1	2	SYT1	2	YTHDF3
2	DSEL	2	HNRPC	2	LRRC8A	2	NRN1	2	PPM1E	2	SEC24A	2	SYT6	2	ZBTB10
2	EDAR	2	HOXA1	2	LRRTM2	2	NXT2	2	PRDM10	2	SCN2B	2	TAPT1	2	ZBTB2
2	EHMT1	2	HOXB9	2	MAB21L2	2	OPHN1	2	PRICKLE2	2	SCOC	2	TESK2	2	ZBTB38
2	EIF2C4	2	HOXC11	2	MAFG	2	PAFAH1B1	2	PRKCB1	2	SCRT1	2	TFAP2A	2	ZBTB44
2	ELAVL2	2	HTR2C	2	MAPK3	2	PAPD5	2	PRKRIR	2	SEC24A	2	THBS1	2	ZDHHC21
2	EMX2	2	IDS	2	MAPKAP1	2	PAPOLA	2	PROSAPIP1	2	SELS	2	TAPT1	2	ZDHHC9
2	EPHA7	2	IGF2BP1	2	MARCKS	2	PAX6	2	PRPF38B	2	44085	2	TESK2	2	ZFX
2	EPHA8	2	IGF2BP2	2	MED13	2	PBX3	2	PRPF4B	2	SERTAD2	2	TFAP2A	2	ZFYVE20
2	EPM2AIP1	2	IGSF3	2	MEGF9	2	PCDH17	2	PTGFRN	2	SETD5	2	THBS1	2	ZFYVE9
2	EPN2	2	IPO11	2	MEOX2	2	PCDHGA1	2	PTPN2	2	SFRS5	2	TIMP2	2	ZDHHC9
2	FAM104A	2	IQGAP1	2	MEX3B	2	PCDHGA11	2	PTPRD	2	SH3TC2	2	TLOC1	2	ZFX
2	FAM131B	2	ITGB1	2	MFN1	2	PCDHGA12	2	PURA	2	SHANK3	2	TMED9	2	ZFYVE20
2	FAM133B	2	ITK	2	MGAT2	2	PCDHGA2	2	RAB1A	2	SIDT1	2	TMEM117	2	ZFYVE9
2	FAM53B	2	JMJD1B	2	MGEA5	2	PCDHGA6	2	RAB22A	2	SLC12A8	2	TMEM189	2	ZIC1
2	FAM60A	2	JMJD3	2	MIER2	2	PCDHGA8	2	RAB24	2	SLC20A2	2	TMF1	2	ZIC4
2	FAM83A	2	JPH4	2	MLL	2	PCDHGB3	2	RAB5A	2	SLC22A4	2	TNRC6B	2	ZIC5
2	FBXO21	2	KCNIP2	2	MLL2	2	PCDHGB7	2	RAB5B	2	SLC25A16	2	TP63	2	ZMIZ1
2	FBXW11	2	KCNT2	2	MN1	2	PCGF5	2	RAB5C	2	SLC30A4	2	TRIM10	2	ZNF281
2	FLJ10815	2	KIM0280	2	MOBKL1A	2	PDE4A	2	RAPH1	2	SLC30A7	2	TSGA14	2	ZNF654
2	FLJ14154	2	KIM0355	2	MPPED2	2	PDS5B	2	RASGRP1	2	SLC37A3	2	UBE2D1	2	ZNF706
2	FLYWCH1	2	KIM0408	2	MRPS25	2	PGRMC1	2	RBMS3	2	SLC39A10	2	UBE2D3		
2	FMNL3	2	KIM1729	2	MSL2L1	2	PHF15	2	RBMXL2	2	SLC5A3	2	UBE2E1		
2	FNDC4	2	KIM1967	2	MTF1	2	PHF17	2	RCN2	2	SLC6A8	2	UBE2NL		
2	FOXN2	2	KIAA2018	2	MYB	2	PHF21B	2	RCOR1	2	SLC6A9	2	UBFD1		
2	FOXN3	2	KLF13	2	MYCL1	2	PHLPPL	2	REEP1	2	SMCR7L	2	UBLCP1		
2	FOXO4	2	KLHDC5	2	MYRIP	2	PIK3CD	2	RELN	2	SMG1	2	USP9X		
2	FOXP1	2	KLHL14	2	NAV1	2	PIM1	2	REPS2	2	SNAPC3	2	VCPIP1		
2	FXR1	2	KLHL28	2	NAV2	2	PLAG1	2	RFX1	2	SOX12	2	VEGFA		
2	GGA2	2	KTELC1	2	NDST1	2	PLAGL2	2	RFX4	2	SOX5	2	VGLL2		
2	GPC4	2	LARP4	2	NECAP1	2	PLS3	2	RFXDC2	2	SOX6	2	VPS8		
2	GPM6B	2	LASP1	2	NEUROD1	2	POGZ	2	RIMBP2	2	SPON1	2	WDR37		

Pancreatic β-cell Pituitary Both Hypothalamus

Table 3: List of *Human miR-7* predicted targets – Targets were predicted using Targetscan, PicTar, and PITA target prediction algorithms. # indicates number of target prediction

algorithms that predict the gene to be regulated by *miR-7*. Colored font indicates verified *miR-7* predicted target in pancreas, pituitary, hypothalamus, or both.

CONSERVATION OF *MIR-7* TARGET REGULATION IN MAMMALS

The mature *miR-7* RNA has perfectly identical sequence conservation between *Drosophila* and mammals (Figure 7). My findings indicate that *miR-7* regulates Dilp2 release in *Drosophila* IPCs, just as it regulates insulin secretion in mouse β-cells[155]. This led me to ask whether the *miR-7* regulation of these predicted targets is similarly conserved in mammals. TargetScan and Pictar were used to predict *miR-7* target genes in the human genome. Using the same search parameters and stringency as the *Drosophila* search, I found 571 human genes that were predicted targets (Table 3). I then determined whether each *Drosophila* and human candidate gene had an ortholog in the other species, and cross-referenced the two lists to find orthologs in both species that are predicted *miR-7* targets. Of the 571 candidates in humans and 97 candidates in *Drosophila*, only 10 pairs of candidates were orthologous to one another. Strikingly, one of these ten pairs includes the *Drosophila cpa* gene, which was also identified in my RNAi screen (Figure 21).

Figure 23 - Identification of orthologous miR-7 predicted targets

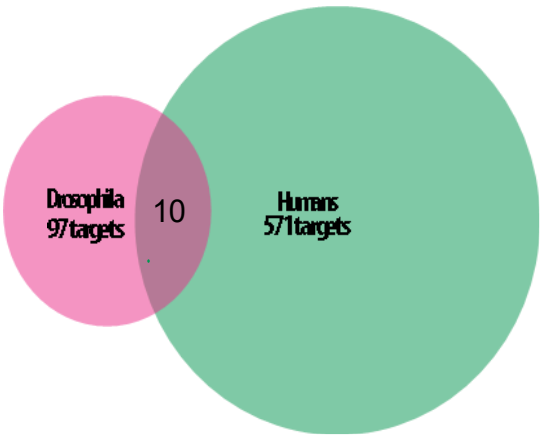

DROSOPHILA	HUMAN	FUNCTION
CPA	CAPZA1	F-actin capping
Daughterless	TCF12	Developmental transcription factor
Ghost	Sec24C	Cop II vesicle coat protein
Brown	ABCG4	ATP binding cassette protein
Rasputin	G3BP2	Ras signaling component
iHog	Boc	Hedgehog signaling component
Orai	Olf186-F	Calcium channel protein
Falafel	SMEK1	Rac signal transduction
SRPK	SRPK2	Protein kinase
Mito	Slc25a23	Mitochondrial membrane carrier

Figure 23 - Identification of orthologous *miR-7* predicted targets - (A) Identified predicted targets in *Drosophila* and in humans were analyzed to determine orthologs in the other species. Cross referencing of the two lists identified orthologs in both species that are predicted *miR-7* targets. **(B)** Of the 571 candidates in humans and 97 candidates in *Drosophila*, only 10 pairs of candidates were orthologous to one another, with *cpa/capZA1* as the top orthologous predicted target identified from the analysis.

QPCR ANALYSIS OF ORTHOLOGOUS *MIR-7* PREDICTED TARGETS IN DROSOPHILA BRAINS

I first sought to determine whether any of the 10 conserved orthologous *miR-7* targets is regulated by *miR-7* in *Drosophila* IPCs. There are only fourteen IPCs in the *Drosophila* brain, therefore detecting transcript changes in such a small subset of cells would be difficult in the context of thousands of other neurons. In addition to being expressed in Drosophila IPCs, *miR-7* is expressed in many neurons of the *Drosophila* brain. I therefore decided to perform a pan-neuronal knockdown of *miR-7* by expressing the *miR-7* sponge under the control of the ELAV-Gal4 driver. In addition to driving expression in post-mitotic neurons, ELAV-Gal4 also drives expression in postmitotic neurons in the brain, ELAV-Gal4 also drives expression in neuroblasts and in glia [156]. If *miR-7* regulates a target in *Drosophila* neurons, I predicted that knockdown of *miR-7* should result in an increase in their mRNA levels, while overexpression of *miR-7* should result in a decrease in mRNA levels. RT-qPCR assays showed that *miR-7* regulates some of these predicted targets in neurons, with *miR-7* knockdown increasing the levels of *cpa, sec24c, rasputin, OLF186F*, and *mito* (Figure 24). The converse experiment was performed, where *miR-7* was overexpressed in postmitotic neurons. However this proved to be lethal and no viable animals could be recovered for experiments.

Figure 24 - Regulation of orthologous predicted targets in Drosophila brain

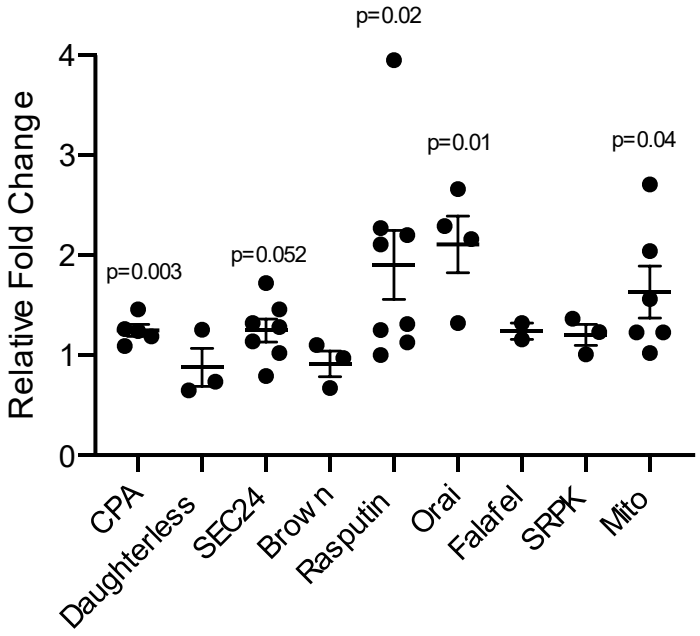

Figure 24 - Regulation of orthologous predicted targets in Drosophila brain - Fold change in brain mRNA levels of orthologous *miR-7* predicted targets – ELAV-Gal4 driver was used to overexpress the *miR-7* sponge in postmitotic neurons. Fold change in levels of orthologous *miR-7* predicted targets were measured in wandering third instar larvae by RT-qPCR.

MIRNA PROFILING OF ORTHOLOGOUS *MIR-7* PREDICTED TARGETS IN B-CELL PANCREAS

The *miR-7* sequence has been strongly conserved across the animal kingdom, and its expression in insulin secretory cells has been conserved across both vertebrates and invertebrates. Given this observation, I wondered whether the conserved targets regulated by *miR-7* in *Drosophila* could also be under *miR-7* regulation in a mouse model. There are publicly deposited microarray datasets from ß-cells of wildtype and *miR-7* loss-of-function mutant mice (104). There are also datasets from ß-cells of wildtype and *miR-7* overexpression (104). I downloaded the datasets and analyzed those 10 orthologous mouse genes. It appears that *CapzA1, TCF12, Boc, Srpk2*, and *Slc25a23* might be regulated by *miR-7* in pancreatic β-cells. A caveat is that I could not perform statistical testing on the data to see if fold-changes were significant. However, given that *cpa* and *mito* are regulated by *miR-7* in *Drosophila* (Figure 23), it suggests that conserved regulation by *miR-7* occurs for *cpa(capzA1*), and *mito(slc25a23*).

Figure 25 - Regulation of orthologous miR-7 predicted targets in pancreatic β-cells

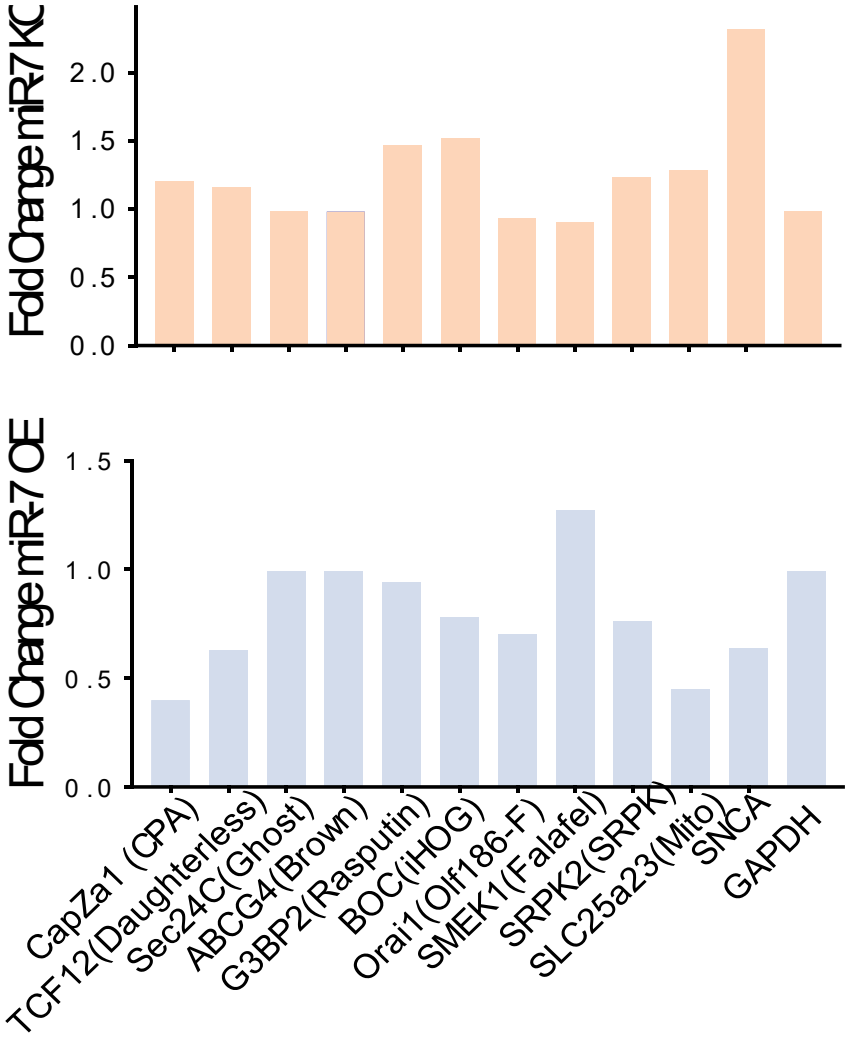

Figure 25 - Regulation of orthologous *miR-7* predicted targets in pancreatic β-cells - published dataset of genome wide transcriptomics from wildtype and *miR-7* knockdown mouse pancreatic β-cells, and *miR-7* overexpression MIN6 cell lines was analyzed to determine changes in the levels of the 10 orthologous *miR-7* predicted targets. SNCA is a previously characterized *miR-7* target that was shown play roles in regulating insulin secretion.

CONSERVATION OF *MIR-7* TARGET REGULATION IN THE PITUITARY

In addition to being expressed in pancreatic β-cells, *miR-7* shows conserved expression in the vertebrate pituitary gland[157]. However in contrast to its role in pancreatic β-cells where it inhibits secreted insulin, *miR-7* role in pituitary cells is to promote secretion [157], suggesting its mechanism of action may have diverged in different cell types. I sought to determine how mouse *miR-7* impacts its regulation of identified orthologous targets in the pituitary gland. *TCF12 and Srpk2* are abnormally elevated in *miR-7* mutant pituitary cells (Figure 25). Interestingly, *CapzA1* and *Boc*, targets found to be elevated in β-cells, actually decreased in the pituitary (Figure 25). Taken together, these results suggest that *miR-7* regulatory roles in neurosecretory cell functions might also demonstrate some cell type dependency, and that its function may have diverged in different contexts in certain cell types.

Figure 26 - Regulation of orthologous predicted targets in the pituitary

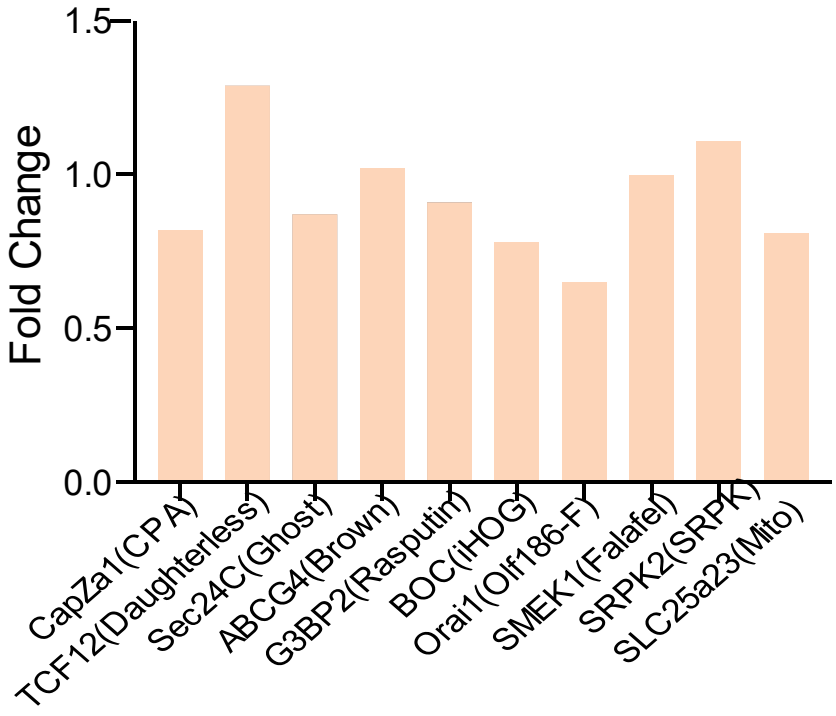

Analysis by Brian Eder

Figure 26 - Regulation of orthologous predicted targets in the pituitary - RNASeq analysis of *miR-7* knockout pituitaries. Relative fold changes of *miR-7* orthologous predicted targets from RNA-seq analysis of pituitaries isolated from *miR-7* knockout mice[157].

Figure 27 - miR-7 predicted target regulation across organisms and cell types

Predicted Target	Drosophila Neurons	Pancreatic β-cell	Pituitary
CPA (CAPZA1)	Y	Y	
DAUGHTERLESS (TCF12)		Y	Y
GHOST (SEC24C)	Y		
BROWN (ABCG4)			
RASPUTIN (G3BP2)	Y	Y	
IHOG (BOC)		Y	
OLF186-F (ORAI1)	Y		
FALAFEL (SMEK1)			
SRPK (SRPK2)		Y	Y
MITO (SLC25A23)	Y	Y	

Figure 27 - *miR-7* predicted target regulation across organisms and cell types - regulation of orthologous *miR-7* predicted targets in *Drosophila* neurons, vertebrate pancreatic β-cells or vertebrate pituitary. Y indicates regulation by *miR-7* of the precited target by *miR-7*.

Discussion

In this chapter, bioinformatic analysis was performed to identify predicted *miR-7* targets in *Drosophila* IPCs and in mammalian pancreatic β-cells. Of 97 predicted *miR-7* target genes in *Drosophila*, I have identified *E(spl)my*, *E(spl)m3, cpa*, and *dachs* as potential mediators of *miR-7*'s effects on organismal growth. Knockdown of expression of any one of these four genes in IPCs inhibited organismal growth, a phenotype that mimics *miR-7* overexpression in IPCs. Characterization of the *E(spl)* and *cpa* IPC phenotypes will be covered in the next chapter. Follow up experiments have not been performed on *dachs* mutant animals. However roles of *dachs* in Dilp regulation in *Drosophila* have been previously described [35,39]. In *Drosophila*, *dachs* is one of the earliest markers of developing IPCs, and in fully differentiated IPCs *dachs* along with the *Drosophila* Pax6 ortholog, *eyeless*, cooperatively bind the Dilp5 gene to activate its expression[50, 55]. Dach's role in differentiated pancreatic β-cells has yet to be determined, however it is known to play a role in promoting pancreatic β-cell proliferation during development[64]. Interestingly, Dachs's binding partner, Pax6 is targeted by *miR-7*. However, *eyeless* is not thought to be regulated by *miR-7*[118]. Nonetheless, these results suggest *miR-7* has been maintained in this role of regulating Dilp production, albeit not necessarily through the same target. While the list of orthologous *miR-7* targets does not include the ortholog of *dachs*, decreasing stringency of the prediction does identify Dachshund as a *miR-7* target in mammals. In the future, investigating *miR-7*'s interactions with *dachs* in *Drosophila* and in

vertebrates would be a direction worth pursuing in order to further determine the extent of *miR-7*'s role in regulating insulin function.

Cross-species target predictions were used as a means of identifying a conserved role for *miR-7*. Analysis of predicted targets for *miR-7* in the *Drosophila* vs human genome shows expansion between the two lineages. Algorithms identify 97 predicted targets for *miR-7* in *Drosophila*, while human predicted target analysis identifies 571 predicted targets. Interestingly, analysis to identify overlap of these predicted genes shows only ten shared predicted targets between the two lineages, with the top predicted target encoding the F-actin capping protein, Capping Protein Alpha. Other orthologous predicted targets that are regulated by *miR-7* in *Drosophila* include the RNA binding protein Rasputin, and the calcium channel protein Orai (OLF186-F) and Mito (Figure 24).

Additional analyses were performed to verify *miR-7* regulation of orthologous predicted targets in mammals because I was interested in identifying a conserved role for *miR-7* in insulin secretory cell types. Of the predicted targets in mouse, only the mouse orthologs of *cpa* and *mito* appear to be regulated by *miR-7* in pancreatic β-cells. These orthologous targets could be playing a role in regulating IPC secretory functions, as proper regulation of actin dynamics and mitochondrial metabolism of glucose is an important step in the insulin secretory process[31, 158, 159]. Additional experiments will need to be performed to determine how *miR-7* regulation of these targets impacts IPC function.

Further analysis utilizing datasets from the pituitary, another neuroendocrine cell type, fails to identify *miR-7* regulation of either of these predicted targets, suggesting some cell type

specificity to *miR-7*'s function in secretory cells (Figure 27). Interestingly however, another actin regulatory protein, Profilin2, was shown to be regulated by *miR-7* in both pancreatic β-cells and in the pituitary[157]. Taken together, these results suggest that a conserved mechanism for *miR-7*'s regulation of neuroendocrine cells may be through its regulation of the actin cytoskeleton. However, there is cell and organism specificity to *miR-7*s regulatory functions.

CHAPTER 4: *MIR-7* AND ENHANCER OF SPLIT

Introduction

Notch signaling is an ancient signaling pathway, present throughout metazoa, that regulates processes ranging from cell fate identity, proliferation, differentiation, and apoptosis[160]. The Notch pathway is initiated when the Notch ligand, Delta, binds to the Notch transmembrane receptor, resulting in cleavage and internalization of receptor intercellular domain, its translocation to the nucleus, where it activates transcription of downstream genes[160]. One of the most well-studied Notch downstream genes in mice belongs to the Enhancer of split family - Hes1.

Notch and Hes1 play roles in specifying cell fate at different stages of pancreatic development. During early development, Notch and Hes1 regulate specification acinar vs endocrine and ductal cell fates, with high levels of Notch signaling indicating endocrine and ductal fates, while low levels promote acinar fate[161]. Endocrine cell fates are assigned during the secondary transition, and are governed by interactions between Notch and the endocrine fate regulator Ngn3 [24, 162]. Ngn3 is expressed in a pulse, and the timing and amplitude of these pulses are necessary for proper specification of different cell types in the pancreatic lineage[162]. The first pulse of Ngn3 specifies α cell fates. Following α cell fate specification, Ngn3 is downregulated, and then is expressed in a second, higher amplitude pulse during the secondary transition[24, 162]. This secondary transition Ngn3 pulse promotes β-cell fates during the first half, and δ cell fates during the second half[24, 162]. Following down-regulation of Ngn3 expression, the tertiary transition occurs. During this stage, the different endocrine cell types undergo additional rounds of proliferation and organize into islet structures[24]. Ngn3 levels are directly antagonized by Notch signaling component Hes1[163]. This interplay between Hes-1-mediated regulation of Ngn3 levels ensures proper specification of all the different endocrine fates. Disruption of Notch signaling results in depletion of multipotent progenitors and premature endocrine differentiation, with differentiated cells primarily acquiring glucagon-producing cell fates[163].

Notch signaling plays a role during IPC development in *Drosophila* as well, however the precise contributions are still in dispute. Hwang et al showed that during early development of the IPC neuroblast from the epithelial placode, loss of Notch signaling inhibits non IPC fates, with loss of Notch signaling resulting in all cells from the placode assuming IPC neuroblast fate[51]. However, in direct contrast to these findings, Kim et al found that Notch signaling promotes IPC cell fates and that loss of Notch signaling results in IPC hypoplasia[53].

I had found that the proneural factor Atonal is required for *miR-7* gene transcription in IPCs (Figure 12). In the *Drosophila* eye, Atonal is repressed by Notch signaling through the *E(spl)* genes, which are orthologous to mammalian Hes1 [142] (Figure 28). The *atonal* gene is transiently expressed during photoreceptor differentiation, and this expression is dependent on its interactions with *miR-7* and *E(spl)* genes[142]. Activation of the EGF receptor during differentiation results in the activation of *atonal*, whose protein product directly binds and activates *miR-7* transcription. *miR-7* feeds back and indirectly increases Atonal protein levels by repressing *E(spl)* gene expression [142]. In addition to Atonal, another target of *miR-7* in the eye, Yan, is also expressed in IPCs. Loss of function of Yan did not affect IPC specification, however the effect of Yan on IPC function was not assayed[51].

My RNAi screen of predicted *miR-7* targets involved in regulating IPC control of growth identified the *E(spl)my* and *E(spl)m3* genes. In this chapter, I perform additional experiments characterizing Dilp levels in *E(Spl)* mutants to determine their effects on IPC function.

Figure 28 - Factors regulating differentiation in the Drosophila Eye

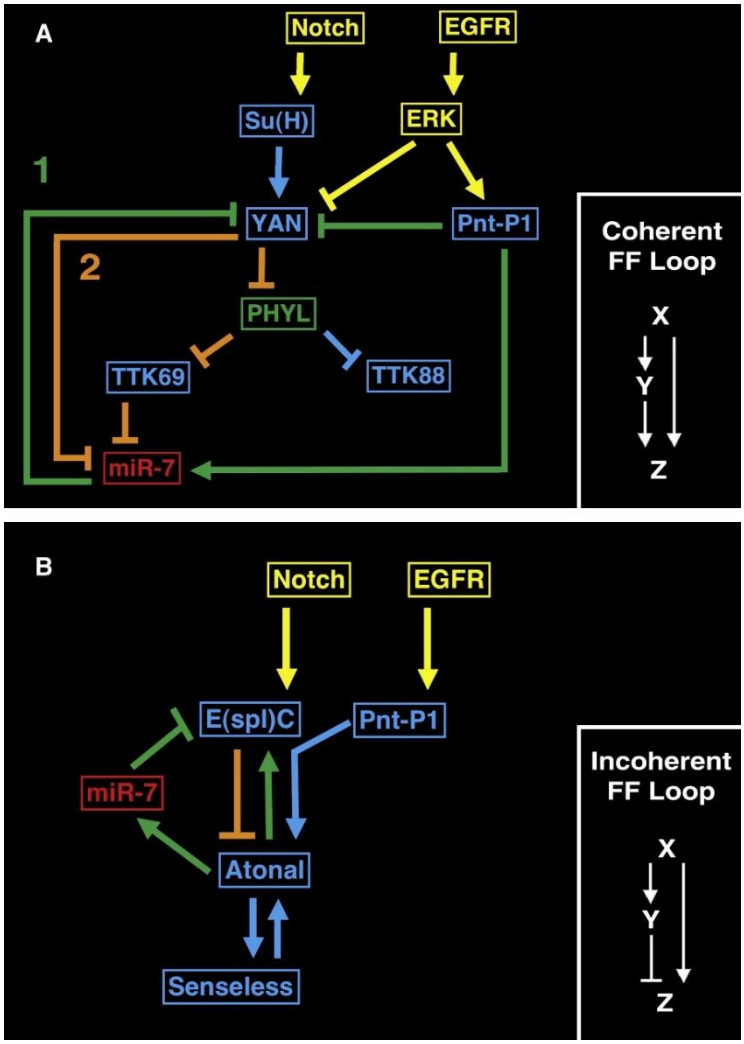

Figure 28 - Factors regulating differentiation in the Drosophila Eye – *miR-7*, E(spl) and the Drosophila NeuroD1 ortholog, Atonal, are integral parts of a network of feedback and feedforward loops that promote robust development of the Drosophila eye.

Results

My RNAi screen identified the predicted *miR-7* target genes *E(spl)my* and *E(spl)m3* as genes that significantly impacted IPC-dependent growth (Figure 22). These genes have previously been shown to be directly repressed by *miR-7*, and in the eye they also inhibit *miR-7* expression through a feedback mechanism [142]. I first quantified Dilp2 transcript levels by RT-qPCR and showed that specific knockdown of either *E(Spl)* gene by RNAi in IPCs had no effect on Dilp2 transcript abundance (Figure 29). Brain-stored Dilp2HF protein levels increased with knockdown of *E(spl)m3* and *E(spl)my*, however circulating Dilp2HF did not show a statistically significant difference with knockdown of either *E(spl)* gene (Figure 29).

I additionally visualized IPCs to determine how RNAi of these genes affected Dilp2HF localization. Imaging of Dilp2HF seems to show slight accumulation of Dilp2HF in IPCs, with knockdown of either *E(spl)my* or *E(spl)m3* (Figure 30).

Many genes expressed in the eye are also expressed in IPCs. *miR-7* transcription in the eye was shown to be inhibited by the transcriptional repressor Yan (Li et al 2009). In order to determine whether Yan was also expressed in IPCs, I visualized Yan expression by co-immunostaining IPC Dilp2HF and anti Yan antibody, and results showed co-expression in IPCs of wandering third instar larvae (Figure 31). I next assayed previously identified *miR-7* regulators in the eye, Pointed, Atonal, and Tramtrack69 for RNAi phenotypes related to IPC function and wing growth. Knockdown of none of the genes had any effect on growth (Figure 32).

Figure 29 - Insulin phenotyping of enhancer of split RNAi

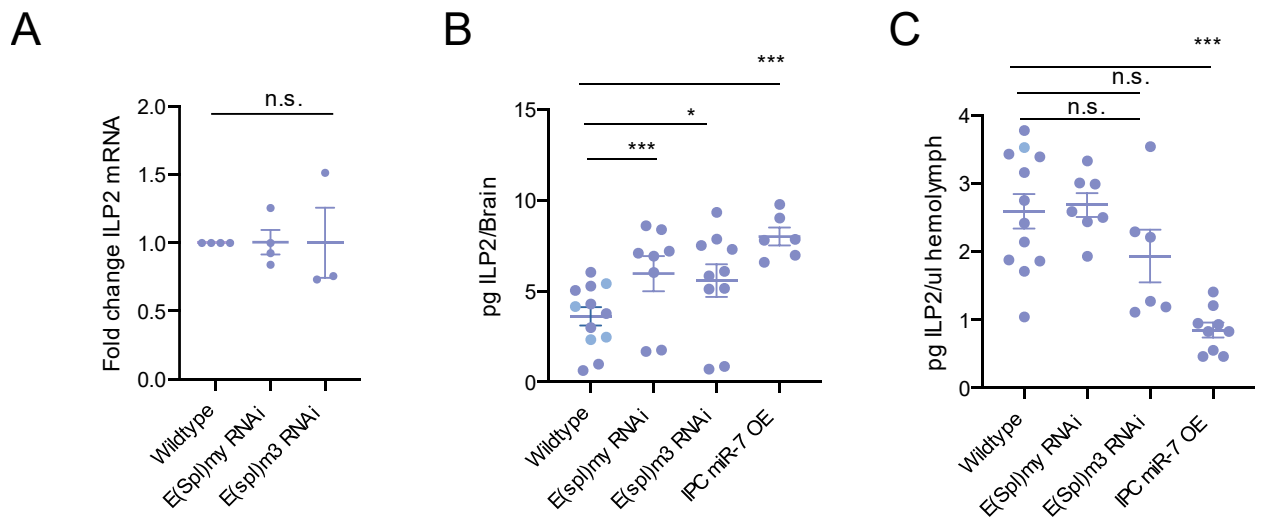

Figure 29 - Insulin phenotyping of enhancer of split RNAi – Dilp2 mRNA, and stored or circulating Dilp2HF levels were quantified in the brains or hemolymph of wandering third instar larvae. Each condition is matched with a wildtype control line that contains the *Dilp2-Gal4* driver used in each experiment **(A)** qPCR was performed on larval brains to determine fold change Dilp2HF transcripts with RNAi. **(B)** ELISA assay on larval brains to quantify stored brain Dilp2HF levels **(C)** ELISA Assay on larval hemolymph to quantify circulating Dilp2HF levels.

Figure 30- IPC Dilp2HF in E(Spl)my and E(Spl)m3 RNAi animals

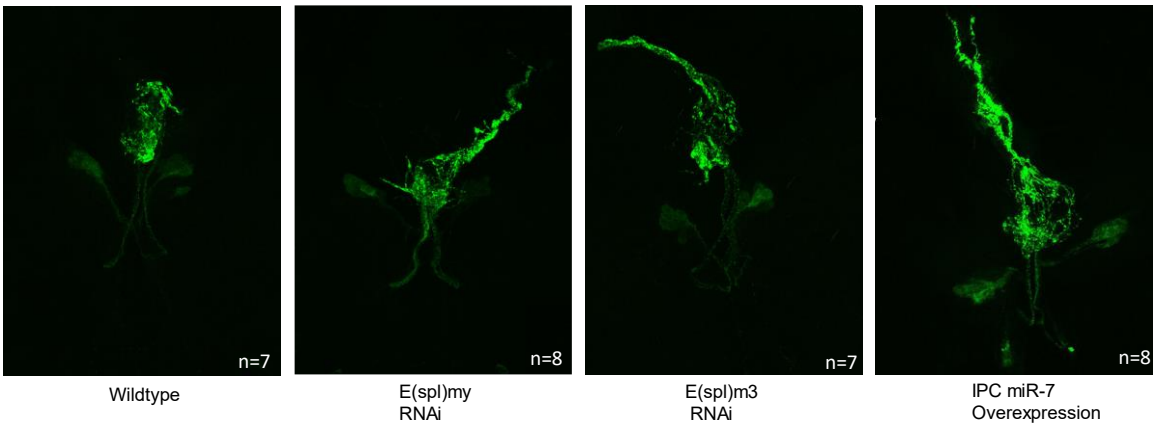

Figure 30- IPC Dilp2HF in E(Spl)my and E(Spl)m3 RNAi animals – immunofluorescence of IPCs of Enhancer of split genes E(spl)my and E(spl)m3 RNAi animals. RNAi was performed by expressing double-stranded RNA in IPCs under the *Dilp2gal4* driver. Each condition is matched with a wildtype control line that contains the *Dilp2-Gal4* driver used in each experiment. Anti-HA antibody was used to visualize Dilp2HF.

Figure 31 - Yan is expressed in IPCs

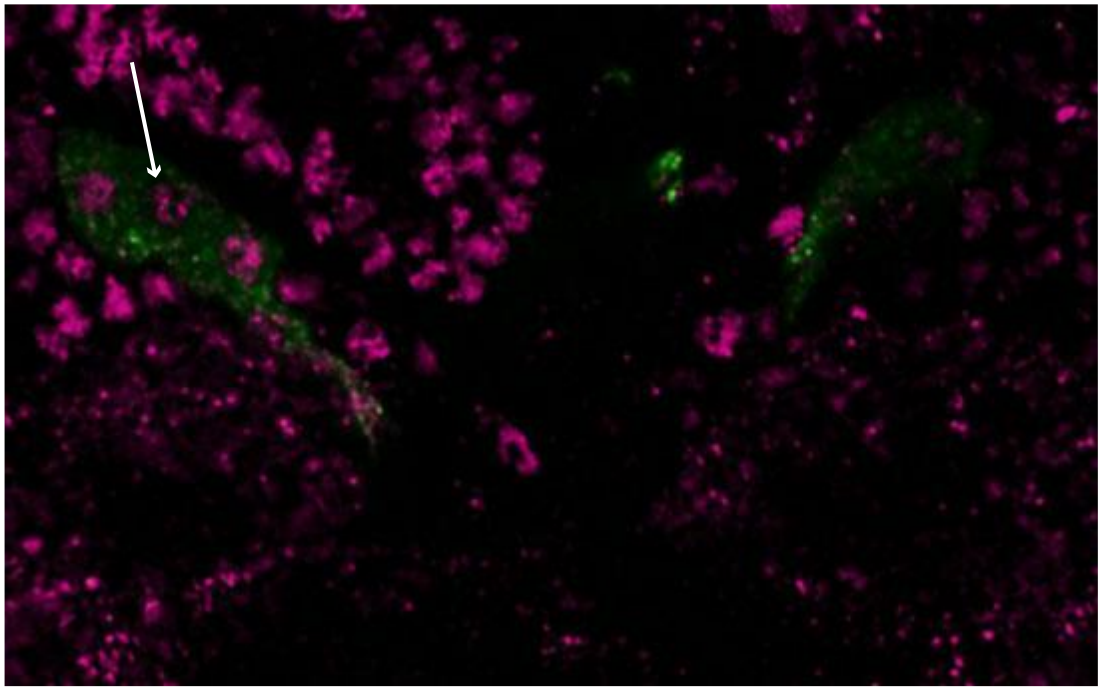

Figure 31 - Yan is expressed in IPCs - Image shows antibody stain against Yan protein in brains of wildtype wandering 3rd instar larvae. IPC are in marked with antibody stain against Dilp2HF in green, and cell nuclei is in purple. White arrow indicates *miR-7* enhancer expression with IPC.

Figure 32 - Growth regulation by eye miR-7 enhancer regulators in IPCs

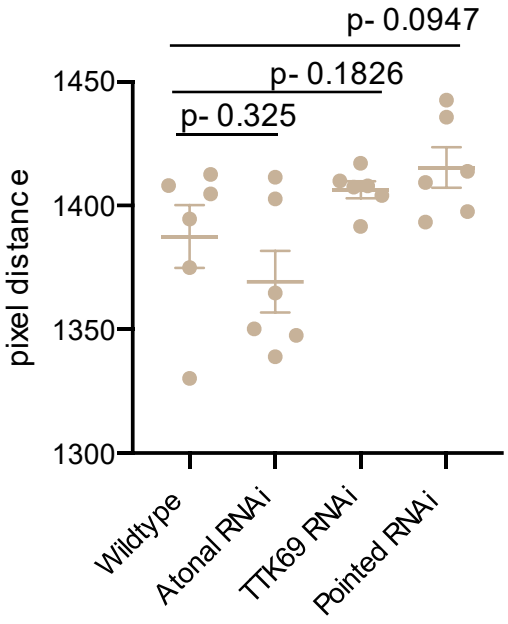

Figure 32 - Growth regulation by eye *miR-7* enhancer regulators in IPCs – The function of Atonal, Tramtrack69, and pointed RNAi animals was characterized by measuring effect of knockdown on growth. Target genes were knocked down by expressing RNAi under the control of the *Dilp2gal4* driver. Each condition is matched with a wildtype control line that contains the *Dilp2-Gal4* driver used in each experiment. Wing growth was measured as the distance between the wing margin and the anterior crossvein.

Discussion

I have identified *E(spl)my* and *E(spl)m3* as potential *miR-7* targets in IPCs. Mutants appear to show no effects on IPC cell numbers, however they increase IPC Dilp2HF protein abundance. If the factors regulating eye differentiation are also playing a role in regulating IPCs, a potential explanation for the observed increase in IPC Dilp2 is through a loss of *E(spl)*-mediated repression of *atonal*. *Atonal* has not been shown to play a role in regulating Dilp2 transcripts, however its vertebrate ortholog, NeuroD1 does activate insulin gene expression.

Although no change in circulating Dilp2HF level was detected, *E(spl)* mutants appeared to show Dilp2HF accumulation in IPCs. In the eye, Atonal also activates expression of the *miR-7* enhancer. This activation of the *miR-7* enhancer was also shown to hold true in IPCs. The accumulation phenotype might be due to increased *miR-7*-mediated inhibition of secretion. Therefore, *miR-7* may function as a barrier to protect circulating insulin levels from changes in brain insulin.

Preliminary analyses shows that in addition to *atonal* and *E(spl)* genes, a previously characterized *miR-7* transcriptional repressor Yan, is also expressed in IPCs, and that other factors shown to regulate *miR-7* may also play roles in regulating IPC function. RNAi of either Atonal, Tramtrack69, or Pointed failed to identify a significant effect on IPC function. These results are very preliminary however, and future experiments with larger sample sizes can more conclusively determine what role, if any, these genes play in regulating IPC function.

Using the current method of determining conservation, the *E(spl)* human ortholog, Hes1 was not identified as a *miR-7* target. However, the stringency used to identify these orthologous predicted

targets was set very high in order to maximize the chances that the targets predicted were bona fide targets. Relaxing the stringency does in fact identify Hes1 as a predicted target. With *miR-7* being induced by Ngn3 and NeuroD1, and Hes1-mediated repression of Ngn3 being integral for endocrine specification to proceed in pancreatic β-cells, it is likely that *miR-7* is an unidentified player in the network of factors regulating Ngn3 levels during endocrine differentiation.

CHAPTER 5: *MIR-7* AND CPA

Introduction

INSULIN SECRETION IN PANCREATIC B-CELLS

Insulin vesicle exocytosis occurs at peripheral regions of the β-cell. Vesicles containing secretory components undergo membrane fusion in a SNARE-dependent manner to release their contents. Insulin secretion occurs in a biphasic manner[31]. In the first phase, predocked vesicles known as the readily releasable pool undergo calcium-induced membrane fusion in response to glucose. This pool consists of a very small percentage (~1%) of the pancreatic β-cell insulin population[31]. Following the exocytosis of the reserve pool comes a second more sustained phase of insulin secretion. In this phase, a more intracellularly localized insulin pool, known as the reserve pool, is mobilized to the plasma membrane to undergo subsequent rounds of exocytosis[31].

The amplitude of insulin released during the second phase of insulin secretion is much lower than in the first phase. However because this process is sustained from minutes to hours, the sheer duration of the process means that the majority of released β-cell insulin is released during this phase[31]. Sustained exocytosis is tightly coupled to endocytosis. In this step, previously fused synaptic vesicles are internalized and removed from the cell membrane. This process is important for recycling secretory vesicle proteins for subsequent rounds of exocytosis, ensuring constant cell membrane volume and adequate membrane tension, and preventing excessive accumulation of secretory machinery at the plasma membrane [164].

Mutations that block endocytosis in pancreatic β-cells also inhibit additional rounds of insulin exocytosis[165].

THE ACTIN CYTOSKELETON AND INSULIN SECRETION

Exocytosis and endocytosis of insulin secretion is heavily dependent on dynamic changes in the actin cytoskeleton. Pancreatic β-cell actin is arranged in a dense network at the cell cortex, and global depolymerization with actin destabilizing drugs leads to an increase in insulin exocytosis[31, 166]. This led to the conclusion that actin's role in exocytosis is primarily an inhibitory one, with the actin cytoskeleton serving as a barrier that prevents vesicles from accessing the plasma membrane[167]. Genetic studies and the utilization of more advanced imaging techniques however, have demonstrated that actin's role in the insulin secretory process is more nuanced, with actin and its associated proteins also playing roles to promote the various stages of the exocytic and endocytic processes [31, 168, 169].

At its most basic unit, actin exists as a G-actin monomer, and with the assistance of various actin nucleation proteins, these monomers can assemble into filamentous F-actin (Figure 33). F-actin can exist as long linear filaments or as shorter branched filaments, and association with different protein nucleators determines whether linear or branched forms predominate. Capping of the filament tips by capping proteins stabilizes these structures, preventing association or dissociation of G-actin from barbed ends [170]. The Ena/Vasp and formin family of proteins antagonize the action of capping proteins by promoting growth of barbed ends through the addition of G-actin (Figure 33). The dynamic growth and shrinkage of F-

actin structures provide the driving force to power cellular processes like exocytosis and endocytosis [171].

Actin is a key player at multiple steps in the biphasic response of insulin to glucose. In the first phase, F-actin plays an inhibitory role by serving as an anchor to tether membrane-localized vesicles to the SNARE machinery and preventing their fusion [172]. The actin-severing protein Cofilin promotes the initial phase of insulin secretion by severing the anchored vesicles from F-actin [172, 173]. F-actin plays a much more important role in the second phase in a process that is orchestrated by the cell polarity regulator Cdc42[173, 174]. In response to glucose, Cdc42 initiates a signaling cascade that activates actin cytoskeletal rearrangements that promote the second phase of insulin release (Figure 33). Cdc42 initiates a signaling pathway through the p21 protein kinase PAK1, a consequence being the remodeling of cortical F-actin filaments[169, 173, 175]. Additionally, Cdc42 activates the effector protein N-WASP, which goes on to activate branching nucleator Arp2/3[173]. The net effect of these Cdc42-dependent actions is to promote secretion of insulin from pancreatic β-cells (Figure 34).

CAPPING PROTEIN AND ACTIN CONSERVATION

I previously showed *miR-7* to be a negative regulator of Dilp2 secretion from *Drosophila* IPCs. However it remained unclear through what mechanism *miR-7* does this. Studies of *miR-7* targets in the previous chapter identified *Drosophila cpa* and its mammalian ortholog *CapZA1* as top candidates affecting insulin or Dilp2 function. These genes encode Capping Protein α (CPA). CPA and capping protein β (CPB) form the capping protein heterodimer complex, which

binds to barbed ends of actin filaments and prevents additional polymerization or depolymerization (Figure 33). I hypothesize that *CPA* could be involved in insulin and Dilp2 secretion[176].

Figure 33 – The dendritic nucleation model of actin assembly

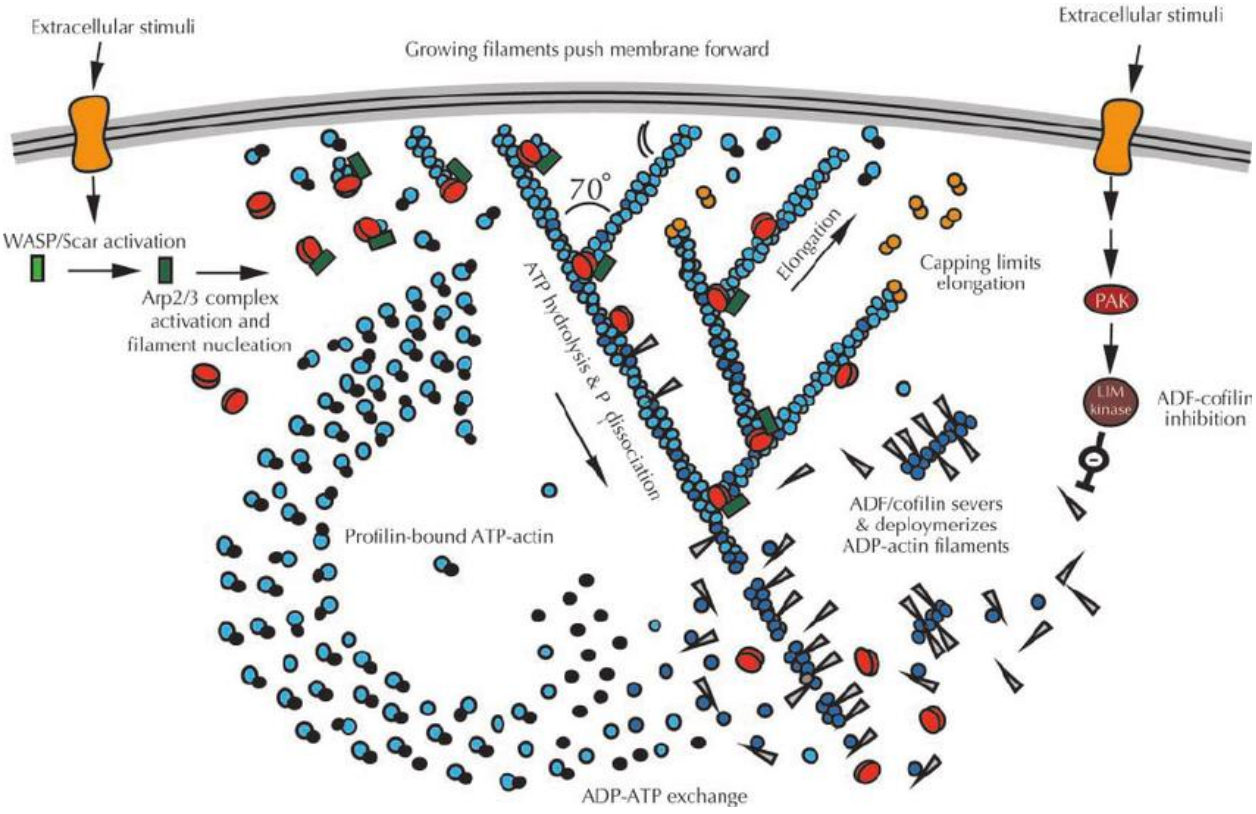

Image from Miller et al 2002

Figure 33 – The dendritic nucleation model of actin assembly – The dendritic nucleation model explains the mechanism of actin assembly at the leading edge of migrating cells, and can be applied to explain actin mechanics of fusing vesicles. In response to glucose, activation of CDC42 initiates a signaling pathway that regulates actin assembly. Arp2/3 complex is activated by Wasp proteins downstream of Cdc42, with activation of arp2/3 resulting in the formation of new actin branches. Cdc42 also activates PAK1 and LIM kinase, which phosphorylates cofilin and inhibits it ability to sever actin filaments. Actin polymerization occurs at the free growing barbed ends, and the force generated by actin growth leads to membrane protrusion. Capping proteins terminate growth at barbed ends, stabilizing the branched actin structure, and funneling G actin monomers for growth at newly formed barbed ends, thereby restricting pushing forces toward the cell membrane.

Figure 34 - Actin's role in the insulin secretory process

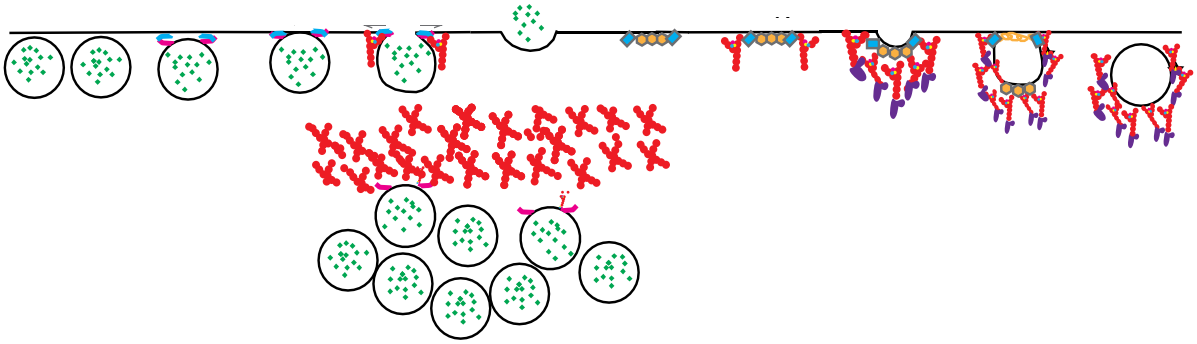

Figure 34 - Actin's role in the insulin secretory process - actin plays a role in the exocytosis and endocytosis of insulin containing vesicles. Actin forms a barrier at the cell cortex. This barrier prevents insulin vesicles from prematurely accessing the cell membrane. Actin plays a role in vesicle docking steps by tethering insulin vesicles to the SNARE machinery at the plasma membrane. Arp2/3-dependent formation of an actin cage around fusing vesicles helps provide the force for insulin vesicles to fuse to plasma membrane. Actin may additionally provide membrane tension necessary for fusion pore dilation during insulin secretion. Lastly, actin provides a driving force for vesicle retrieval and membrane scission during endocytosis.

Results

VALIDATION OF *MIR-7* REGULATION OF CPA

Bioinformatics predicted *cpa* as the top orthologous target of *miR-7*. However it remained to be determined whether *cpa* was active in regulating the function of *Drosophila* IPCs. If a target gene directly mediates the effect of *miR-7* on growth control I reasoned that RNAi knockdown of the gene specifically in IPCs would resemble *miR-7* overexpression. The simplest phenotypic readout of growth control is adult body size, and *miR-7* overexpression causes adults to weigh less than normal (Figure 14). Adult body size scales proportionally with wing blade length: the distance between points where the third longitudinal vein intersects the wing margin and anterior crossvein [92]. *miR-7* overexpression in IPCs reduced wing blade length as expected (Figure 35). When I next crossed *Dilp2-Gal4* to *UAS-cpa(RNAi)* and measured blade length of affected animals, it resulted in decreased wing length, similar to the decrease seen with *miR-7* overexpression (Figure 35).

If *miR-7* represses the expression of *cpa* as computationally predicted, I expected to be able to observe this regulation in vivo. Therefore, I knocked down *miR-7* in all brain neurons using a pan-neuronal Gal4 driving the *miR-7* Sponge, and then measured *cpa* mRNA levels in the brain. As predicted, the level of *cpa* mRNA increased when *miR-7* was knocked down (Figure 35).

Figure 35 - CPA RNAi phenocopies miR-7 inhibition of wing growth

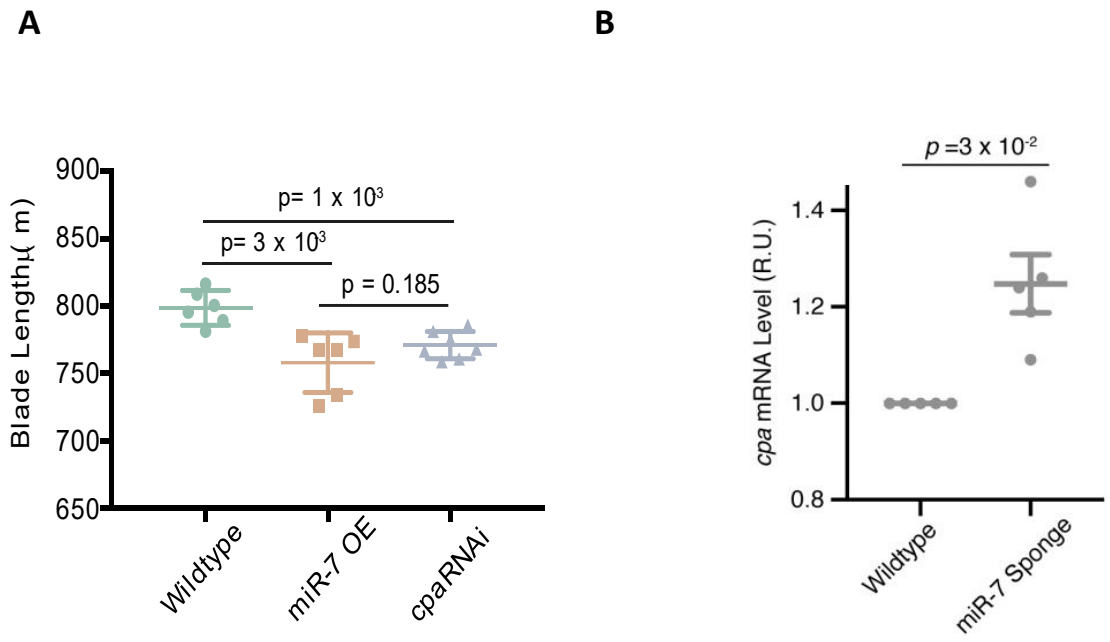

Figure 35 - CPA RNAi phenocopies *miR-7* inhibition of wing growth - (A) Blade lengths of males that contain *Dilp2-Gal4* and either overexpress *miR-7* (OE) or an RNAi hairpin directed against the *cpa* gene. Each condition is matched with a wildtype control line that contains the *Dilp2-Gal4* driver used in each experiment. Error bars are standard deviations, and *p* values are from two-tailed student T-tests. **(B)** Level of *cpa* mRNA in larval brains from animals that have *miR-7* knocked down in all neurons by the *miR-7* sponge. Measurements made by RT-qPCR are presented in relative units normalized to wildtype replicates.

There are two predicted *miR-7* binding sites in the *cpa* 3'UTR. The first binding site is an 8mer match to the *miR-7* seed, and it shows high levels of sequence conservation that extend from *Drosophila* to mammals. The second binding site is an offset 6mer match to the seed, and does not show as high a degree of conservation (Figure 36). To verify that *cpa* is indeed a direct target of *miR-7*, its 3'UTR was fused to a luciferase reporter gene and transfected into *Drosophila* S2 cells. To test for specificity of *miR-7* regulation, the first, the second, or both *miR-7* binding sites were mutated in the reporter gene. The wildtype and mutant reporters were cotransfected with plasmids mediating Gal4-driven expression of UAS-*miR-7*, in order to ensure sufficient levels of *miR-7* RNA. Interestingly, mutation of either the first or the second binding site resulted in a 1.5 fold increase in luciferase expression (Figure 36). Mutation of both binding sites however, resulted in a 2.3 fold increase in luciferase expression (Figure 36). Taken together, these results demonstrate that these two sites function additively to mediate *miR-7* regulation of *cpa* transcripts.

To determine whether *miR-7* regulates *cpa* expression in mammalian pancreatic β-cells, I turned to data from mouse experiments[104]. Both humans and mice contain three paralogous genes encoding *miR-7* isoforms. The major *miR-7* paralogs are identical in sequence between the two species, and they are predicted regulators of *capping protein alpha* homologs in both mouse (*Capza1*) and human (*CAPZA1*). Therefore, I analyzed a published dataset of genome-wide transcript levels from mouse β-cells. This dataset contains transcriptomics from wildtype β-cells, as well as β-cells in which *miR-7* paralogs were either knocked out or overexpressed. I focused attention on *Capza1* mRNA levels that were quantitated in these

samples. Strikingly, there was an increase in *Capza1* mRNA levels in *miR-7a-2* knockout β-cells (Figure 38). Conversely, there was a decrease in *Capza1* mRNA levels when any one of the three *miR-7* paralogs was overexpressed in β-cells (Figure 38). This result indicates that mouse *Capza1* is repressed by *miR-7* in pancreatic β-cells.

Figure 36 - Luciferase assay of CPA 3'UTR

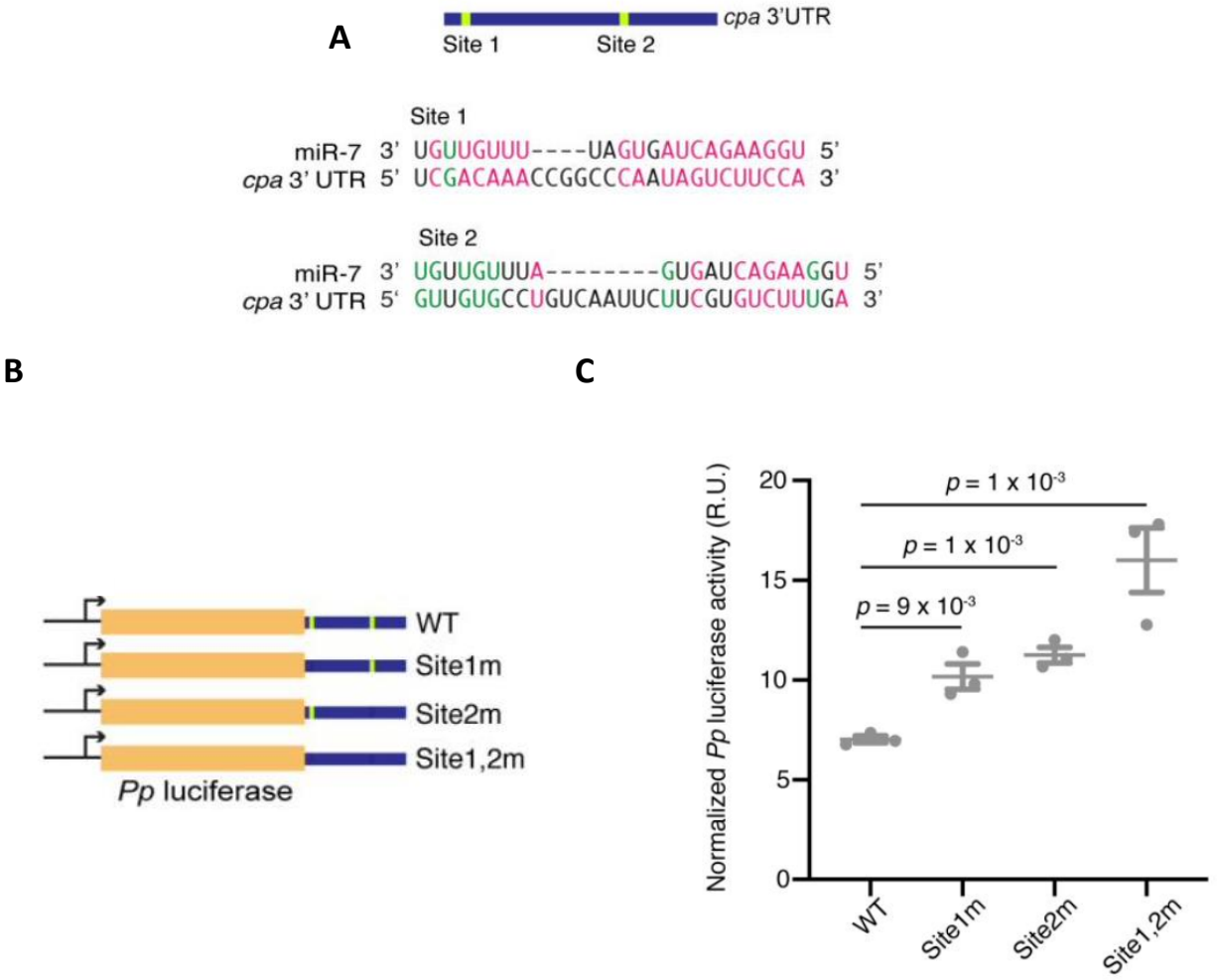

Figure 36 - Luciferase assay of CPA 3'UTR - Alignment of the human *miR-7*-1-5p strand with its predicted binding site in the 3' UTR of human *CAPZA1*. Alignment of the mouse *miR-7*a-1-5p strand with its predicted binding site in the 3' UTR of mouse *Capza1*. Watson-Crick base-pairs are highlighted in red and GU wobble base-pairs are highlighted in green **(B)** Schematic showing firefly luciferase fused to the *cpa* 3'UTR in reporter genes. Wildtype (WT) and mutant 3'UTRs used in reporters are shown. **(C)** Firefly luciferase activity from the different reporter genes normalized to Renilla luciferase in S2 cells expressing *miR-7*.

DILP2 PHENOTYPING OF CPA

If *miR-7* acts through *cpa* to regulate Dilp2 secretion in *Drosophila* IPCs, then RNAi should phenocopy some of the effects seen with *miR-7* overexpression in IPCs. I first quantified *Dilp2HF* transcript levels in IPCs. Quantification *Dilp2HF* transcript levels in IPCs of *cpa* RNAi animals showed that as predicted, RNAi had no effect on transcripts (Figure 37). I next assayed *cpa* RNAi animals to measure changes in stored brain and circulating Dilp2HF peptide levels. *miR-7* overexpression in IPCs increased stored brain Dilp2HF while decreasing the levels of Dilp2HF in circulation (Figure 37). RNAi of *cpa* resulted in increase in the levels of stored brain Dilp2HF and decreased circulating Dilp2HF (Figure 37). Interestingly, this effect was at a degree that was indistinguishable from the decrease seen with *miR-7* overexpression (Figure 37). From these experiments I conclude that *cpa* is required to stimulate Dilp2HF release from IPCs.

Figure 37 - Insulin phenotyping of cpa RNAi

A

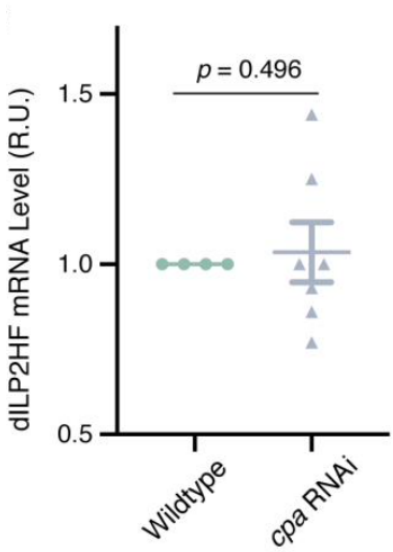

B

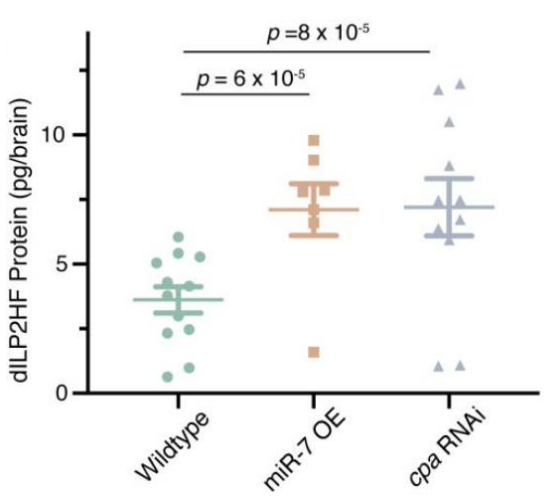

C

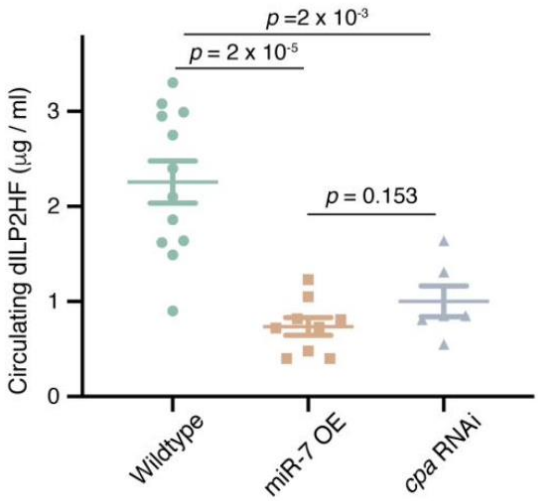

Figure 37 - Insulin phenotyping of cpa RNAi - (A) *Dilp2* mRNA levels in larval brains from wildtype animals or animals that have a RNAi knockdown of *cpa* in IPCs. Measurements made by RT-qPCR are presented in relative units. **(B)** Stored brain Dilp2HF peptide (by weight) in larvae that have *miR-7* overexpression (OE) or RNAi knockdown of *cpa* in IPCs. Each condition is matched with a wildtype control line that contains the *Dilp2-Gal4* driver used in each experiment. There was no significant difference between *miR-7* OE and *cpa* RNAi levels of Dilp2HF (p = 0.76, t test). **(C)** Concentration of Dilp2HF peptide in larval hemolymph from animals that have *miR-7* overexpression (OE) or RNAi knockdown of *cpa* in IPCs. For panels E - H, error bars represent the standard error of the mean, and p values are derived from unpaired two-tailed student T-tests.

Figure 38 – miR-7 regulation of CPA in pancreatic β-cells

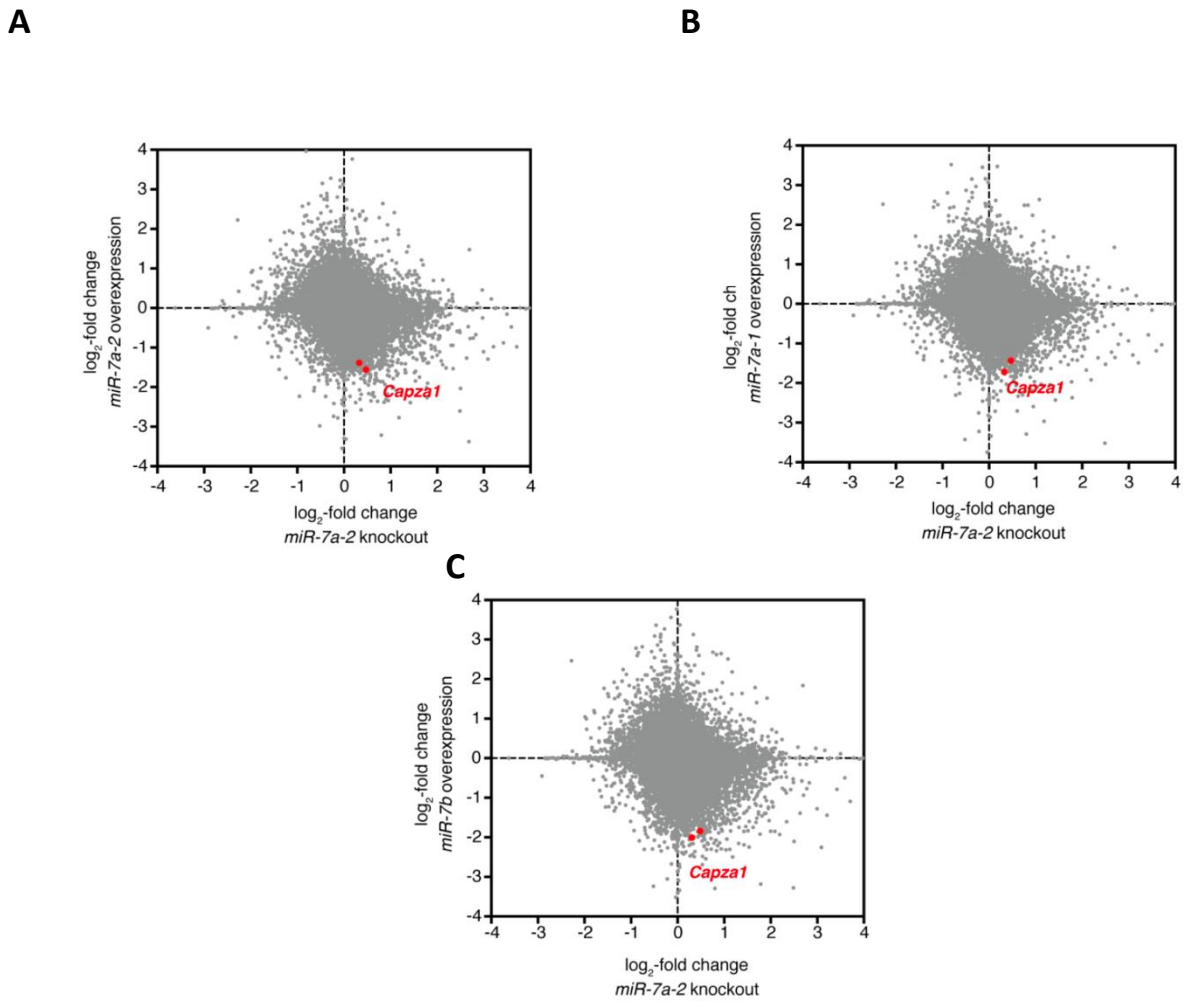

Figure 38 – *miR-7* regulation of CPA in pancreatic β-cells - Scatter plots of all mRNAs (grey).The Y axis shows the $\log_2$fold difference in mRNA levels from MIN6 cell lines overexpressing a *miR-7* paralog vs. not overexpressing the paralog. The X axis shows the $\log_2$fold difference in mRNA level pancreatic islets isolated from *miR-7*a-2 knockout mice vs. wildtype mice. Highlighted in red are the two replicate samples measured for the *Capza1* mRNA in each experiment. **(A)** MIN cells overexpressing *miR-7*a-1 vs. *miR-7*a-2 knockout islets. **(B)** MIN cells overexpressing *miR-7*a-2 vs. *miR-7*a-2 knockout islets. **(C)** MIN cells overexpressing *miR-7*b vs. *miR-7*a-2 knockout islets.

Discussion

Here, I have demonstrated that *cpa* expression is inhibited by *miR-7* in *Drosophila* and mouse insulin secretory cells, and that CPA promotes Dilp2 secretion from *Drosophila* IPCs. It is unclear precisely how CPA stimulates Dilp2 secretion but it might be via regulation of vesicle exocytosis or endocytosis. The dendritic nucleation model predicts that in order for Arp2/3 branching and additional polymerization to persist in a cell, free barbed ends must be capped to limit the addition and dissociation of G actin monomers[171]. The force generated by actin polymerization downstream of Arp2/3 has been shown to drive steps of exocytosis and endocytosis[168, 176-181]. Capping protein has been proposed to function in this pathway by stabilizing existing branches while funneling free G-actin to selectively grow at new branches[171]. In this way, growth and movement can occur only in specific regions.

A role for CPA in the insulin secretory pathway hasn't been previously characterized. However studies in other systems have shown a role for capping protein during exocytosis and endocytosis. In a reconstituted cell free system, it was demonstrated that in the presence of Arp2/3 and G-actin, low levels of capping protein generated pushing forces on the plasma membrane, likely similar to what is seen during vesicle exocytosis[182]. Higher capping protein concentrations are necessary for inward membrane curvature, and high capping protein concentrations along with the presence of nonmuscle myosin II enables vesicles to undergo scission[182].

Studies of endocytic vesicles of *cpa* mutant yeast buds provide some in vivo support for these observations. Yeast buds mutant for either subunit of capping protein show significant defects in the first phase of endocytosis, which corresponds to vesicle scission. Mutant buds show reduced dynamics in actin patches and actin cables, and this corresponds to reduction in the ability of vesicles to move away from the plasma membrane [178, 183]. In addition to defects in this first phase of movement, later stages of vesicle movement away from the plasma membrane are also compromised[183].

In budding yeast, either too much or too little capping protein inhibits actin patch movement and efficient endocytosis[178]. Additional studies need to be performed in order to determine whether this mechanism holds true in *Drosophila* IPCs and in pancreatic β-cells. However, the need for tight control of capping protein levels could provide an explanation for why this interaction with *miR-7* is so important as to be conserved over such long evolutionary timespans.

CHAPTER 6: GENERAL DISCUSSION AND FUTURE DIRECTIONS

In my thesis, I have found that *miR-7* is a conserved repressor of secreted insulin in *Drosophila* and in humans, and that *miR-7* regulation occurs through a conserved target, the actin capping protein *cpa.* This finding adds *miR-7* to the growing list of microRNAs that play conserved roles in regulating insulin secretory cell function[84, 184, 185]. This leads to a number of questions, including why this specific class of molecules are utilized in this pathway, and why the interactions have shown such strong conservation. Many of these identified miRNAs inhibit the insulin secretory function of these cells, leading to another question of why these molecules are embedded in pathways they are supposed to inhibit.

A recent publication from our lab provides one possible explanation for some of these questions. Cassidy et al demonstrated a role for repressors in orchestrating developmental processes by synchronizing gene expression with metabolic state[186]. Activated genes need to be downregulated in a timely manner in order to ensure expression of the next gene in the sequence, and repressors are necessary to perform this role. Utilizing mutations in a variety of repressors, including microRNA mutants, Cassidy et al demonstrated that loss of microRNA regulation increases the amplitude and duration of developmental activators, resulting in defects in developmental patterning[186]. This phenomenon is highly dependent on metabolic rate. Slowing down development by genetically ablating the IPCs renders these repressors dispensable, with mutants rescuing gene expression amplitude and duration and restoring normal phenotype[186].

Parallels can be drawn between gene regulation during development and miRNA regulation of metabolic processes. Circulating metabolite levels must be maintained in order to ensure that growth proceeds in a proper manner and that metabolism is maintained at a steady

state. The interplay between secreted hormones such as insulin and glucagon ensure proper regulation of these processes. Peaks in one secreted hormone correspond with troughs in the other, and this pattern is essential for proper signal reception and maintenance of metabolic processes[187, 188]. *In vivo*, insulin is expressed in short 10-minute bursts and longer 80-minute ultradian pulses[189, 190]. Feeding increases the amplitude of these pulses, however the peaks are quickly brought down and the pulse frequency remains the same[191, 192]. Diabetic patients and their first-degree relatives often show disruptions in both fast and ultradian pulses, suggesting that their maintenance of normal insulin oscillatory pattern is important for proper regulation of blood glucose levels [193, 194].

Certain gene regulatory motifs can result in pulsed gene expression[195]. The kinase *Cdc42* is deployed to the plasma membrane in response to glucose to promote insulin secretion[169]. Downstream *Cdc42* effectors, *Arp2/3* and *Cpa* are likely also similarly deployed[173]. At the same time, *miR-7* is activated to inhibit this pathway. These interactions result in an incoherent feedforward loop, a gene regulatory motif that is suited for generating uniform levels of output in response to varying levels of input[195]. In response to the upstream glucose signal, the kinase acts fast to promote insulin secretion, while *miR-7*, acting more slowly, shuts it off. This provides a potential explanation for why miRNAs are embedded in this process. Perhaps *miR-7* regulation of *cpa* has been maintained over such long evolutionary distances because it functions in a pathway that is highly attuned to the levels and the timing of its expression, allowing β-cells to mount an adequate response to a wide range of nutritional inputs.

Growth phenotypes were observed in IPC *miR-7* mutants, however no phenotypes of circulating glucose or triglycerides levels were observed. This could be a result of the nutritional status of the animals. Cassidy et al found that slowing development by ablating the IPCs diminished the amplitude of activator gene expression and reduced the penetrance of miRNA mutant phenotypes[186]. A similar effect might be at play with *miR-7* regulation of Dilps. Further stressing the insulin secretion capacity of these cells by feeding animals a high sugar diet and quantifying secreted insulin might show altered kinetics. Additionally, maintaining *miR-7* mutant animals on a strict low nutrient diet might diminish the growth difference between wildtype and mutant animals.

Quantifying *Cpa* levels and *miR-7* activity in response to varying glucose levels can help determine how this response is regulated. The utilization of miRNA silencing sensors in live imaging approaches can provide a useful readout for measuring *miR-7* activity [144]. In order to understand the consequences of *miR-7* action on glucose levels, insulin and glucose fluctuations can be measured to determine how these vary with different levels of *miR-7* and *cpa*. The impact of these changes on insulin signal reception can also be measured by utilizing fluorescent sensors for insulin signal reception[196]. If *miR-7* does indeed play a role in downregulating insulin amplitude, then this approach could be a useful tool to answer a number of questions, including determining the outer limit of glucose at which miRNA repression is no longer able rescue insulin amplitude and how miRNA regulation changes with variance in parameters such as aging, obesity, and circadian time.

miR-7 is expressed in various neurosecretory cell types, including in glucagon-secreting α cells, in the pituitary, and in the hypothalamus[118, 157, 197]. In contrast to its role in

inhibiting insulin secretory cells, *miR-7* promotes secretion in the pituitary[157]. Evolutionarily, the pituitary is more closely related to glucagon secreting α cells and AKH cells, suggesting it may function through similar mechanisms in these cell types[50]. Upstream stimuli that elicit insulin secretion actually inhibit the α cell secretory ability[198]. Given these observations, miRNA regulation may be more important to limit the amount of time that the neurons are inhibited, and glucagon cell targets should be anti-correlated to insulin cell targets. Future work should focus on determining *miR-7*s role in AKH secretion and its downstream targets in corpora cardiaca neurons.

With broad expression of *miR-7* in secretory cells, one possibility is that it is also released into circulation to exert some function [199]. miR-375 is secreted from pancreatic β-cells during conditions inversely associated with insulin secretion[200]. A function for secreted miR-375 is not yet known, however other instances of miRNAs that are secreted to regulate a target in distant tissue have been recorded [201, 202]. Perhaps miRNAs could be secreted to synchronize β-cell status with insulin target tissue. miRNAs expressed in β-cells including *miR-7*, miR-375, and Let-7 have been shown to regulate the IGF and insulin receptors[203, 204]. An intriguing possibility is that miRNAs could be released from IPCs to modulate expression of components of insulin/IGF reception in target tissue. This hypothesis can be tested by expressing a tagged *miR-7* in IPCs and performing qRT-PCR on hemolymph and tissues to assay for its presence. Ability of secreted *miR-7* to regulate targets can be tested by expressing *miR-7* specifically in IPCs of null mutant animals and assaying activity of *miR-7* sensors in target tissue.

Targeted delivery of miRNA mimics and antagomiRs are gaining traction as a way to treat disease[205, 206]. With *miR-7*'s role as a regulator of secreted insulin, manipulating *miR-7* levels may provide a means to better control blood glucose levels for Type II Diabetes patients. Studies suggest that insulin administered in pulses is better at maintaining blood glucose than non-pulsed insulin[207]. If miRNAs are found to play roles in regulating these pulses, then miRNA therapy may one day be utilized to rescue the defective pulses characteristic of Type II Diabetes.

One frequently cited limitation of using non canonical models such as *Drosophila* for endocrinology is that the distant evolutionary relationships of endocrine systems of mammals make it difficult to uncover common mechanisms. However, as I have shown here, using evolution as a guiding constraint can help reveal the fundamental ways in which organisms function.

Chapter 7: Methods

METHODS

Genetics

For all experiments, *Drosophila melanogaster* was raised using standard lab conditions and food. Stocks were either obtained from the Bloomington Stock Center, from listed labs, or were derived in our laboratory. A summary of the *Drosophila* genes manipulated in this study is listed in Table 1.

To gener*ate miR-7* null mutant animals, I crossed two different deletion mutants together and made a trans-heterozygous *miR-7Δ1*/*Df(2R)exu1* mutant. The *miR-7Δ1* mutant chromosome deletes the pre-*miR-7* sequence, while the *Df(2R)exu1* chromosome deletes *miR-7* along with 17 other genes. None of these 17 other genes is known to be involved in miRNA biology.

To specifically misexpress genes in IPCs, I used *Dilp2-Gal4* transgenic lines with the transgene inserted either on chromosome II or III. The *Dilp2-Gal4* transgene fuses the *Dilp2* gene promoter to the yeast *Gal4* gene open reading frame. *Gal4* encodes a transcription factor in yeast that binds to upstream activating sequences (UAS) in target yeast genes and activates the transcription of those genes. If Gal4 is expressed in *Drosophila* cells, it does not activate any fly genes but will activate any transgene that bears a UAS element. These UAS transgenes are routinely kept as independent lines, and when crossed with a Gal4 transgenic line, the UAS transgene will be expressed in cells that contain Gal4. *Dilp2-Gal4* is specifically expressed in brain IPCs9. I used a number of different UAS transgenic lines in combination with *Dilp2-Gal4*. *Drosophila* genetics frequently requires construction of stocks in which 4 or more of the 6

chromosomes must be put together so that particular transgenes or mutations are combined into one animal. This combination then facilitates perturbing one or more genes at the same time plus having genetic reporters of such perturbations. I “juggled” several chromosomes when putting together genotypes related to *Dilp2-Gal4*, and it was technically more straightforward to use particular *Dilp2-Gal4* chromosomes for particular genotypes.

To genetically ablate the IPCs of the brain, animals were constructed bearing a *Dilp2-Gal4* gene on chromosome III and a *UAS-Reaper* (*Rpr*) gene on chromosome II. *Rpr* is a pro-apoptotic gene that is sufficient to kill cells in which it is expressed35. Examination of *Dilp2-Gal4 UAS-Rpr* larval brains showed that they almost completely lacked IPCs (data not shown).

To overexpress *miR-7* in IPCs, I used a *UAS-miR-7* transgene in which a 432 bp DNA fragment containing the *miR-7* precursor is downstream of the UAS-driven promoter36. This was combined with the *Dilp2-Gal4* transgene located on chromosome III. To knockdown *miR-7* in IPCs, I used a *UAS-miR-7 Sponge* transgene in which the UAS-driven promoter sits upstream of GFP coding sequence and a sponge sequence in the 3'UTR37. The sponge sequence consists of 10 tandem binding sites for *miR-7*, with base mismatches at positions 9-12. This *UAS-miR-7 Sponge* transgene was combined with the *Dilp2-Gal4* transgene located on chromosome II. For all wildtype controls involving IPC-specific expression of transgenes, I used animals that contained the matching *Dilp2-Gal4* transgenic line. To knockdown *miR-7* in all brain neurons, *UAS-miR-7 Sponge* was combined with *Elav-Gal4*. Wildtype controls had only *Elav-Gal4*.

To mark IPCs, I used either *UAS-mCD8::mRFP* or *UAS-DsRed.nls*. The former expresses a mouse CD8 transmembrane domain fused to the N-terminus of mRFP38. The latter expresses dsRed with a nuclear localization tag at the C-terminus39

To determine whether *miR-7* RNA is expressed in IPCs, I used a *miR-7* transcriptional enhancer driving GFP40. This consists of a 349 bp region upstream from the *miR-7* transcription start site. The *miR-7* enhancer region was placed upstream a minimal promoter (TATA) and sequence encoding for a nuclear localized GFP was placed downstream of this region. The *miR-7* enhancer contains two binding sites for the bHLH factor Atonal, which was previously demonstrated to regulate enhancer activity in the eye40. To determine if bHLH factors regulate of enhancer activity in IPCs, I used animals that expressed GFP under the control of the *miR-7* enhancer, but with the two bHLH binding sites mutated40.

To assay *miR-7* silencing activity in IPCs, I utilized miRNA silencing sensors. The *miR-7* sensor expresses GFP under the control of the tubulin promoter and with a 3'UTR that contains two perfectly complementary *miR-7* binding sites41. The control sensor drives GFP under the control of the same tubulin promoter, however there are no *miR-7* binding sites in the 3'UTR41.

To quantify stored and circulating Dilp2 levels, I used flies expressing Dilp2HF25. These flies are null mutant for the endogenous *Dilp2* gene, but express a genomic *Dilp2* transgene that has been tagged with an HA epitope at the B-chain carboxy terminus and a FLAG epitope at the A-chain amino terminus.

To identify *miR-7* regulatory targets, RNAi lines were obtained from Bloomington Drosophila Stock Resource Center or from the Vienna Drosophila Resource Center. Each RNAi line has a UAS promoter that drives a double-stranded hairpin RNA corresponding to an annotated *Drosophila* gene42. Each line was crossed to *Dilp2-Gal4* animals, and progeny bearing both transgenes were assayed. A summary of the genetic constructs is listed in Table 2.

Body Weight Measurement

All *Drosophila* to be weighed were raised at 25°C. Adult females were weighed no more than 24 hours after eclosion, and batches of 20-50 animals were counted and weighed on a Mettler analytical balance. Larvae undergoing the pupal molt were identified as "white prepupae", and batches of these animals were counted and weighed on a Mettler analytical balance. For either adults or larvae, the total weight of a batch was divided by the number of animals in the batch to derive a mean weight per individual. Multiple batches were independently weighed, and mean weights calculated. All data shown represent the mean of these mean estimates. Wildtype controls were animals with one copy of the *Dilp2-Gal4* gene located on either the second or third chromosome. The insertion site of the *Dilp2-Gal4* gene in control lines was matched to its *miR-7* perturbation since I found that different insertion lines caused animals to vary in weight. The cause might be linked to Gal4 itself mildly affecting IPC function.

Adult Wing Measurement

Length of the adult wing scales proportionally with total size of adult *Drosophila*. To measure wing length, wings from 3-5 day old adult male flies were preserved in 70% (v/v) ethanol. Preserved wings were mounted in 70% (v/v) glycerol and imaged using a Zeiss Axiophot microscope and a 4x objective. Images were digitized using the Zeiss Zen imaging software. To measure wing blade length, the distance between the anterior crossvein and wing margin (point where it intersects with the L3 longitudinal vein) was measured using the Microruler package in ImageJ software.

Metabolite Measurements

Triglycerides – To determine total body triglycerides, five wandering third instar larvae were homogenized in freshly made phosphate buffered saline (PBS) + 0.05% (v/v) Tween-20 (Sigma). Homogenate was heated to 70°C, centrifuged at 3000 x g, and then at 3500 x g. Following centrifugation, 25 µl supernatant was added to 100 µl Infinity Triglycerides Reagent (Thermo Scientific) and incubated at 37°C for 10 minutes (min). Absorbance at 540 nm was measured to determine total triglycerides. Following triglyceride measurements, total protein was determined by the Bradford assay.

To determine levels of circulating triglycerides, hemolymph was extracted from wandering third instar larvae as described43 and diluted 1:10 in PBS. Samples were heated at 70°C for 5 min and then centrifuged for 10 min at 16000 x g. Five µl supernatant was added to 100 ul Infinity

Triglyceride Reagent (Thermo Scientific), and samples were incubated at 37°C for 10min. Absorbance at 540 nm was measured using a Biotek Synergy 4 microplate reader.

Glucose – To measure circulating glucose levels, porcine kidney trehalase (Sigma) was diluted 1:1000 (v/v) in Infinity Glucose Reagent (Thermo Scientific), and pH was adjusted to 6.5 with HCl. One µl of hemolymph was extracted from wandering third instar larvae and added to 100 µl Glucose Reagent supplemented with trehalase, and samples were incubated overnight at 37°C. Absorbance at 340 nm was measured using the Biotek Synergy4 microplate reader.

ELISA Assay of Brain and Circulating Dilp2HF

To measure circulating Dilp2HF levels, 2.5 µg/ml anti-FLAG antibody44 (Sigma-Aldrich F1804) in 0.2 M sodium bicarbonate pH 9.4 buffer was incubated overnight in wells of an ELISA plate (Nunc Immuno Module, Thermo Scientific 468667). Following two washing steps, wells were blocked overnight in PBS + 2% (w/v) BSA (Sigma). Three µl of hemolymph was extracted from male wandering third instar larvae and added to 37 µl PBS. Hemolymph samples were centrifuged at 16000 x g for 5 min. 35 µl of supernatant was added to 5 µl PBS + 2% (v/v) Tween-20 supplemented with rat anti-HA-antibody conjugated to horseradish peroxidase45 (Roche 12013819001) (1:500 v/v dilution from stock). This was added to one well of a blocked ELISA plate, and incubated overnight at 4°C. Wells were washed with PBS+ 0.2% (v/v) Tween-20 and developed using 100 µl One Step Ultra TMB – ELISA Substrate (Thermo Scientific 34029) for 30 minutes at room temperature. Reactions were stopped with 100 µl 2 M sulfuric acid, and absorbance was measured at 450 nm.

To measure stored brain Dilp2HF levels, three brains were dissected from wandering third instar larvae and homogenized in 150 µl PBS + 1% (v/v) Triton-X100. Samples were vortexed for 5 min and then centrifuged at 16000 x g for 5 min. 35 µl supernatant was used to perform the ELISA assay, as described above. Total brain protein levels were determined by Bradford assay.

Tissue Preparation and Imaging

Brains of male wandering third instar larvae were dissected and fixed for 60 min at room temperature in 4% (w/v) paraformaldehye (Sigma) in PBS. Washes were performed using PBS. Brain tissue was mounted in Vectashield and images were collected using a Leica SP5 laser scanning confocal microscope. Fluorophores were excited sequentially using the 488 and 561 laser lines. When comparing conditions, samples were imaged side by side on the same slide, using identical parameters between conditions. Images were collected as Z-stacks, with optical section thickness set to 2.98 µm for *miR-7* sensor and reporter images, while images of the *miR-7* sponge had an optical section thickness of 2.52 µm. Imaging was performed with the 40X oil objective lens, with 1.25 NA, and 1024 x 1024 resolution. All scans were done with the bidirectional scanner, and line averaging was set to 6x. Offset was set to zero, and gain was adjusted to minimize overexposure of the brightest sections.

RNA Extraction and RT-qPCR

Seven to ten brains from male wandering third instar larvae were dissected in PBS and homogenized in 200 µl TRIzol Reagent (Invitrogen). RNA was extracted according to the manufacturer's instructions. SuperScript III reverse transcriptase (Thermo) was used for reverse transcription of RNA. The reaction was primed using oligo-dT and random 9mer primers (2:1 molar ratio). 25 ng cDNA was used as a template for each qPCR reaction using SyBr Green. Gene

mRNA levels were normalized to β-tubulin mRNA level using the standard delta-delta Ct method. Primers used are listed below:

CPA mRNA -

Forward – CGCCACCAATTGTCGCCTTT Reverse – AGCGCAGATCTCGAGCTTGA

Dilp2HF mRNA

Forward – GGACGCCCTCAATCCCCTGC Reverse – CGCCTCCGGACTTCAGCCAG

Beta Tubulin

Forward - GCAGTTCACCGCTATGTTCA Reverse – CGGACACCAGATCGTTCAT

Prediction of *miR-7* Targets

The algorithms PicTar, Sloan-Kettering, PITA, MiRTE, miRanda, and TargetScan were used to predict *miR-7* targets in annotated *Drosophila melanogaster* genes40. For prediction of *miR-7* targets in annotated human genes, PicTar, TargetScan, and PITA were used40. Genes predicted by three or more algorithms for *Drosophila*, and two or more algorithms for humans were considered to be predicted targets. Human orthologs of *Drosophila* predicted targets were determined using Ensembl, InParanoid, and Orthology Matrix40.

Luciferase Assays of *miR-7* sites in the CPA 3'UTR

The annotated 3’UTR of the *cpa* gene (2R:21059062..21059883 [+], Dmel release 5.57) was synthesized as a gBlock (IDT) and inserted into the pMT-GL3 plasmid, which expresses the firefly luciferase gene under the control of a copper-inducible metallothionein promoter46. Construction of this reporter involved swapping the *Drosophila cpa* 3'UTR for the SV40 3'UTR

present in pMT-GL3. Each predicted *miR-7* binding site in the *cpa* 3'UTR was mutated singly or together to generate three different mutant reporters. Site 1 (2R:21059118-21059126) was mutated from GTCTTCCA to GCTCCCCA. Site 2 (2R:21059595-21059601) was mutated from GTCTTT to GTGGGG.

To perform luciferase assays, *Drosophila* S2 cells were cultured in Schneider's media supplemented with 10% FBS and seeded at a density of 2x106 cells per ml prior to transfection. Cells were co-transfected with pMT-Ren, which is a control reporter for Renilla luciferase46, and pMT-GL3 containing either a wildtype or mutant *cpa* 3'UTR. These were transfected at a 1:10 molar ratio, respectively, Cells were also transfected with UAS-*miR-7* and Ubiquitin-Gal4 plasmids. Transfections were performed with Effectene Transfection Reagent (Qiagen) according to manufacturer's protocol. To induce reporter expression, Cu2SO4 was added to 0.5 mM final concentration. Twenty four hours after induction, cells were lysed, and luciferase assays were performed using the Dual Luciferase Assay system (Promega). Luciferase activities were quantified using the Glomax Luminometer, and Firefly luciferase activity was normalized as the ratio of Firefly to Renilla enzymatic activities per sample.

Analysis of Mouse β-cell Transcriptomics

Microarray data was downloaded from GEO (accession no. GSE48195)28. Scatterplots were rendered in Prism 8 (Graphpad).

REFERENCES

1. Murtaugh, L.C., *Pancreas and beta-cell development: from the actual to the possible.* Development, 2007. **134**(3): p. 427-438.
2. Noguchi, G.M. and M.O. Huising, *Integrating the inputs that shape pancreatic islet hormone release.* Nature Metabolism, 2019. **1**(12): p. 1189-1201.
3. Seymour, P.A. and M. Sander, *Historical Perspective: Beginnings of the β-Cell.* Current Perspectives in β-Cell Development, 2011. **60**(2): p. 364-376.
4. Kim, S.K. and D.A. Melton, *Pancreas development is promoted by cyclopamine, a Hedgehog signaling inhibitor.* Proceedings of the National Academy of Sciences, 1998. **95**(22): p. 13036-13041.
5. Hebrok, M., S.K. Kim, and D.A. Melton, *Notochord repression of endodermal Sonic hedgehog permits pancreas development.* Genes & Development, 1998. **12**(11): p. 1705-1713.
6. Harrison, K.A., et al., *Pancreas dorsal lobe agenesis and abnormal islets of Langerhans in Hlxb9-deficient mice.* Nature Genetics, 1999. **23**(1): p. 71-75.
7. Spence, J.R., et al., *Sox17 regulates organ lineage segregation of ventral foregut progenitor cells.* Developmental cell, 2009. **17**(1): p. 62-74.
8. Li, H., et al., *Selective agenesis of the dorsal pancreas in mice lacking homeobox gene Hlxb9.* Nature Genetics, 1999. **23**(1): p. 67-70.
9. Martín, M., et al., *Dorsal pancreas agenesis in retinoic acid-deficient Raldh2 mutant mice.* Developmental Biology, 2005. **284**(2): p. 399-411.
10. Ahlgren, U., et al., *Independent requirement for ISL1 in formation of pancreatic mesenchyme and islet cells.* Nature, 1997. **385**(6613): p. 257-260.
11. Bhushan, A., et al., *Fgf10 is essential for maintaining the proliferative capacity of epithelial progenitor cells during early pancreatic organogenesis.* Development, 2001. **128**(24): p. 5109-5117.
12. Pulkkinen, M.-A., et al., *The IIIb isoform of fibroblast growth factor receptor 2 is required for proper growth and branching of pancreatic ductal epithelium but not for differentiation of exocrine or endocrine cells.* Mechanisms of Development, 2003. **120**(2): p. 167-175.
13. Jonckheere, N., et al., *Analysis of mPygo2 mutant mice suggests a requirement for mesenchymal Wnt signaling in pancreatic growth and differentiation.* Developmental biology, 2008. **318**(2): p. 224-235.
14. Ahnfelt-Rønne, J., et al., *Mesenchymal Bone Morphogenetic Protein Signaling Is Required for Normal Pancreas Development.* Diabetes, 2010. **59**(8): p. 1948-1956.
15. Fujikura, J., et al., *Notch/Rbp-j signaling prevents premature endocrine and ductal cell differentiation in the pancreas.* Cell Metabolism, 2006. **3**(1): p. 59-65.
16. Esni, F., et al., *Notch inhibits Ptf1 function and acinar cell differentiation in developing mouse and zebrafish pancreas.* Development, 2004. **131**(17): p. 4213-4224.
17. Georgia, S., et al., *p57 and Hes1 coordinate cell cycle exit with self-renewal of pancreatic progenitors.* Developmental Biology, 2006. **298**(1): p. 22-31.
18. Schaffer, A.E., et al., *Nkx6 transcription factors and Ptf1a function as antagonistic lineage determinants in multipotent pancreatic progenitors.* Developmental cell, 2010. **18**(6): p. 1022-1029.

19. Scavuzzo, M.A., et al., *Endocrine lineage biases arise in temporally distinct endocrine progenitors during pancreatic morphogenesis.* Nature Communications, 2018. **9**(1): p. 3356.
20. Gu, C., et al., *Pancreatic beta cells require NeuroD to achieve and maintain functional maturity.* Cell metabolism, 2010. **11**(4): p. 298-310.
21. Naya, F.J., et al., *Diabetes, defective pancreatic morphogenesis, and abnormal enteroendocrine differentiation in BETA2/neuroD-deficient mice.* Genes Dev, 1997. **11**(18): p. 2323-34.
22. Collombat, P., et al., *Opposing actions of Arx and Pax4 in endocrine pancreas development.* Genes & development, 2003. **17**(20): p. 2591-2603.
23. Wang, Q., et al., *Ghrelin is a novel target of Pax4 in endocrine progenitors of the pancreas and duodenum.* Dev Dyn, 2008. **237**(1): p. 51-61.
24. Rukstalis, J.M. and J.F. Habener, *Neurogenin3: a master regulator of pancreatic islet differentiation and regeneration.* Islets, 2009. **1**(3): p. 177-84.
25. Bratanova-Tochkova, T.K., et al., *Triggering and Augmentation Mechanisms, Granule Pools, and Biphasic Insulin Secretion.* Diabetes, 2002. **51**(suppl 1): p. S83-S90.
26. Rorsman, P., et al., *The Cell Physiology of Biphasic Insulin Secretion.* Physiology, 2000. **15**(2): p. 72-77.
27. Hoenig, M. and G.W. Sharp, *Glucose induces insulin release and a rise in cytosolic calcium concentration in a transplantable rat insulinoma.* Endocrinology, 1986. **119**(6): p. 2502-7.
28. Ashcroft, F.M., D.E. Harrison, and S.J. Ashcroft, *Glucose induces closure of single potassium channels in isolated rat pancreatic beta-cells.* Nature, 1984. **312**(5993): p. 446-8.
29. Cook, D.L. and N. Hales, *Intracellular ATP directly blocks K+ channels in pancreatic B-cells.* Nature, 1984. **311**(5983): p. 271-273.
30. CURRY, D.L., L.L. BENNETT, and G.M. GRODSKY, *Dynamics of Insulin Secretion by the Perfused Rat Pancreas.* Endocrinology, 1968. **83**(3): p. 572-584.
31. Wang, Z. and D.C. Thurmond, *Mechanisms of biphasic insulin-granule exocytosis - roles of the cytoskeleton, small GTPases and SNARE proteins.* Journal of cell science, 2009. **122**(Pt 7): p. 893-903.
32. Daniel, S., et al., *Identification of the docked granule pool responsible for the first phase of glucose-stimulated insulin secretion.* Diabetes, 1999. **48**(9): p. 1686-1690.
33. Barg, S., et al., *A Subset of 50 Secretory Granules in Close Contact With l-Type Ca²⁺ Channels Accounts for First-Phase Insulin Secretion in Mouse β-Cells.* Diabetes, 2002. **51**(suppl 1): p. S74-S82.
34. Renström, E., et al., *Cooling inhibits exocytosis in single mouse pancreatic B-cells by suppression of granule mobilization.* The Journal of physiology, 1996. **494 (Pt 1)**(Pt 1): p. 41-52.
35. Joshi, R.L., et al., *Targeted disruption of the insulin receptor gene in the mouse results in neonatal lethality.* Embo j, 1996. **15**(7): p. 1542-7.
36. Baker, J., et al., *Role of insulin-like growth factors in embryonic and postnatal growth.* Cell, 1993. **75**(1): p. 73-82.
37. Xu, Y., et al., *How IGF-II Binds to the Human Type 1 Insulin-like Growth Factor Receptor.* Structure, 2020. **28**(7): p. 786-798.e6.
38. Kavran, J.M., et al., *How IGF-1 activates its receptor.* Elife, 2014. **3**.
39. Bach, L.A., *The insulin-like growth factor system: towards clinical applications.* The Clinical biochemist. Reviews, 2004. **25**(3): p. 155-164.
40. Li, G., et al., *Insulin at physiological concentrations selectively activates insulin but not insulin-like growth factor I (IGF-I) or insulin/IGF-I hybrid receptors in endothelial cells.* Endocrinology, 2005. **146**(11): p. 4690-6.

41. Benyoucef, S., et al., *Characterization of insulin/IGF hybrid receptors: contributions of the insulin receptor L2 and Fn1 domains and the alternatively spliced exon 11 sequence to ligand binding and receptor activation.* The Biochemical journal, 2007. **403**(3): p. 603-613.
42. Hakuno, F. and S.I. Takahashi, *IGF1 receptor signaling pathways.* J Mol Endocrinol, 2018. **61**(1): p. T69-t86.
43. Boucher, J., Y.-H. Tseng, and C.R. Kahn, *Insulin and insulin-like growth factor-1 receptors act as ligand-specific amplitude modulators of a common pathway regulating gene transcription.* The Journal of biological chemistry, 2010. **285**(22): p. 17235-17245.
44. Xia, X., et al., *Growth Hormone-Releasing Hormone and Its Analogues: Significance for MSCs-Mediated Angiogenesis.* Stem Cells International, 2016. **2016**: p. 8737589.
45. Hawkes, C.P. and A. Grimberg, *Insulin-Like Growth Factor-I is a Marker for the Nutritional State.* Pediatric endocrinology reviews : PER, 2015. **13**(2): p. 499-511.
46. Wan, X., et al., *Dietary protein-induced hepatic IGF-1 secretion mediated by PPARγ activation.* PloS one, 2017. **12**(3): p. e0173174-e0173174.
47. Hedman, C.A., et al., *The IGF-system is not affected by a twofold change in protein intake in patients with type 1 diabetes.* Growth Hormone & IGF Research, 2005. **15**(4): p. 304-310.
48. Russell-Jones, D.L., et al., *Intraperitoneal insulin is more potent than subcutaneous insulin at restoring hepatic insulin-like growth factor-I mRNA levels in the diabetic rat: a functional role for the portal vascular link.* J Mol Endocrinol, 1992. **9**(3): p. 257-63.
49. Rulifson, E.J., S.K. Kim, and R. Nusse, *Ablation of insulin-producing neurons in flies: growth and diabetic phenotypes.* Science, 2002. **296**(5570): p. 1118-20.
50. Wang, S., et al., *The origin of islet-like cells in Drosophila identifies parallels to the vertebrate endocrine axis.* Proceedings of the National Academy of Sciences, 2007. **104**(50): p. 19873-19878.
51. Hwang, H.J. and E. Rulifson, *Serial specification of diverse neuroblast identities from a neurogenic placode by Notch and Egfr signaling.* Development (Cambridge, England), 2011. **138**(14): p. 2883-2893.
52. Kim, S.K. and E.J. Rulifson, *Conserved mechanisms of glucose sensing and regulation by Drosophila corpora cardiaca cells.* Nature, 2004. **431**(7006): p. 316-320.
53. Park, S., et al., *Specification of Drosophila Corpora Cardiaca Neuroendocrine Cells from Mesoderm Is Regulated by Notch Signaling.* PLOS Genetics, 2011. **7**(8): p. e1002241.
54. Nässel, D.R. and J.V. Broeck, *Insulin/IGF signaling in Drosophila and other insects: factors that regulate production, release and post-release action of the insulin-like peptides.* Cellular and Molecular Life Sciences, 2016. **73**(2): p. 271-290.
55. Okamoto, N., Y. Nishimori, and T. Nishimura, *Conserved role for the Dachshund protein with Drosophila Pax6 homolog Eyeless in insulin expression.* Proceedings of the National Academy of Sciences, 2012. **109**(7): p. 2406-2411.
56. Clements, J., et al., *Conserved role for the Drosophila Pax6 homolog Eyeless in differentiation and function of insulin-producing neurons.* Proceedings of the National Academy of Sciences, 2008. **105**(42): p. 16183-16188.
57. Docherty, J.E.B., et al., *Mio acts in the Drosophila brain to control nutrient storage and feeding.* Gene, 2015. **568**(2): p. 190-195.
58. Ikeya, T., et al., *Nutrient-Dependent Expression of Insulin-like Peptides from Neuroendocrine Cells in the CNS Contributes to Growth Regulation in Drosophila.* Current Biology, 2002. **12**(15): p. 1293-1300.
59. Grönke, S., et al., *Molecular evolution and functional characterization of Drosophila insulin-like peptides.* PLoS genetics, 2010. **6**(2): p. e1000857-e1000857.

60. Geminard, C., E.J. Rulifson, and P. Leopold, *Remote control of insulin secretion by fat cells in Drosophila.* Cell Metab, 2009. **10**(3): p. 199-207.
61. Kim, J. and T.P. Neufeld, *Dietary sugar promotes systemic TOR activation in Drosophila through AKH-dependent selective secretion of Dilp3.* Nature communications, 2015. **6**: p. 6846-6846.
62. Clements, J., et al., *Conserved role for the Drosophila Pax6 homolog Eyeless in differentiation and function of insulin-producing neurons.* Proceedings of the National Academy of Sciences of the United States of America, 2008. **105**(42): p. 16183-16188.
63. Okamoto, N., Y. Nishimori, and T. Nishimura, *Conserved role for the Dachshund protein with Drosophila Pax6 homolog Eyeless in insulin expression.* Proc Natl Acad Sci U S A, 2012. **109**(7): p. 2406-11.
64. Kalousova, A., et al., *Dachshund homologues play a conserved role in islet cell development.* Developmental biology, 2010. **348**(2): p. 143-152.
65. Park, S., et al., *A Genetic Strategy to Measure Circulating Drosophila Insulin Reveals Genes Regulating Insulin Production and Secretion.* PLOS Genetics, 2014. **10**(8): p. e1004555.
66. Kréneisz, O., et al., *Glucose increases activity and Ca2+ in insulin-producing cells of adult Drosophila.* Neuroreport, 2010. **21**(17): p. 1116-1120.
67. Colombani, J., et al., *A Nutrient Sensor Mechanism Controls Drosophila Growth.* Cell, 2003. **114**(6): p. 739-749.
68. Fridell, Y.-W.C., et al., *Increased uncoupling protein (UCP) activity in Drosophila insulin-producing neurons attenuates insulin signaling and extends lifespan.* Aging, 2009. **1**(8): p. 699-713.
69. Arntfield, M.E. and D. van der Kooy, *β-Cell evolution: How the pancreas borrowed from the brain.* BioEssays, 2011. **33**(8): p. 582-587.
70. Turque, N., et al., *Pax-QNR/Pax-6, a paired box- and homeobox-containing gene expressed in neurons, is also expressed in pancreatic endocrine cells.* Molecular Endocrinology, 1994. **8**(7): p. 929-938.
71. Roncero, I., et al., *Expression of glucose transporter isoform GLUT-2 and glucokinase genes in human brain.* Journal of Neurochemistry, 2004. **88**(5): p. 1203-1210.
72. Devaskar, S.U., et al., *Insulin gene expression and insulin synthesis in mammalian neuronal cells.* Journal of Biological Chemistry, 1994. **269**(11): p. 8445-8454.
73. van Arensbergen, J., et al., *Derepression of Polycomb targets during pancreatic organogenesis allows insulin-producing beta-cells to adopt a neural gene activity program.* Genome research, 2010. **20**(6): p. 722-732.
74. Schuurmans, C. and F. Guillemot, *Molecular mechanisms underlying cell fate specification in the developing telencephalon.* Current Opinion in Neurobiology, 2002. **12**(1): p. 26-34.
75. Jensen, J., *Gene regulatory factors in pancreatic development.* Developmental Dynamics, 2004. **229**(1): p. 176-200.
76. Atouf, F., P. Czernichow, and R. Scharfmann, *Expression of Neuronal Traits in Pancreatic Beta Cells: IMPLICATION OF NEURON-RESTRICTIVE SILENCING FACTOR/REPRESSOR ELEMENT SILENCING TRANSCRIPTION FACTOR, A NEURON-RESTRICTIVE SILENCER.* Journal of Biological Chemistry, 1997. **272**(3): p. 1929-1934.
77. Cao, J., et al., *Insight into insulin secretion from transcriptome and genetic analysis of insulin-producing cells of Drosophila.* Genetics, 2014. **197**(1): p. 175-192.
78. Rayburn, L.Y.M., et al., *The proprotein convertase amontillado (amon) is required during Drosophila pupal development.* Developmental biology, 2009. **333**(1): p. 48-56.
79. Davidson, J.K., et al., *Insulin assays and light microscopical studies of digestive organs in protostomian and deuterostomian species and in coelenterates.* General and Comparative Endocrinology, 1971. **17**(2): p. 388-401.

80. Iser, W.B., M.S. Gami, and C.A. Wolkow, *Insulin signaling in Caenorhabditis elegans regulates both endocrine-like and cell-autonomous outputs.* Developmental biology, 2007. **303**(2): p. 434-447.
81. Falkmer, S., *Immunocytochemical studies of the evolution of islet hormones.* Journal of Histochemistry & Cytochemistry, 1979. **27**(9): p. 1281-1282.
82. Lynn, F.C., et al., *MicroRNA Expression Is Required for Pancreatic Islet Cell Genesis in the Mouse.* Diabetes, 2007. **56**(12): p. 2938-2945.
83. Fu, X., et al., *MicroRNA-26a targets ten eleven translocation enzymes and is regulated during pancreatic cell differentiation.* Proceedings of the National Academy of Sciences, 2013. **110**(44): p. 17892-17897.
84. Poy, M.N., et al., *miR-375 maintains normal pancreatic alpha- and beta-cell mass.* Proc Natl Acad Sci U S A, 2009. **106**(14): p. 5813-8.
85. Li, X., *miR-375, a microRNA related to diabetes.* Gene, 2014. **533**(1): p. 1-4.
86. Keller, D.M., et al., *Characterization of Pancreatic Transcription Factor Pdx-1 Binding Sites Using Promoter Microarray and Serial Analysis of Chromatin Occupancy.* Journal of Biological Chemistry, 2007. **282**(44): p. 32084-32092.
87. Sebastiani, G., et al., *MicroRNA-124a is hyperexpressed in type 2 diabetic human pancreatic islets and negatively regulates insulin secretion.* Acta Diabetologica, 2015. **52**(3): p. 523-530.
88. Poy, M.N., et al., *A pancreatic islet-specific microRNA regulates insulin secretion.* Nature, 2004. **432**(7014): p. 226-230.
89. Baroukh, N., et al., *MicroRNA-124a Regulates Foxa2 Expression and Intracellular Signaling in Pancreatic β-Cell Lines.* Journal of Biological Chemistry, 2007. **282**(27): p. 19575-19588.
90. Pascal, L., G. Sonia, and R. Romano, *Regulation of the expression of components of the exocytotic machinery of insulin-secreting cells by microRNAs.* Biological Chemistry, 2008. **389**(3): p. 305-312.
91. Wu, Q. and M.R. Brown, *SIGNALING AND FUNCTION OF INSULIN-LIKE PEPTIDES IN INSECTS.* Annual Review of Entomology, 2006. **51**(1): p. 1-24.
92. Suh, Y.S., et al., *Genome-wide microRNA screening reveals that the evolutionary conserved miR-9a regulates body growth by targeting sNPFR1/NPYR.* Nature Communications, 2015. **6**: p. 7693.
93. Varghese, J., S.F. Lim, and S.M. Cohen, *Drosophila miR-14 regulates insulin production and metabolism through its target, sugarbabe.* Genes & development, 2010. **24**(24): p. 2748-2753.
94. Boulan, L., D. Martín, and M. Milán, *bantam miRNA Promotes Systemic Growth by Connecting Insulin Signaling and Ecdysone Production.* Current Biology, 2013. **23**(6): p. 473-478.
95. Colombani, J., et al., *Antagonistic Actions of Ecdysone and Insulins Determine Final Size in Drosophila.* Science, 2005. **310**(5748): p. 667-670.
96. Jin, H., V.N. Kim, and S. Hyun, *Conserved microRNA miR-8 controls body size in response to steroid signaling in Drosophila.* Genes & development, 2012. **26**(13): p. 1427-1432.
97. Hyun, S., et al., *Conserved MicroRNA miR-8/miR-200 and Its Target USH/FOG2 Control Growth by Regulating PI3K.* Cell, 2009. **139**(6): p. 1096-1108.
98. Lee, G.J., J.W. Jun, and S. Hyun, *MicroRNA miR-8 regulates multiple growth factor hormones produced from Drosophila fat cells.* Insect Molecular Biology, 2015. **24**(3): p. 311-318.
99. Honegger, B., et al., *Imp-L2, a putative homolog of vertebrate IGF-binding protein 7, counteracts insulin signaling in Drosophila and is essential for starvation resistance.* Journal of biology, 2008. **7**(3): p. 10-10.
100. Osterbur, D.L., et al., *Genes expressed during imaginal discs morphogenesis: IMP-L2, a gene expressed during imaginal disc and imaginal histoblast morphogenesis.* Developmental Biology, 1988. **129**(2): p. 439-448.

101. Lozano, J., R. Montañez, and X. Belles, *MiR-2 family regulates insect metamorphosis by controlling the juvenile hormone signaling pathway.* Proceedings of the National Academy of Sciences of the United States of America, 2015. **112**(12): p. 3740-3745.
102. Wild, S., et al., *Global prevalence of diabetes: estimates for the year 2000 and projections for 2030.* Diabetes Care, 2004. **27**(5): p. 1047-53.
103. Warram, J.H., et al., *Slow Glucose Removal Rate and Hyperinsulinemia Precede the Development of Type II Diabetes in the Offspring of Diabetic Parents.* Annals of Internal Medicine, 1990. **113**(12): p. 909-915.
104. Perley, M.J. and D.M. Kipnis, *Plasma insulin responses to oral and intravenous glucose: studies in normal and diabetic sujbjects.* The Journal of clinical investigation, 1967. **46**(12): p. 1954-1962.
105. Zimmet, P., *Globalization, coca-colonization and the chronic disease epidemic: can the Doomsday scenario be averted?* Journal of Internal Medicine, 2000. **247**(3): p. 301-310.
106. Diamond, J., *The double puzzle of diabetes.* Nature, 2003. **423**(6940): p. 599-602.
107. Florez, J.C., *Newly identified loci highlight beta cell dysfunction as a key cause of type 2 diabetes: Where are the insulin resistance genes?* Diabetologia, 2008. **51**(7): p. 1100.
108. Grant, S.F.A., et al., *Variant of transcription factor 7-like 2 (TCF7L2) gene confers risk of type 2 diabetes.* Nature Genetics, 2006. **38**(3): p. 320-323.
109. Saxena, R., et al., *Common Single Nucleotide Polymorphisms in TCF7L2 Are Reproducibly Associated With Type 2 Diabetes and Reduce the Insulin Response to Glucose in Nondiabetic Individuals.* Diabetes, 2006. **55**(10): p. 2890-2895.
110. Cauchi, S., et al., *TCF7L2 is reproducibly associated with type 2 diabetes in various ethnic groups: a global meta-analysis.* Journal of Molecular Medicine, 2007. **85**(7): p. 777-782.
111. Zhou, Y., et al., *TCF7L2 is a master regulator of insulin production and processing.* Human molecular genetics, 2014. **23**(24): p. 6419-6431.
112. Jennings, B.H., *Drosophila – a versatile model in biology & medicine.* Materials Today, 2011. **14**(5): p. 190-195.
113. Palanker Musselman, L., et al., *A high-sugar diet produces obesity and insulin resistance in wild-type Drosophila.* Disease Models & Mechanisms, 2011. **4**(6): p. 842-849.
114. Prochnik, S.E., D.S. Rokhsar, and A.A. Aboobaker, *Evidence for a microRNA expansion in the bilaterian ancestor.* Dev Genes Evol, 2007. **217**(1): p. 73-7.
115. Wienholds, E., et al., *MicroRNA Expression in Zebrafish Embryonic Development.* Science, 2005. **309**(5732): p. 310-311.
116. Correa-Medina, M., et al., *MicroRNA miR-7 is preferentially expressed in endocrine cells of the developing and adult human pancreas.* Gene Expr Patterns, 2009. **9**(4): p. 193-9.
117. Bravo-Egana, V., et al., *Quantitative differential expression analysis reveals miR-7 as major islet microRNA.* Biochemical and Biophysical Research Communications, 2008. **366**(4): p. 922-926.
118. Kredo-Russo, S., et al., *Pancreas-enriched miRNA refines endocrine cell differentiation.* Development, 2012. **139**(16): p. 3021-31.
119. Wang, Y., et al., *MicroRNA-7 regulates the mTOR pathway and proliferation in adult pancreatic β-cells.* Diabetes, 2013. **62**(3): p. 887-895.
120. Latreille, M., et al., *MicroRNA-7a regulates pancreatic β cell function.* J Clin Invest, 2014. **124**(6): p. 2722-35.
121. Broughton, S.J., et al., *Longer lifespan, altered metabolism, and stress resistance in Drosophila from ablation of cells making insulin-like ligands.* Proceedings of the National Academy of Sciences of the United States of America, 2005. **102**(8): p. 3105-3110.
122. Saltiel, A.R. and C.R. Kahn, *Insulin signalling and the regulation of glucose and lipid metabolism.* Nature, 2001. **414**(6865): p. 799-806.

123. D'ERCOLE, A.J., et al., *Expression of Insulin-Like Growth Factor I Stimulates Normal Somatic Growth in Growth Hormone-Deficient Transgenic Mice.* Endocrinology, 1990. **127**(3): p. 1033-1040.
124. D'ERCOLE, A.J., et al., *Growth Enhancement of Transgenic Mice Expressing Human Insulin-Like Growth Factor I*.* Endocrinology, 1988. **123**(6): p. 2827-2833.
125. DeChiara, T.M., A. Efstratiadis, and E.J. Robertsen, *A growth-deficiency phenotype in heterozygous mice carrying an insulin-like growth factor II gene disrupted by targeting.* Nature, 1990. **345**(6270): p. 78-80.
126. Melloul, D., S. Marshak, and E. Cerasi, *Regulation of insulin gene transcription.* Diabetologia, 2002. **45**(3): p. 309-326.
127. Evans-Molina, C., et al., *Glucose regulation of insulin gene transcription and pre-mRNA processing in human islets.* Diabetes, 2007. **56**(3): p. 827-835.
128. Colombani, J., et al., *A Nutrient Sensor Mechanism Controls Drosophila Growth.* Cell, 2003. **114**(6): p. 739-749.
129. Brogiolo, W., et al., *An evolutionarily conserved function of the Drosophila insulin receptor and insulin-like peptides in growth control.* Current Biology, 2001. **11**(4): p. 213-221.
130. Ikeya, T., et al., *Nutrient-dependent expression of insulin-like peptides from neuroendocrine cells in the CNS contributes to growth regulation in Drosophila.* Curr Biol, 2002. **12**(15): p. 1293-300.
131. Liu, Y., et al., *Drosophila insulin-like peptide 1 (DILP1) is transiently expressed during non-feeding stages and reproductive dormancy.* Scientific reports, 2016. **6**: p. 26620-26620.
132. Slaidina, M., et al., *A Drosophila insulin-like peptide promotes growth during nonfeeding states.* Developmental cell, 2009. **17**(6): p. 874-884.
133. Jaszczak, J.S., et al., *Growth Coordination During Drosophila melanogaster Imaginal Disc Regeneration Is Mediated by Signaling Through the Relaxin Receptor Lgr3 in the Prothoracic Gland.* Genetics, 2016. **204**(2): p. 703-709.
134. Garofalo, R.S., *Genetic analysis of insulin signaling in Drosophila.* Trends in Endocrinology & Metabolism, 2002. **13**(4): p. 156-162.
135. Böhni, R., et al., *Autonomous Control of Cell and Organ Size by CHICO, a Drosophila Homolog of Vertebrate IRS1–4.* Cell, 1999. **97**(7): p. 865-875.
136. Weinkove, D., et al., *Regulation of imaginal disc cell size, cell number and organ size by Drosophila class IA phosphoinositide 3-kinase and its adaptor.* Current Biology, 1999. **9**(18): p. 1019-1029.
137. Verdu, J., et al., *Cell-autonomous regulation of cell and organ growth in Drosophila by Akt/PKB.* Nature Cell Biology, 1999. **1**(8): p. 500-506.
138. Scanga, S.E., et al., *The conserved PI3'K/PTEN/Akt signaling pathway regulates both cell size and survival in Drosophila.* Oncogene, 2000. **19**(35): p. 3971-3977.
139. Tikhanovich, I., J. Cox, and S.A. Weinman, *Forkhead box class O transcription factors in liver function and disease.* Journal of gastroenterology and hepatology, 2013. **28 Suppl 1**(0 1): p. 125-131.
140. Cohen, P. and S. Frame, *The renaissance of GSK3.* Nature Reviews Molecular Cell Biology, 2001. **2**(10): p. 769-776.
141. Tessmar-Raible, K., et al., *Conserved sensory-neurosecretory cell types in annelid and fish forebrain: insights into hypothalamus evolution.* Cell, 2007. **129**(7): p. 1389-400.
142. Li, X., et al., *A MicroRNA Imparts Robustness against Environmental Fluctuation during Development.* Cell, 2009. **137**(2): p. 273-282.
143. Kredo-Russo, S., et al., *Regulation of pancreatic microRNA-7 expression.* Exp Diabetes Res, 2012. **2012**: p. 695214.

144. Stark, A., et al., *Identification of Drosophila MicroRNA targets.* PLoS biology, 2003. **1**(3): p. E60-E60.
145. Loya, C.M., et al., *Transgenic microRNA inhibition with spatiotemporal specificity in intact organisms.* Nature methods, 2009. **6**(12): p. 897-903.
146. Naya, F.J., et al., *Diabetes, defective pancreatic morphogenesis, and abnormal enteroendocrine differentiation in BETA2/neuroD-deficient mice.* Genes & development, 1997. **11**(18): p. 2323-2334.
147. Glick, E., D. Leshkowitz, and M.D. Walker, *Transcription Factor BETA2 Acts Cooperatively with E2A and PDX1 to Activate the Insulin Gene Promoter.* Journal of Biological Chemistry, 2000. **275**(3): p. 2199-2204.
148. Cho, J.-H. and M.-J. Tsai, *The role of BETA2/NeuroD1 in the development of the nervous system.* Molecular Neurobiology, 2004. **30**(1): p. 35-47.
149. Xu, H., et al., *The circular RNA Cdr1as, via miR-7 and its targets, regulates insulin transcription and secretion in islet cells.* Sci Rep, 2015. **5**: p. 12453.
150. Friedman, R.C., et al., *Most mammalian mRNAs are conserved targets of microRNAs.* Genome research, 2009. **19**(1): p. 92-105.
151. Lin, Y.-C., et al., *Human TRIM71 and Its Nematode Homologue Are Targets of let-7 MicroRNA and Its Zebrafish Orthologue Is Essential for Development.* Molecular Biology and Evolution, 2007. **24**(11): p. 2525-2534.
152. Yue, D., H. Liu, and Y. Huang, *Survey of Computational Algorithms for MicroRNA Target Prediction.* Current genomics, 2009. **10**(7): p. 478-492.
153. McGeary, S.E., et al., *The biochemical basis of microRNA targeting efficacy.* Science, 2019. **366**(6472): p. eaav1741.
154. Carthew, R.W. and E.J. Sontheimer, *Origins and Mechanisms of miRNAs and siRNAs.* Cell, 2009. **136**(4): p. 642-655.
155. Latreille, M., et al., *MicroRNA-7a regulates pancreatic beta cell function.* J Clin Invest, 2014. **124**(6): p. 2722-35.
156. Berger, C., et al., *The commonly used marker ELAV is transiently expressed in neuroblasts and glial cells in the Drosophila embryonic CNS.* Dev Dyn, 2007. **236**(12): p. 3562-8.
157. Ahmed, K., et al., *Loss of microRNA-7a2 induces hypogonadotropic hypogonadism and infertility.* The Journal of clinical investigation, 2017. **127**(3): p. 1061-1074.
158. Hoffman, N.E., et al., *SLC25A23 augments mitochondrial Ca2+ uptake, interacts with MCU, and induces oxidative stress–mediated cell death.* Molecular Biology of the Cell, 2014. **25**(6): p. 936-947.
159. Kennedy, E. and C. Wollheim, *Role of mitochondrial calcium in metabolism-secretion coupling in nutrient-stimulated insulin release.* Diabetes & metabolism, 1998. **24**: p. 15-24.
160. Gazave, E., et al., *Origin and evolution of the Notch signalling pathway: an overview from eukaryotic genomes.* BMC Evolutionary Biology, 2009. **9**(1): p. 249.
161. Masjkur, J., et al., *Endocrine Pancreas Development and Regeneration: Noncanonical Ideas From Neural Stem Cell Biology.* Diabetes, 2016. **65**(2): p. 314-30.
162. Johansson, K.A., et al., *Temporal Control of Neurogenin3 Activity in Pancreas Progenitors Reveals Competence Windows for the Generation of Different Endocrine Cell Types.* Developmental Cell, 2007. **12**(3): p. 457-465.
163. Jensen, J., et al., *Control of endodermal endocrine development by Hes-1.* Nature Genetics, 2000. **24**(1): p. 36-44.
164. Liang, K., L. Wei, and L. Chen, *Exocytosis, Endocytosis, and Their Coupling in Excitable Cells.* Frontiers in Molecular Neuroscience, 2017. **10**(109).

165. Fan, F., et al., *Dynamin 2 regulates biphasic insulin secretion and plasma glucose homeostasis.* The Journal of clinical investigation, 2015. **125**(11): p. 4026-4041.
166. Heaslip, A.T., et al., *Cytoskeletal dependence of insulin granule movement dynamics in INS-1 beta-cells in response to glucose.* PloS one, 2014. **9**(10): p. e109082-e109082.
167. Kalwat, M.A. and D.C. Thurmond, *Signaling mechanisms of glucose-induced F-actin remodeling in pancreatic islet β cells.* Experimental & Molecular Medicine, 2013. **45**(8): p. e37-e37.
168. Wen, P.J., et al., *Actin dynamics provides membrane tension to merge fusing vesicles into the plasma membrane.* Nature communications, 2016. **7**: p. 12604-12604.
169. Wang, Z., E. Oh, and D.C. Thurmond, *Glucose-stimulated Cdc42 signaling is essential for the second phase of insulin secretion.* The Journal of biological chemistry, 2007. **282**(13): p. 9536-9546.
170. Bear, J.E. and F.B. Gertler, *Ena/VASP: towards resolving a pointed controversy at the barbed end.* Journal of Cell Science, 2009. **122**(12): p. 1947-1953.
171. Nicholson-Dykstra, S., H.N. Higgs, and E.S. Harris, *Actin Dynamics: Growth from Dendritic Branches.* Current Biology, 2005. **15**(9): p. R346-R357.
172. Thurmond, D.C., et al., *Glucose-Stimulated Insulin Secretion Is Coupled to the Interaction of Actin with the t-SNARE (Target Membrane Soluble N-Ethylmaleimide-Sensitive Factor Attachment Protein Receptor Protein) Complex.* Molecular Endocrinology, 2003. **17**(4): p. 732-742.
173. Uenishi, E., et al., *Actin dynamics regulated by the balance of neuronal Wiskott-Aldrich syndrome protein (N-WASP) and cofilin activities determines the biphasic response of glucose-induced insulin secretion.* The Journal of biological chemistry, 2013. **288**(36): p. 25851-25864.
174. Guček, A., et al., *Fusion pore regulation by cAMP/Epac2 controls cargo release during insulin exocytosis.* eLife, 2019. **8**: p. e41711.
175. Kalwat, M.A., et al., *A p21-activated kinase (PAK1) signaling cascade coordinately regulates F-actin remodeling and insulin granule exocytosis in pancreatic β cells.* Biochem Pharmacol, 2013. **85**(6): p. 808-16.
176. Ma, W., et al., *Arp2/3 nucleates F-actin coating of fusing insulin granules in pancreatic β cells to control insulin secretion.* Journal of Cell Science, 2020. **133**(6): p. jcs236794.
177. Bretou, M., et al., *Cdc42 controls the dilation of the exocytotic fusion pore by regulating membrane tension.* Molecular Biology of the Cell, 2014. **25**(20): p. 3195-3209.
178. Kim, K., et al., *Actin-based Motility during Endocytosis in Budding Yeast.* Molecular Biology of the Cell, 2006. **17**(3): p. 1354-1363.
179. Mooren, O.L., B.J. Galletta, and J.A. Cooper, *Roles for Actin Assembly in Endocytosis.* Annual Review of Biochemistry, 2012. **81**(1): p. 661-686.
180. Kochubey, O., A. Majumdar, and J. Klingauf, *Imaging Clathrin Dynamics in Drosophila melanogaster Hemocytes Reveals a Role for Actin in Vesicle Fission.* Traffic, 2006. **7**(12): p. 1614-1627.
181. Galletta, B.J., D.Y. Chuang, and J.A. Cooper, *Distinct roles for Arp2/3 regulators in actin assembly and endocytosis.* PLoS biology, 2008. **6**(1): p. e1-e1.
182. Dürre, K., et al., *Capping protein-controlled actin polymerization shapes lipid membranes.* Nature communications, 2018. **9**(1): p. 1630-1630.
183. Kaksonen, M., C.P. Toret, and D.G. Drubin, *A Modular Design for the Clathrin- and Actin-Mediated Endocytosis Machinery.* Cell, 2005. **123**(2): p. 305-320.
184. Hu, D., et al., *Identification of miR-9 as a negative factor of insulin secretion from beta cells.* Journal of Physiology and Biochemistry, 2018. **74**(2): p. 291-299.
185. Duan, J., et al., *miR-29a Negatively Affects Glucose-Stimulated Insulin Secretion and MIN6 Cell Proliferation via Cdc42/β-Catenin Signaling.* International Journal of Endocrinology, 2019. **2019**: p. 5219782.

186. Cassidy, J.J., et al., *Repressive Gene Regulation Synchronizes Development with Cellular Metabolism.* Cell, 2019. **178**(4): p. 980-992.e17.
187. Hope, K.M., et al., *Regulation of α-Cell Function by the β-Cell in Isolated Human and Rat Islets Deprived of Glucose: the "Switch-off" Hypothesis.* Diabetes, 2004. **53**(6): p. 1488-1495.
188. Raju, B. and P.E. Cryer, *Loss of the Decrement in Intraislet Insulin Plausibly Explains Loss of the Glucagon Response to Hypoglycemia in Insulin-Deficient Diabetes.* Documentation of the Intraislet Insulin Hypothesis in Humans, 2005. **54**(3): p. 757-764.
189. Lang, D.A., et al., *Cyclic oscillations of basal plasma glucose and insulin concentrations in human beings.* N Engl J Med, 1979. **301**(19): p. 1023-7.
190. Simon, C. and G. Brandenberger, *Ultradian Oscillations of Insulin Secretion in Humans.* Diabetes, 2002. **51**(suppl 1): p. S258-S261.
191. Pørksen, N., et al., *Human insulin release processes measured by intraportal sampling.* American Journal of Physiology-Endocrinology and Metabolism, 2002. **282**(3): p. E695-E702.
192. Schmitz, O., et al., *On high-frequency insulin oscillations.* Ageing Research Reviews, 2008. **7**(4): p. 301-305.
193. Hunter, S.J., et al., *Association between insulin secretory pulse frequency and peripheral insulin action in NIDDM and normal subjects.* Diabetes, 1996. **45**(5): p. 683-6.
194. O'Rahilly, S., R.C. Turner, and D.R. Matthews, *Impaired pulsatile secretion of insulin in relatives of patients with non-insulin-dependent diabetes.* N Engl J Med, 1988. **318**(19): p. 1225-30.
195. Alon, U., *Network motifs: theory and experimental approaches.* Nature Reviews Genetics, 2007. **8**(6): p. 450-461.
196. Britton, J.S., et al., *Drosophila's Insulin/PI3-Kinase Pathway Coordinates Cellular Metabolism with Nutritional Conditions.* Developmental Cell, 2002. **2**(2): p. 239-249.
197. Gao, Y., et al., *MicroRNA miR-7 and miR-17-92 in the Arcuate Nucleus of Mouse Hypothalamus Regulate Sex-Specific Diet-Induced Obesity.* Mol Neurobiol, 2019. **56**(11): p. 7508-7521.
198. Le Marchand, S.J. and D.W. Piston, *Glucose suppression of glucagon secretion: metabolic and calcium responses from alpha-cells in intact mouse pancreatic islets.* The Journal of biological chemistry, 2010. **285**(19): p. 14389-14398.
199. Knudsen, L.A., et al., *The MicroRNA Repertoire in Enteroendocrine Cells: Identification of miR-375 as a Potential Regulator of the Enteroendocrine Lineage.* Endocrinology, 2015. **156**(11): p. 3971-3983.
200. Sedgeman, L.R., et al., *Beta cell secretion of miR-375 to HDL is inversely associated with insulin secretion.* Scientific Reports, 2019. **9**(1): p. 3803.
201. Zhou, Y., et al., *A secreted microRNA disrupts autophagy in distinct tissues of Caenorhabditis elegans upon ageing.* Nat Commun, 2019. **10**(1): p. 4827.
202. Thomou, T., et al., *Adipose-derived circulating miRNAs regulate gene expression in other tissues.* Nature, 2017. **542**(7642): p. 450-455.
203. Luo, J., et al., *miR-375 Suppresses IGF1R Expression and Contributes to Inhibition of Cell Progression in Laryngeal Squamous Cell Carcinoma.* BioMed Research International, 2014. **2014**: p. 374598.
204. Jung, H.J. and Y. Suh, *Regulation of IGF -1 signaling by microRNAs.* Frontiers in genetics, 2015. **5**: p. 472-472.
205. Rech, M., et al., *AntagomiR-103 and -107 Treatment Affects Cardiac Function and Metabolism.* Molecular Therapy - Nucleic Acids, 2019. **14**: p. 424-437.
206. Hanna, J., G.S. Hossain, and J. Kocerha, *The Potential for microRNA Therapeutics and Clinical Research.* Frontiers in Genetics, 2019. **10**(478).
207. Dong, S., et al., *Effects of Periodic Intensive Insulin Therapy: An Updated Review.* Current therapeutic research, clinical and experimental, 2019. **90**: p. 61-67.

208. Riedl, J., et al., *Lifeact: a versatile marker to visualize F-actin.* Nature Methods, 2008. **5**(7): p. 605-607.

APPENDIX

Imaging IPCs to identify pathways leading to insulin secretory defects

Lifeact-GFP, was used to visualize the cytoskeleton in IPCs. Lifeact is a yeast derived peptide that binds both F-actin and G-actin[208]. Preliminary analysis of Lifeact images does not show clear differences between *miR-7* overexpression and wildtype actin in IPCs. It is possible that CPA might be affecting actin at the level of motility and live imaging of the cytoskeleton might be a better approach toward determining defects with *miR-7* overexpression. Attempts to image the cytoskeleton however did not yield insightful results due to technical limitations.

Figure 39 - Imaging F-actin cytoskeleton with Lifeact GFP

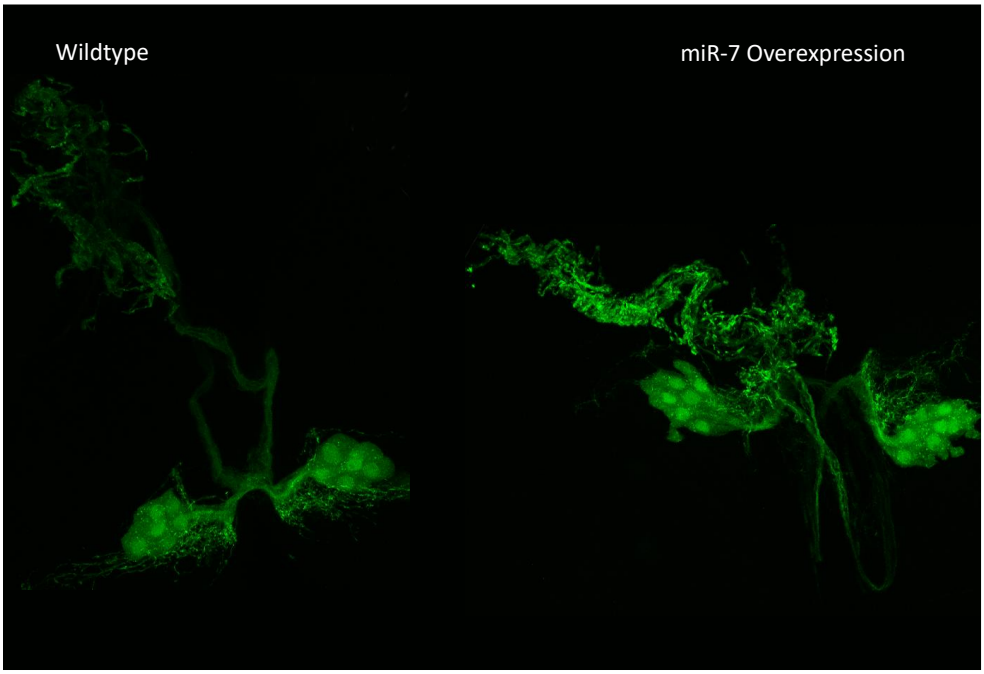

Figure 39: Imaging F-actin cytoskeleton with Lifeact GFP - GFP-bound actin-binding peptide Life-act is expressed in IPCs under the control of the Dilp2Gal4 driver. Left shows wildtype IPC, while right shows Lifeact staining in IPCs with *miR-7* overexpression.

Secretory defects observed in IPCs might be Dilp specific. In order to assess the general secretory abilities of IPCs, a GFP-tagged rat atrial natriuretic factor (ANF-GFP) was expressed in IPCs along with UAS*miR-7*. This peptide was expressed under the control of the Dilp2gal4 driver, and should be secreted like any other IPC peptide. Unlike IPC Dilp however, this peptide is exogenous, and not subject to endogeneous Dilp processing steps. This thereby allows us to explore IPC secretory abilities in a more isolated context. Interestingly, I observed that the levels of this peptide increased with *miR-7* overexpression relative to controls, suggesting that IPC secretion might be affected at a generalized level. This GFP does come with the caveat that it is expressed under the control of the Dilp2gal4 UAS system, it therefore doesn't rule out the possibility that the effects seen might be due to differential regulation of Dilp2 transcription as a result of *miR-7* overexpression.

Figure 40 - Anf-GFP levels increase with miR-7 overexpression

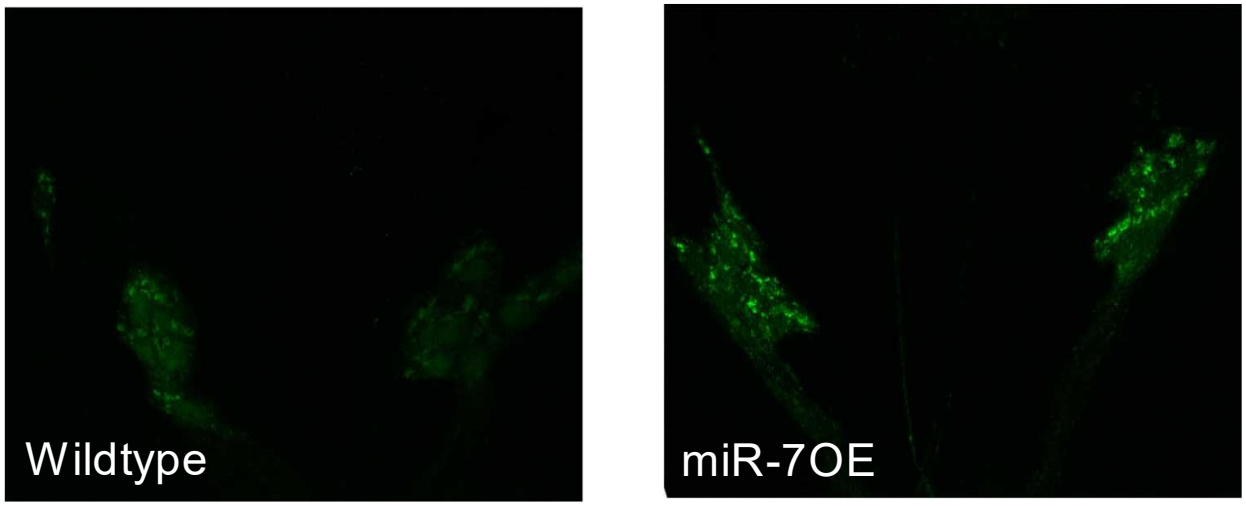

Figure 40: Expression of Anf-GFP in IPCs - GFP-tagged rat atrial natriuretic factor (ANF-GFP) was expressed under the control of the Dilp2gal4 driver. Left shows expression in wildtype IPCs while right shows expression in IPCs when *miR-7* is overexpressed.